MICROFLUIDIC DEVICES FOR PERFORMING MULTIPLEXED IMMUNOASSAYS AND NUCLEIC ACID TESTS

Emily Anna Oblath

A dissertation submitted to the faculty of the University of North Carolina at Chapel Hill in partial fulfillment of the requirements for the degree of Doctor of Philosophy in the Department of Chemistry.

Chapel Hill
2012

Approved by:

J. Michael Ramsey

James W. Jorgenson

R. Mark Wightman

Kevin M. Weeks

Marcey L. Waters

ABSTRACT

EMILY ANNA OBLATH: Microfluidic Devices for Performing Multiplexed Immunoassays and Nucleic Acid Tests
(Under the direction of J. Michael Ramsey)

This work describes the development of microfluidic devices to perform multiplexed immunoassays and nucleic acid tests for point-of-care (POC) diagnostics. Diagnostic testing is usually performed at centralized laboratories, imposing a significant delay in treatment. In contrast, POC testing is performed by the primary healthcare provider, and the results can be used to implement proper treatment immediately. Saliva can be an ideal sample for POC diagnostics since it is easily collected and contains many disease biomarkers. This work focuses on using saliva to monitor and diagnose pulmonary diseases. Cytokine biomarkers are measured as early indicators for asthma or cystic fibrosis, while DNA is characterized to identify bacteria that can cause respiratory infections.

The first device described uses sandwich immunoassays to measure cytokines. The polydimethylsiloxane (PDMS)-glass hybrid chip integrated microfluidic channels with a 900-well microarray. The wells were loaded with antibody-functionalized microspheres from a random mixture. An encoding strategy was used for multiplexed assays so that microspheres functionalized with antibodies for one analyte could be distinguished from microspheres for another analyte. Optimization of the assay for reduced analysis time and a low limit of detection is described for two cytokines, VEGF

and IL-8. The optimized assay required less than one hour, and the theoretical limits of detection were found to be well below physiological levels reported in the literature.

A second device was developed to integrate DNA extraction and polymerase chain reaction (PCR) amplification for the detection of bacteria found in saliva. Sample extraction is a particularly challenging problem for POC, PCR-based diagnostics. In this device, DNA extraction was accomplished by filtering samples through an aluminum oxide membrane (AOM) integrated with a PDMS-glass channel structure. Parallel reaction wells located above the AOM were used to perform multiplexed analyses. Several designs and detection strategies were explored as the device was optimized. The final format incorporated 7 reaction wells and real-time detection with fluorescent probes or an intercalating dye. Detection of as little as 8-12 copies of purified template DNA was achieved. The successful identification of bacteria and spiked genomic DNA in saliva is also described.

Dedicated to my mom
and in memory of my dad

ACKNOWLEDGEMENTS

I would like to thank my advisor, J. Michael Ramsey, for the opportunity to work in his research group and for his support and guidance of my research. I also thank all the members of the Ramsey group for their help over the past 5 years. In particular, J.P. Alarie, Hamp Henley, and Patty Dennis were indispensable for teaching me how to use the instruments in lab, for helpful discussions when experiments didn't work, and for their many contributions to my research. Finally, I would like to thank my family and friends for their support throughout my time in graduate school.

TABLE OF CONTENTS

LIST OF TABLES

Table

LIST OF FIGURES

Figure

LIST OF ABBREVIATIONS AND SYMBOLS

AF488	Alexa Fluor® 488 streptavidin conjugate
AOM	Aluminum oxide membrane
BOE	Buffered oxide etchant
bp	Base pairs
BSA	Bovine serum albumin
CCD	Charge-coupled device
CE	Capillary electrophoresis
CNC	Computer numeric controlled
C_t	Cycle threshold
DI	Deionized
DNA	Deoxyribonucleic acid
dNTPs	Deoxyribonucleotides
DRIE	Deep reactive-ion etching
EDTA	Ethylenediaminetetraacetic acid
ELISA	Enzyme-linked immunosorbent assay
EMCCD	Electron multiplying charge-coupled device
EtBr	Ethidium bromide
FAM	Carboxyfluorescein
FIB	Focused ion beam
fM	Femtomolar
g	Grams
gDNA	Genomic deoxyribonucleic acid

hr	Hour
IaBkQ	Iowa Black® Dark Quencher FQ
IL-8	Interleukin-8
KCl	Potassium chloride
keV	Kiloelectron volt
LiCl	Lithium chloride
LOC	Lab-on-a-chip
LOD	Limit of detection
M	Molar
mg	Milligrams
$MgCl_2$	Magnesium chloride
min	Minutes
mL	Milliliters
mM	Millimolar
mol	Moles
mRNA	Messenger ribonucleic acid
MRSA	Methicillin-resistant *Staphylococcus aureus*
ms	Milliseconds
MSSA	Methicillin-susceptible *Staphylococcus aureus*
μg	Micrograms
μm	Micrometers
μTAS	Micro total analysis system
nA	Nanoamps

NaCl	Sodium chloride
NCBI	National Center for Biotechnology Information
ng	Nanograms
nm	Nanometers
nmol	Nanomoles
PBP	Penicillin-binding protein
PBS	Phosphate buffered saline
PCR	Polymerase chain reaction
PDMS	Poly(dimethylsiloxane)
PEG	Polyethylene glycol
pg	Picograms
POC	Point-of-care
PVP	Polyvinylpyrrolidone
RNA	Ribonucleic acid
RTD	Resistance temperature detector
rt-PCR	Real-time polymerase chain reaction
rxn	Reaction
s	Seconds
SDS	Sodium dodecyl sulfate
S/N	Signal-to-noise ratio
SSC	Saline sodium citrate buffer
TBS	Tris-buffered saline
TE	Tris-ethylenediaminetetraacetic acid

UV	Ultraviolet
VEGF	Vascular endothelial growth factor
W	Watt

CHAPTER 1

INTRODUCTION TO POINT-OF-CARE SALIVARY DIAGNOSTICS

1.1 Microfluidics and Point-of-care Diagnostics

Microfluidics concerns the behavior and manipulation of fluids on the micro-scale. It can be used as a strategy for taking macro-scale techniques and procedures and adapting them onto a device to perform the same actions on the microscale. Ideally, microfluidics would integrate all the steps for a procedure usually performed on the bench top into a single device, a micro total analysis system (μTAS) or Lab-on-a-chip (LOC).[1-4] Often that device can take the form of a small chip, something comparable to a microscope slide, that contains millimeter- to micrometer-scale fluidic channels and features for manipulating and transporting fluids from one region of the chip to another.[3, 5, 6] If possible, the chip would provide sample-in answer-out capability, with little or no interaction from the user.[1, 3-5, 7-11] The detection method of the 'answer' could be integrated as part of the chip or could be housed in a separate instrument.[11, 12]

The initial motivation for miniaturization with microfluidics was to improve performance in applications requiring high resolution separations and sensitive detection.[3, 5] The decreased size of LOC devices also leads to other advantages including lower consumption of sample and reagents, lower cost, and shorter analysis times.[3, 5, 11, 12] Much of the early research focused on fabricating functional microscale components such as pumps, valves, and chemical sensors.[3] This early work created silicon-based devices using microfabrication techniques developed in the semiconductor industry.[3, 5] Device

materials eventually moved towards polymers, such as poly(dimethysiloxane) (PDMS), that are more suitable for biological samples, require less complex fabrication procedures for components like pumps and valves, and are less expensive.[3, 5, 9] Further research shifted towards integrating multiple steps, such as separation and detection, onto a single device.[3, 5, 7, 9] This led to the potential for automation of analytical techniques with extremely easy to use devices, one of the biggest advantages of microfluidics.[1, 5, 11]

The sample-in answer-out promise of microfluidics makes it extremely well suited for point-of-care (POC) diagnostics. The goal of POC diagnostics is to perform analyses at or near where the patient is receiving care.[13, 14] An ideal test would be fast enough for the patient to receive results while waiting in the doctor's office, emergency room, or at home. Current diagnostic testing typically takes place at centralized labs.[11, 13-15] Samples must be collected, sometimes at the point-of-care, sometimes at a separate testing site such as a LabCorp or Quest Diagnostics lab, and then packaged and transported to the testing facilities for analysis. Depending on the tests ordered and the frequency at which the results are reported, the results may not be available to the care providers for many days.[14-16] It may take even longer for the results to be communicated to the patient and for any necessary treatment decisions to be made. POC testing reduces the turn-around time to get results, eliminates sample packaging and transportation costs, decreases labor costs, and lowers the chances of contaminated, mislabeled, and lost samples.[15, 16] The fast turn-around time of POC testing can even improve patient outcomes, particularly for test results that impact a critical decision in patient care.[15] An automated sample-in answer-out LOC would be ideal for these tests, reducing the time

required and need for trained personnel at a centralized laboratory to obtain the information necessary to monitor or make treatment decisions.

1.2 Saliva

Whole saliva is made up of components from many sources. It contains secretions from the parotid, submandibular, sublingual, and minor salivary glands, crevicular fluid from the oral mucosa, as well as bacteria, leukocytes, and sloughed epithelial cells.[17] Each salivary gland contributes different mixtures of proteins to the whole saliva.[18] Saliva serves many purposes important for both oral health and overall health. The continuous flow of saliva washes bacteria and food out of the mouth, and the saliva also acts as a buffer, neutralizing acid and protecting tooth enamel.[18] Saliva also begins digesting food as it is eaten, and aids in swallowing the food.[18] Without saliva, teeth would quickly decay and the mouth would be vulnerable to infections. Individuals with chronically dry mouth, such as those with Sjögren's syndrome, often develop serious problems with tooth decay and cavities.[19]

Saliva contains a huge number of analytes and possible biomarkers that come from all of its components, making it a good candidate for diagnostic tests. Blood and urine are two of the most commonly used samples for diagnostic tests. In some instances blood is the only choice, but for many analytes saliva can be used instead.[16, 20] Most analytes found in blood and urine can also be found in saliva, although they are often present in lower concentrations.[16, 20, 21] Many steroid, hormone, drug, and antibody levels in saliva have been found to correlate well with those found in blood or urine, although this is not true in all cases.[16, 20] Antibodies to HIV, protein biomarkers for cancer, and inflammatory cytokines are just a few of the analytes that have been detected in saliva.[22-

[24] Levels and types of bacteria in saliva have been linked to periodontal health, bad breath, and pancreatic cancer.[25-27] If analyte levels correlate with those found in other samples and lower analyte concentration is not a critical problem, saliva offers many advantages over blood samples. Saliva is easier to obtain with painless, non-invasive collection that does not require phlebotomy. Collecting saliva is less dangerous than blood collection for the person doing the collecting, and, with fewer privacy concerns, it is easier to maintain a chain of custody for saliva samples than for urine samples.[16, 20]

There are many ways to collect both whole saliva and saliva from individual glands. The most basic collection method is unstimulated collection of whole saliva through draining or drooling. The patient allows saliva to drain out of their mouth into a container with minimal mouth movement.[28] Evaporation during the collection time can be problematic for the draining method, so spitting can be used as an alternative although it does have a stimulating effect on the saliva flow.[28] Chewing on paraffin wax or unflavored chewing gum, and introducing citric acid to the mouth have also been used to stimulate saliva flow for collection.[28, 29] Swabs and commercially available absorbent pads can also be used for whole saliva collection.[28, 29] Suction methods can be used to collect either whole saliva or secretions from the individual glands, but require more training and specialized equipment, and are more invasive for the patient.[28]

The method used to collect and store saliva for diagnostic testing depends on the analytes and biomarkers being targeted, but there are also some general properties of saliva that must be considered for all analytes. The most important consideration is that the methods used to collect samples must be consistent for a given test.[17, 29] This includes collecting repeated samples in the same way, collecting samples at the same time of day

and under the same environmental conditions, and limiting eating and drinking for a period of time, usually 1-2 hours, prior to sample collection.[17, 30, 31] Flow rates and composition of saliva can vary greatly between samples, even for the same individual, so saliva may sometimes be better suited for qualitative tests than for quantitative tests.[18, 20, 29]

If the target analytes include protein or enzyme biomarkers, care must be taken to preserve them until the analysis is performed. The bacteria and digestive enzymes found in saliva have proteolytic activity and will alter the concentrations of proteins in the sample if not stopped.[17, 29] Collecting saliva on ice can slow or stop the degradation of proteins in the sample.[17, 29] The addition of protease inhibitors such as EDTA, phenylmethanesulfonylfluoride, soy bean trypsin inhibitor, and E-64 (an epoxide-based cysteine protease inhibitor) to the collection vials can also be helpful for slowing protein degradation.[29] Sodium azide can also be added to slow bacterial growth and thus slow protein breakdown, but it will interfere in downstream analysis if an enzyme-linked immunosorbent assay (ELISA) is used.[29] The salivary proteins can also be lost from adsorbing to the surfaces of the collection device if materials such as glass are present.[17] If an absorbent pad or swab is used for saliva collection, the analytes must be compatible with the material chosen. Another consideration is that highly prevalent proteins in saliva can sometimes affect or obscure the detection of low abundance proteins.[32] Mucins are high molecular weight, heavily glycosylated proteins that are prevalent in saliva.[29] Mucin aggregates are responsible for the viscoelastic properties of saliva.[29] They can be precipitated out of the sample, reducing viscosity concerns, but since mucin-protein complexes can form, precipitation of the mucins can lead to a loss of protein

biomarkers.[17, 29] Alpha amylase is another highly prevalent protein in saliva, and it can be selectively removed to allow detection of lower abundance proteins.[32] As with the removal of mucins, this is only useful if the biomarker proteins are not also removed.

If the purpose of the saliva sample is for bacterial culture, the collection conditions will not affect the results as much as for proteins.[17] Because saliva is constantly flowing, bacteria will be constantly shed from the surfaces in the mouth.[33] The biggest effect on saliva samples for culture is the behavior of the patient. Diet, tooth-cleaning habits, and whether the patient has taken antibiotics recently will all affect the levels and types of bacteria found in the mouth.[33] Some patients use more effective toothbrushing that is different from their usual habits prior to visiting the dentist.[33] This can temporarily lower the amounts of bacteria in the mouth but, since the behavior usually does not continue after the visit to the dentist, levels will quickly return to normal.[33] A final consideration in collecting saliva for bacterial culture is that culture media appropriate for the target organisms should be used during any storage or transport steps to keep the bacteria viable.[17]

If the target analytes are nucleic acids, care must be taken to avoid their breakdown before analysis. Salivary RNA biomarkers have been identified, and if those are to be measured special care must be taken to stabilize the RNA.[29] Ambient temperature RNA stabilizers are available commercially and can be added to the samples after collection, but storage at or below -20 °C is still recommended.[29, 31] DNA degrades more slowly, so stabilization is not as critical.[31] If the target analytes include DNA or RNA from the bacteria or other microorganisms found in saliva, the same considerations regarding bacteria levels and patient behavior prior to collection for bacterial culture will

apply. Many biomarkers, including proteins and some salivary RNA, are primarily found in saliva supernatant, and a centrifugation step is often incorporated before storage and analysis of the sample.[29] This is not the case for genomic DNA (gDNA) from human cells and other microorganisms that is instead found in the solid components of saliva.[31]

Saliva is an attractive sample for use with POC testing and LOC since it is easy to collect.[16, 21] However, because of its mucin aggregates and viscous nature, saliva can be incompatible with microfluidic devices.[30] Sample processing must be performed after collection to prevent the sample from clogging or fouling the microfluidic device. Freeze-thaw cycles and centrifugation can greatly decrease viscosity, but are not very practical in a POC setting.[29] Filters have been used instead to remove large proteins and any particles from the sample.[30] As with any other processing step, it must be verified that the filter doesn't also remove the analyte from the sample.

1.3 Immunoassays

For protein analytes, an immunoassay is often the analytical method of choice.[34] Immunoassays are tests that use antibody-antigen interactions to detect analytes in the sample such as hormones, cytokines, and other antibodies.[34-36] The immunoassay principle was first described by Yalow and Berson in 1959 with an assay for insulin that used radioactive labels for detection.[37] Their assay was a competitive immunoassay, in which a labeled antigen competes with unlabeled antigen in the sample for a limited number of antibody binding sites. The proportion of labeled antigen bound to the antibodies is measured and the concentration of sample antigen determined.[35] For a competitive immunoassay, the signal is inversely proportional to the analyte concentration.

Another type of immunoassay is the reagent excess or sandwich immunoassay, which uses two antibodies. The first antibody is immobilized onto a surface and captures the antigen from the sample. A wash step removes unbound sample, and a labeled secondary antibody is brought in that will bind to the antigen-antibody complex on the surface. Unbound secondary antibody is then washed away and the signal from the surface measured to determine the concentration.[35] Because they rely on two antibodies specific to the antigen, sandwich immunoassays are less likely than some other types of immunoassays to return false positive results.[38] The low background, due to signal increasing with analyte concentration, also tends to make sandwich assays more sensitive.[38] One drawback to sandwich immunoassays is that finding two antibodies with different binding sites is difficult for some antigens.[38] Radioactive labels were originally used for immunoassays, but fluorescent labels have become much more common.[34, 36, 38, 39] If an enzyme is used as the label for a sandwich immunoassay, it is known as an ELISA.[35, 40] ELISAs add an additional step by bringing in the substrate to react with the enzyme and then detecting the product of that reaction. The amplification resulting from the enzyme reaction makes ELISAs even more sensitive than standard sandwich assays.[35, 40]

For some analytes, immunoassays are the only practical method for quantitation.[34] The recognition of antigens by antibodies is extremely specific, and complex biological samples, such as blood, plasma, urine, and saliva can be used.[34-36] Immunoassays can be designed with low limits of detection for a large number of analytes, and can be designed to be very fast and simple to use, with commercial kits available for many different analytes.[34-36] Immunoassays can be so fast and user-friendly that they are used for POC

devices like home pregnancy tests. The advantages of immunoassays make it an attractive technique to use in a LOC device for protein biomarkers in saliva. All types of immunoassays have been adapted onto microfluidic devices, with sandwich assays and ELISAs being very common.[41] Multiplexed immunoassays for more than one analyte have been performed on microfluidic devices. One strategy for multiplexing is to use microarrays. With microarray devices the capture antibodies are immobilized in an array on a surface within the microfluidic device and the assays for all analytes are performed simultaneously.[22, 42-46]

Adapting immunoassays onto microfluidic devices for POC diagnostics combines the advantages of immunoassays with those of microfluidics, but it requires some special considerations compared to immunoassays performed under standard conditions in microtiter plates. The surface area-to-volume ratios in microfluidic devices are very high, so the characteristics of the surface and its compatibility with immunoassays are a concern. Surface modification with a coating or the addition of blocking buffers to reagent solutions is often necessary to prevent adsorption of antigen or other reagents to the channel walls.[44, 47-49] Another consideration is that at the small scale of microfluidic channels, fluid flow is laminar. If diffusion is not sufficient enough to transport antigens or secondary antibodies to the immobilized capture antibody (for a sandwich assay), mixers may need to be designed into the device.[48] Many types of mixers have been developed for microfluidic devices that can be used if necessary.[8-10] A final consideration for immunoassays in microfluidic devices is the integration of some sort of internal calibration on-chip to account for chip-to-chip or run-to-run variations.[48] Unlike

with microtiter plates, it can be difficult to generate a calibration curve on a microfluidic device.

1.4 Detection and Identification of Bacteria

In addition to targeting protein analytes, diagnostic tests are also performed to detect bacteria and other microorganisms that cause infectious diseases. Currently, collected samples are usually sent to a centralized laboratory for cell culture.[14, 50-52] After culture, the bacteria are identified by their phenotypic characteristics. Morphologic features, growth variables, gram staining, and the growth media are just a few of the characteristics that can be used to identify the species.[53, 54] To identify the particular strain of bacteria, susceptibility to antibiotics, protein profiles, and bacteriophage analysis can be used.[53, 54] Culture-based tests are adequate for some situations, but there are many drawbacks.[55] Culture methods are slow and labor intensive, often taking several days for results to be returned.[50, 51, 53-55] If antibiotic susceptibility must be determined, additional testing time is needed.[56] Many organisms also have similar characteristics, making correct identification difficult.[53] Another problem with culture-based identification is that not all organisms can be cultured.[14, 56-58] The culture methods used with diagnostic samples tend to be biased towards well known, well characterized species.[57]

An alternative to culture methods is to identify bacteria from their DNA using nucleic acid tests. Nucleic acid tests can identify the bacteria in a sample in a few hours, eliminating the need for culture.[54, 59] The polymerase chain reaction (PCR) is frequently used to amplify DNA for nucleic acid tests. PCR was invented in the mid-1980s by Kary Mullis and other scientists at Cetus Corporation.[60, 61] PCR takes advantage of thermostable DNA polymerases, such as *Taq* polymerase, to catalyze the replication of a

specific DNA sequence from a template strand using oligonucleotide primers and deoxynucleotide triphosphates (dNTPs). The reaction cycles through three temperature steps and with each cycle the amount of DNA is theoretically doubled. The first step is denaturation, at a temperature from 90-95 °C, to melt the double-stranded DNA into single-stranded DNA. The second step is annealing, usually at a temperature near 55 °C for about 30 s, to allow the primers to hybridize to the template strands. The final step is extension, at a temperature near 72 °C for 0.5-3 min, where the DNA polymerase extends the primers and replicates the DNA sequence. The 3-step cycle is repeated 30 or more times with a longer denaturation step before the first cycle and a longer extension step after the final cycle. The exponential amplification from thermocycling makes PCR a very sensitive technique – it can be used to detect as little as one copy of template DNA in a sample.

For PCR-based diagnostic testing, samples are still sent to a centralized laboratory for processing. A typical PCR test requires sample preparation steps, expensive equipment and reagents, and trained technicians.[1, 16, 58, 62] Sample preparation steps are necessary because template DNA often needs to be released from the nucleus of the cells and because PCR inhibitors are often present that, if not removed, may cause false negatives.[59, 63] These labor-intensive steps mean that at centralized labs the tests are usually performed once a day in large batches, so the minimum time for obtaining results is about 24 hours.[56, 58] Adapting PCR onto a microfluidic device can make it amenable to POC diagnostics. Some advantages of microfluidic PCR tests over tube-based procedures include lower consumption of expensive reagents, faster cycling times, lower costs per test, and automated processing by minimally trained personnel.[11, 14, 51, 64-67] A

LOC incorporating PCR for diagnostic testing could be portable, with disposable chips to eliminate contamination between samples. Devices could also incorporate parallel processing units to increase throughput and identify multiple strains or species of bacteria simultaneously.[50, 62, 66, 67]

As with any microfluidic device, the exact design and materials used in a PCR chip will vary depending on the application. Regardless of the application, for PCR microfluidics there are two main design strategies. The first strategy is stationary chamber PCR. The PCR solution is kept stationary inside a reaction chamber and the temperature of the chamber is cycled. This design is similar to tube-based PCR testing, and has the advantages of simple chip configuration and great flexibility in the length of the thermocycling steps and in the number of cycles.[1, 14, 66, 67] The second strategy is flow through PCR. The PCR solution continuously flows through different zones of the chip that are held at constant temperatures. This design can achieve extremely fast thermocycling times since only the thermal mass of the sample must be heated and cooled rather than the entire chip. A major drawback of this design is that the number of cycles is usually fixed by the channel layout so it is not as flexible as the chamber design.[1, 14, 66, 67] Either chip design can be integrated with different types of sample processing, heating strategies, and post-PCR analysis and detection of products.[67]

No matter what design and materials are chosen for a microfluidic PCR device, preventing PCR inhibition is a major concern. As with immunoassays, the high surface area-to-volume ratios found in microfluidic devices can be a problem. Adsorption to the channel surfaces can be a problem not only for template DNA in the sample but also for the primers and the *Taq* polymerase.[63, 68] Adsorption of any of the reagents to the

channel surfaces will inhibit PCR, so various passivation strategies are used to reduce or prevent the adsorption. Bovine serum albumin (BSA) and polyvinylpyrrolidone (PVP) are two common PCR additives used for dynamic surface passivation.[67, 68] Static surface passivation by coating the channels with a PCR friendly substance is another way to reduce adsorption.[63, 67] Inhibition can also be caused by materials used in the fabrication of chips, so the fabrication choices may be restricted if a reaction is particularly sensitive.[63, 67] Sample components other than the target DNA are another source of inhibition that can be addressed by integrating sample preparation onto the microchip.[69-73] The extraction technique used will depend on the application.

1.5 Research Goals and Objectives

The focus of the research discussed in this dissertation is the development of a POC microfluidic device that uses saliva samples to diagnose and monitor pulmonary diseases such as asthma and cystic fibrosis, as well as respiratory infections that are common in patients with pulmonary diseases. The targeted saliva components are cytokines, chemokines, and bacterial species that are either biomarkers of disease or causes of infections. The device should be useable without specialized training and should be fully integrated and self-contained, without the need for extensive off-chip sample preparation or signal detection. It was determined that two devices, one targeting proteins via multiplex immunoassays and the other targeting bacterial DNA via PCR would be developed. The potential merging of the two devices into a single device was one of the design criteria, but it was not pursued. PDMS was chosen as the material of choice because it is inexpensive, optically transparent for fluorescence detection

techniques, easy to fabricate devices and prototype potential chip designs, and it is generally compatible with biological systems.[74, 75]

This project is part of a collaboration with the Walt group at Tufts University (biomarker screening and immunoassay development), Ahura Scientific (control instrument development and data acquisition), and the Brodley group at Tufts University (automated data analysis and data mining). Other collaborators include the Oppenheim group at Boston University Medical Center, who have been collecting and tracking saliva samples, and clinicians from Boston University Pulmonary/Boston Medical Center and the Children's Hospital at Harvard University who have been recruiting asthma and cystic fibrosis patients to donate samples for the study.

1.6 References

1. Kricka, L. J.; Wilding, P., Microchip PCR. *Analytical and Bioanalytical Chemistry* 2003, *377*, (5), 820-825.

2. Manz, A.; Graber, N.; Widmer, H. M., Miniaturized Total Chemical Analysis Systems: a Novel Concept for Chemical Sensing. *Sensors and Actuators B-Chemical* 1990, *1*, (1-6), 244-248.

3. Reyes, D. R.; Iossifidis, D.; Auroux, P.-A.; Manz, A., Micro Total Analysis Systems. 1. Introduction, Theory, and Technology. *Analytical Chemistry* 2002, *74*, (12), 2623-2636.

4. West, J.; Becker, M.; Tombrink, S.; Manz, A., Micro Total Analysis Systems: Latest Achievements. *Analytical Chemistry* 2008, *80*, (12), 4403-4419.

5. Whitesides, G. M., The origins and the future of microfluidics. *Nature* 2006, *442*, (7101), 368-373.

6. Walt, D. R., Miniature Analytical Methods for Medical Diagnostics. *Science* 2005, *308*, (5719), 217-219.

7. Arora, A.; Simone, G.; Salieb-Beugelaar, G. B.; Kim, J. T.; Manz, A., Latest Developments in Micro Total Analysis Systems. *Analytical Chemistry* 2010, *82*, (12), 4830-4847.

8. Auroux, P.-A.; Iossifidis, D.; Reyes, D. R.; Manz, A., Micro Total Analysis Systems. 2. Analytical Standard Operations and Applications. *Analytical Chemistry* 2002, *74*, (12), 2637-2652.

9. Dittrich, P. S.; Tachikawa, K.; Manz, A., Micro Total Analysis Systems. Latest Advancements and Trends. *Analytical Chemistry* 2006, *78*, (12), 3887-3907.

10. Vilkner, T.; Janasek, D.; Manz, A., Micro Total Analysis Systems. Recent Developments. *Analytical Chemistry* 2004, *76*, (12), 3373-3386.

11. Weigl, B.; Domingo, G.; LaBarre, P.; Gerlach, J., Towards non- and minimally instrumented, microfluidics-based diagnostic devices. *Lab on a Chip* 2008, *8*, (12), 1999-2014.

12. Janasek, D.; Franzke, J.; Manz, A., Scaling and the design of miniaturized chemical-analysis systems. *Nature* 2006, *442*, (7101), 374-380.

13. Mascini, M.; Tombelli, S., Biosensors for biomarkers in medical diagnostics. *Biomarkers* 2008, *13*, (7-8), 637-657.

14. Park, S.; Zhang, Y.; Lin, S.; Wang, T.-H.; Yang, S., Advances in microfluidic PCR for point-of-care infectious disease diagnostics. *Biotechnology Advances* 2011, *29*, (6), 830-839.

15. Lee-Lewandrowski, E.; Lewandrowski, K., Perspectives on Cost and Outcomes for Point-of-Care Testing. *Clinics in Laboratory Medicine* 2009, *29*, (3), 479-489.

16. Hart, R. W.; Mauk, M. G.; Liu, C.; Qiu, X.; Thompson, J. A.; Chen, D.; Malamud, D.; Abrams, W. R.; Bau, H. H., Point-of-care oral-based diagnostics. *Oral Diseases* 2011, *17*, (8), 745-752.

17. Söderling, E., Practical Aspects of Salivary Analyses. In *Human Saliva: Clincal Chemistry and Microbiology*, Tenovuo, J. O., Ed. CRC Press, Inc.: Baco Raton, FL, 1989; Vol. I, pp 1-24.

18. Amerongen, A. v. N.; Veerman, E. C. I.; Vissink, A., Saliva: Properties and functions. In *Salivary Diagnostics*, Wong, D. T., Ed. Wiley-Blackwell: Ames, Iowa, 2008; pp 27-36.

19. Fox, P. C., Sjögren's syndrome. In *Salivary Diagnostics*, Wong, D. T., Ed. Wiley-Blackwell: Ames, Iowa, 2008; pp 189-197.

20. Hofman, L. F., Human saliva as a diagnostic specimen. *Journal of Nutrition* 2001, *131*, (5), 1621S-1625S.

21. Malamud, D., Saliva as a Diagnostic Fluid. *Dental Clinics of North America* 2011, *55*, (1), 159-178.

22. Blicharz, T. M.; Siqueira, W. L.; Helmerhorst, E. J.; Oppenheim, F. G.; Wexler, P. J.; Little, F. F.; Walt, D. R., Fiber-Optic Microsphere-Based Antibody Array for the Analysis of Inflammatory Cytokines in Saliva. *Analytical Chemistry* 2009, *81*, (6), 2106-2114.

23. Liu, C.; Qiu, X.; Ongagna, S.; Chen, D.; Chen, Z.; Abrams, W. R.; Malamud, D.; Corstjens, P. L. A. M.; Bau, H. H., A timer-actuated immunoassay cassette for detecting molecular markers in oral fluids. *Lab on a Chip* 2009, *9*, (6), 768-776.

24. Tan, W.; Sabet, L.; Li, Y.; Yu, T.; Klokkevold, P. R.; Wong, D. T.; Ho, C.-M., Optical protein sensor for detecting cancer markers in saliva. *Biosensors & Bioelectronics* 2008, *24*, (2), 266-271.

25. Farrell, J. J.; Zhang, L.; Zhou, H.; Chia, D.; Elashoff, D.; Akin, D.; Paster, B. J.; Joshipura, K.; Wong, D. T. W., Variations of oral microbiota are associated with pancreatic diseases including pancreatic cancer. *Gut* 2012, *61*, (4), 582-588.

26. Kurata, H.; Awano, S.; Yoshida, A.; Ansai, T.; Takehara, T., The prevalence of periodontopathogenic bacteria in saliva is linked to periodontal health status and oral malodour. *Journal of Medical Microbiology* 2008, *57*, (5), 636-642.

27. Petti, S.; Pezzi, R.; Cattaruzza, M. S.; Osborn, J. F.; Darca, A. S., Restoration related salivary Streptococcus mutans level: A dental caries risk factor? *Journal of Dentistry* 1997, *25*, (3-4), 257-262.

28. Vissink, A.; Wolff, A.; Veerman, E. C. I., Saliva Collectors. In *Salivary Diagnostics*, Wong, D. T., Ed. Wiley-Blackwell: Ames, Iowa, 2008; pp 37-59.

29. Veerman, E. C. I.; Vissink, A.; Wong, D. T.; Amerongen, A. v. N., Processing and storage of saliva samples. In *Salivary Diagnostics*, Wong, D. T., Ed. Wiley-Blackwell: Ames, Iowa, 2008; pp 69-76.

30. Helton, K. L.; Nelson, K. E.; Fu, E.; Yager, P., Conditioning saliva for use in a microfluidic biosensor. *Lab on a Chip* 2008, *8*, (11), 1847-1851.

31. Jiang, J.; Park, N. J.; Hu, S.; Wong, D. T., A universal pre-analytic solution for concurrent stabilization of salivary proteins, RNA and DNA at ambient temperature. *Archives of Oral Biology* 2009, *54*, (3), 268-273.

32. Deutsch, O.; Fleissig, Y.; Zaks, B.; Krief, G.; Aframian, D. J.; Palmon, A., An approach to remove alpha amylase for proteomic analysis of low abundance biomarkers in human saliva. *Electrophoresis* 2008, *29*, (20), 4150-4157.

33. Bratthall, D.; Carlsson, P., Clinical Microbiology of Saliva. In *Human Saliva: Clincal Chemistry and Microbiology*, Tenovuo, J. O., Ed. CRC Press, Inc.: Boca Raton, FL, 1989; Vol. II, pp 203-241.

34. Gosling, J. P., A Decade of Development in Immunoassay Methodology. *Clinical Chemistry* 1990, *36*, (8), 1408-1427.

35. Davies, C., Introduction to Immunoassay Principles. In *The Immunoassay Handbook*, 2nd ed.; Wild, D., Ed. Nature Publishing Group: New York, NY, 2001; pp 3-40.

36. Luppa, P. B.; Sokoll, L. J.; Chan, D. W., Immunosensors - principles and applications to clinical chemistry. *Clinica Chimica Acta* 2001, *314*, (1-2), 1-26.

37. Yalow, R. S.; Berson, S. A., Assay of Plasma Insulin in Human Subjects by Immunological Methods. *Nature* 1959, *184*, (4699), 1648-1649.

38. Bilitewski, U., Protein-sensing assay formats and devices. *Analytica Chimica Acta* 2006, *568*, (1-2), 232-247.

39. Hage, D. S., Immunoassays. *Analytical Chemistry* 1999, *71*, (12), 294R-304R.

40. Ngo, T. T., Developments in Immunoassay Technology. *Methods* 2000, *22*, (1), 1-3.

41. Kricka, L. J.; Wild, D., Lab-on-a-chip, Micro-, and Nanoscale Immunoassay Systems. In *The Immunoassay Handbook*, 3rd ed.; Wild, D., Ed. Elsevier: New York, NY, 2005; pp 294-309.

42. Barbee, K. D.; Hsiao, A. P.; Roller, E. E.; Huang, X., Multiplexed protein detection using antibody-conjugated microbead arrays in a microfabricated electrophoretic device. *Lab on a Chip* 2010, *10*, (22), 3084-3093.

43. Derveaux, S.; Stubbe, B. G.; Roelant, C.; Leblans, M.; De Geest, B. G.; Demeester, J.; De Smedt, S. C., Layer-by-Layer Coated Digitally Encoded Microcarriers for Quantification of Proteins in Serum and Plasma. *Analytical Chemistry* 2008, *80*, (1), 85-94.

44. Diercks, A. H.; Ozinsky, A.; Hansen, C. L.; Spotts, J. M.; Rodriguez, D. J.; Aderem, A., A microfluidic device for multiplexed protein detection in nano-liter volumes. *Analytical Biochemistry* 2009, *386*, (1), 30-35.

45. Rissin, D. M.; Walt, D. R., Duplexed sandwich immunoassays on a fiber-optic microarray. *Analytica Chimica Acta* 2006, *564*, (1), 34-39.

46. Urbanowska, T.; Mangialaio, S.; Zickler, C.; Cheevapruk, S.; Hasler, P.; Regenass, S.; Legay, F., Protein microarray platform for the multiplex analysis of biomarkers in human sera. *Journal of Immunological Methods* 2006, *316*, (1-2), 1-7.

47. Bange, A.; Halsall, H. B.; Heineman, W. R., Microfluidic immunosensor systems. *Biosensors & Bioelectronics* 2005, *20*, (12), 2488-2503.

48. Henares, T. G.; Mizutani, F.; Hisamoto, H., Current development in microfluidic immunosensing chip. *Analytica Chimica Acta* 2008, *611*, (1), 17-30.

49. Lillehoj, P. B.; Wei, F.; Ho, C. M., A self-pumping lab-on-a-chip for rapid detection of botulinum toxin. *Lab on a Chip* 2010, *10*, (17), 2265-2270.

50. Heo, J.; Hua, S. Z., An Overview of Recent Strategies in Pathogen Sensing. *Sensors* 2009, *9*, (6), 4483-4502.

51. Mairhofer, J.; Roppert, K.; Ertl, P., Microfluidic Systems for Pathogen Sensing: A Review. *Sensors* 2009, *9*, (6), 4804-4823.

52. McPherson, R. A.; Pincus, M. R., ed., *Henry's Clinical Diagnosis and Management by Laboratory Methods*. 21 ed.; Saunders Elsevier: Philadelphia, 2007.

53. Desai, M. J.; Armstrong, D. W., Separation, Identification, and Characterization of Microorganisms by Capillary Electrophoresis. *Microbiology and Molecular Biology Reviews* 2003, *67*, (1), 38-51.

54. Tang, Y. W.; Procop, G. W.; Persing, D. H., Molecular diagnostics of infectious diseases. *Clinical chemistry* 1997, *43*, (11), 2021-2038.

55. Jackowski, M.; Szeliga, J.; Kłodzińska, E.; Buszewski, B., Application of capillary zone electrophoresis (CZE) to the determination of pathogenic bacteria for medical diagnosis. *Analytical and Bioanalytical Chemistry* 2008, *391*, (6), 2153-2160.

56. Doring, G.; Unertl, K.; Heininger, A., Validation criteria for nucleic acid amplification techniques for bacterial infections. *Clinical Chemistry and Laboratory Medicine* 2008, *46*, (7), 909-918.

57. Rogers, G. B.; Daniels, T. W. V.; Tuck, A.; Carroll, M. P.; Connett, G. J.; David, G. J. P.; Bruce, K. D., Studying Bacteria in Respiratory Specimens by Using Conventional and Molecular Microbiological Approaches. *BMC Pulmonary Medicine* 2009, *9*, (14).

58. Sauer-Budge, A. F.; Mirer, P.; Chatterjee, A.; Klapperich, C. M.; Chargin, D.; Sharon, A., Low cost and manufacturable complete microTAS for detecting bacteria. *Lab on a Chip* 2009, *9*, (19), 2803-2810.

59. Mothershed, E. A.; Whitney, A. M., Nucleic acid-based methods for the detection of bacterial pathogens: Present and future considerations for the clinical laboratory. *Clinica Chimica Acta* 2006, *363*, (1-2), 206-220.

60. Saiki, R. K.; Scharf, S.; Faloona, F.; Mullis, K. B.; Horn, G. T.; Erlich, H. A.; Arnheim, N., Enzymatic Amplification of β-Globin Genomic Sequences and Restriction Site Analysis for Diagnosis of Sickle Cell Anemia. *Science* 1985, *230*, (4732), 1350-1354.

61. Bartlett, J. M. S.; Stirling, D., A Short History of the Polymerase Chain Reaction. In *PCR Protocols*, 2nd ed.; Bartlett, J. M. S.; Stirlins, D., Eds. Humana Press: Totowa, NJ, 2003; pp 3-6.

62. Lien, K.-Y.; Liu, C.-J.; Kuo, P.-L.; Lee, G.-B., Microfluidic System for Detection of α-Thalassemia-1 Deletion Using Saliva Samples. *Analytical Chemistry* 2009, *81*, (11), 4502-4509.

63. Wilson, I. G., Inhibition and Facilitation of Nucleic Acid Amplification. *Applied and Environmental Microbiology* 1997, *63*, (10), 3741-3751.

64. Lee, C.-Y.; Lee, G.-B.; Lin, J.-L.; Huang, F.-C.; Liao, C.-S., Integrated microfluidic systems for cell lysis, mixing/pumping and DNA amplification. *Journal of Micromechanics and Microengineering* 2005, *15*, (6), 1215-1223.

65. Yeung, S.-W.; Lee, T. M.-H.; Cai, H.; Hsing, I.-M., A DNA biochip for on-the-spot multiplexed pathogen identification. *Nucleic Acids Research* 2006, *34*, (18), e118.

66. Zhang, C. S.; Xing, D., Miniaturized PCR chips for nucleic acid amplification and analysis: latest advances and future trends. *Nucleic Acids Research* 2007, *35*, (13), 4223-4237.

67. Zhang, C. S.; Xu, J. L.; Ma, W. L.; Zheng, W. L., PCR microfluidic devices for DNA amplification. *Biotechnology Advances* 2006, *24*, (3), 243-284.

68. Kolari, K.; Satokari, R.; Kataja, K.; Stenman, J.; Hokkanen, A., Real-time analysis of PCR inhibition on microfluidic materials. *Sensors and Actuators B-Chemical* 2008, *128*, (2), 442-449.

69. Chen, L.; Manz, A.; Day, P. J. R., Total nucleic acid analysis integrated on microfluidic devices. *Lab on a Chip* 2007, *7*, (11), 1413-1423.

70. Kim, J.; Johnson, M.; Hill, P.; Gale, B. K., Microfluidic sample preparation: cell lysis and nucleic acid purification. *Integrative Biology* 2009, *1*, (10), 574-586.

71. Liu, P.; Mathies, R. A., Integrated microfluidic systems for high-performance genetic analysis. *Trends in Biotechnology* 2009, *27*, (10), 572-581.

72. Mariella, R., Sample preparation: the weak link in microfluidics-based biodetection. *Biomedical Microdevices* 2008, *10*, (6), 777-784.

73. Price, C. W.; Leslie, D. C.; Landers, J. P., Nucleic acid extraction techniques and application to the microchip. *Lab on a Chip* 2009, *9*, (17), 2484-2494.

74. McDonald, J. C.; Duffy, D. C.; Anderson, J. R.; Chiu, D. T.; Wu, H. K.; Schueller, O. J. A.; Whitesides, G. M., Fabrication of microfluidic systems in poly(dimethylsiloxane). *Electrophoresis* 2000, *21*, (1), 27-40.

75. Sia, S. K.; Whitesides, G. M., Microfluidic devices fabricated in poly(dimethylsiloxane) for biological studies. *Electrophoresis* 2003, *24*, (21), 3563-3576.

CHAPTER 2

MICROFLUIDIC BEAD-BASED IMMUNOASSAY CHIP

2.1 Introduction

Microfluidic immunoassays for POC diagnostics have been developed with many different strategies. Chips have been fabricated using silicon, glass, and polymers as the base material, although some materials are better suited for POC immunoassays than others.[1, 2] Silicon does not make a very good substrate since proteins tend to bind to the surface and it is not optically transparent in the UV/visible region of the spectrum often used for optical detection of immunoassay results.[1] Glass is optically transparent and has better surface chemistry for immunoassays than silicon, but polymers, such as PDMS, are also optically transparent and are especially well-suited for mass production.[3] Polymer chips also tend to have reduced manufacturing costs compared with silicon or glass devices with the more expensive fabrication processes only used for the development of the mold. The mold can then be used to make many highly reproducible castings for chips.[1-3]

The type of immunoassay used also varies between chips. Since non-competitive immunoassays such as sandwich assays tend to be more sensitive, they are often used in microfluidic chips.[4] These types of immunoassays require an immobilized capture antibody on a surface, generally one of the channel surfaces in a microfluidic chip. Antibodies can be immobilized through microcontact printing or by chemically tethering

the antibody to the surface.[1, 2, 5] With any immobilization method used, the antibodies need to be oriented properly on the surface to capture antigen from the sample.[1, 2, 5]

The type of signal generated for the detection of antigen varies as well. Fluorescence, surface plasmon resonance, and electrochemical detection methods are the most common.[1, 2, 4] Fluorescence detection is easy to integrate into an immunoassay and it has high sensitivity which makes it the most common form of detection.[1, 2, 5] ELISAs can be performed with a substrate and enzyme that generate a fluorescent product for even greater sensitivity than standard fluorescence detection.[6] One device described was made from a glass slide, used a streptavidin-biotin linkage to immobilize antibodies on a surface, and then used fluorescently labeled reporter probes to detect cancer markers from saliva samples.[7] Another device was made from polymers and incorporated a lateral flow strip with immobilized synthetic HIV envelope peptides to capture antibodies to HIV from saliva samples that were then detected with fluorescently labeled reporters.[8] These are just two examples of the many applications and sample types that microfluidic immunoassays can be designed for.

Since antibody-antigen interactions are very specific, most immunoassays can detect only one analyte. If multiplexed detection from the same sample is desired, antibodies for multiple antigens can be immobilized to a surface in a microarray. Microarrays allow many analytes to be evaluated simultaneously, saving time and reducing the sample volume needed since only one assay is performed.[4, 9-11] Microfluidic devices can incorporate microarrays and the technique has been demonstrated for many applications.[3, 12-14] While microarrays of immobilized antibodies can be fabricated, the current technology for spotting the antibodies is labor-intensive and requires high-

precision, and the antibody-spotting technology makes customizing the selection of antibodies used in each chip difficult.[11, 15-17]

An alternative to immobilizing capture antibodies directly onto a surface is to couple antibodies to microspheres. Microsphere-based immunoassays have a number of advantages over planar assays including better reproducibility in the attachment of capture antibodies to the surface, more flexibility in surface chemistry, and shorter analysis times.[11, 18, 19] Microspheres also have a high surface-to-volume ratio leading to a greater number of capture antibodies available and therefore higher sensitivity compared to planar immunoassays.[15, 16, 20] Microspheres can also be used to form microarrays for multiplexing, and having a prepared library of microspheres with capture antibodies for different analytes means an array can be easily customized for a particular set of targets. Microarrays of antibody-coupled microspheres can be formed by loading microspheres into known locations, or by randomly loading a mixture of microsphere types and decoding the type of microsphere in each location afterwards.[16, 18-22] Decoding of random arrays can be done by doping the microspheres with varying levels of one or more fluorescent dyes or even by photobleaching a barcode onto each microsphere if they are large enough.[11, 16, 23]

The Walt group at Tufts University has developed microsphere-based immunoassays that use fiber optic bundles to form microarrays.[16, 24, 25] Sets of microspheres, or beads, are functionalized with different capture antibodies. Mixtures of beads with different capture antibodies are randomly loaded into fiber optic arrays to perform multiplexed immunoassays. Each type of microsphere is encoded with a unique concentration of europium (Eu^{3+}) dye, which allows them to be identified by fluorescence

intensity after they are loaded into an array.[24-27] Multiple encoding dyes can be used if the multiplexed assay calls for more bead types than can be distinguished using a single dye.[23, 28] The end of the fiber optic bundle containing the array is exposed to reagent solutions over the course of a sandwich assay and the fiber is finally imaged, both for decoding and signal detection, using a custom-built epi-fluorescence microscope with a charge-coupled device (CCD) camera.[23] The Walt group used conventional ELISA methods to identify ten salivary cytokines and chemokines that are potential biomarkers for pulmonary diseases, such as asthma and cystic fibrosis, and developed antibody-functionalized microspheres that were used in fiber optic microarrays to simultaneously measure all ten analytes in saliva supernatant samples from patients with pulmonary diseases.[23, 29]

In this chapter the adaptation of the Walt group's microsphere-based immunoassay onto a microfluidic chip is described. The PDMS/glass hybrid chip contains an 896-well microarray fabricated into a single PDMS layer that also includes all the fluidic channels needed to deliver reagents for the sandwich assay to the array. The optimization of the assay is described and limits of detection in buffer and saliva supernatant were determined for two cytokines.

2.2 Materials and Methods

Materials and Reagents

Sylgard 184 PDMS was obtained from Dow Corning (Midland, MI). PDMS was prepared according to the manufacturer's recommendation with a 10:1 polymer/cross-linker ratio. Trichloro-(1H,1H,2H,2H-perfluorooctyl)silane, 97% (perfluorooctyl silane), poly(ethylene glycol) (PEG) with an average molecular weight of 200 g/mol (PEG 200),

polyvinylpyrrolidone (PVP) with an average molecular weight of 10,000 g/mol, 10x phosphate buffered saline solution (PBS), tris buffered saline with 0.05% Tween 20 (TBS/Tween 20), and DNase/RNase free polyurethane amplification tape (PCR tape) were purchased from Sigma-Aldrich (St. Louis, MO). Fisherbrand plain glass microscope slides (75 mm x 25 mm, 990 μm thick) and isopropyl alcohol were purchased from Thermo Fisher Scientific (Waltham, MA). SEA Block blocking buffer, SuperBlock blocking buffer, Protein Free blocking buffer, Blocker BSA (10% BSA) in PBS, PBS Starting Block blocking buffer, and TBS Starting Block blocking buffer were purchased from Pierce Biotechnology, Inc. (Rockford, IL). PEG with an average molecular weight of 10,000 g/mol (PEG 10k) was purchased from Alfa Aesar (Ward Hill, MA). Buffered oxide etchant (BOE), 10:1, was purchased from Transene (Danvers, MA). 2-[methoxy(polyethyleneoxy)propyl]trimethoxysilane, 90% (PEG-silane) was purchased from Gelest (Morrisville, PA). Streptavidin-Alexa Fluor® 488 (AF488) conjugate was purchased from Invitrogen (Carlsbad, CA). Purified recombinant human vascular endothelial growth factor (VEGF), interleukin-8 (IL-8), and biotin-labeled polyclonal detection antibodies for each cytokine were purchased from R&D Systems, Inc. (Minneapolis, MN). Cytokines and antibodies were reconstituted according to the manufacturer's instructions. Buffer solutions of 1x PBS containing 0.1% PEG 10k (PBS/PEG10k) were prepared from a 10x stock solution diluted with deionized (DI) water filtered with a NANOpure Diamond water purification system (Barnstead International, Dubuque, IA).

Antibody coupled microspheres were provided by collaborators in the Walt group at Tufts University and were made in a manner previously described.[23] Briefly, 3.1 μm

diameter amine-functionalized microspheres are encoded with Europium (III) thenoyltrifluoroacetonate trihydrate at concentrations of either 1.0, 0.5, 0.125, or 0.025 M. These four concentrations can be differentiated based on fluorescence emission intensity upon UV excitation. After encoding, four different cytokine capture antibodies are attached to the different sets of microspheres after which they are stored in TBS Starting Block blocking buffer with 0.05% sodium azide at 4 °C, protected from light.

Chip Fabrication

The chips were fabricated by first making a master mold of the chip design in glass followed by making a complementary mold of the master in PDMS. The final PDMS chips were prepared from the complementary PDMS mold. This has recently been described in detail.[30] Glass master molds were fabricated using a combination of wet chemical etching and focused ion beam (FIB) milling. Channels were patterned onto a glass substrate using standard photolithography techniques and etched to a depth of 30 μm using 10:1 BOE. A 50 nm thick layer of chromium was sputtered onto the glass substrate using an Ion Deposition/Sputter System (South Bay Technology, Inc., San Clemente, CA). Microarrays were milled using a Helios 600 Nanolab Dual Focused Ion Beam System (FEI, Hillsboro, Oregon). Galium ions at an energy of 30 keV and current of 21 nA were used to mill individual microwells to a depth of 2.95 μm and diameter of 2.75 μm with a well center-to-center spacing of 8 μm. Array patterns from 100 wells (10x10) up to 896 wells (28x32) were milled. Assay optimization and limit of detection determination were performed on chips with 896 well arrays.

The glass master was treated with oxygen plasma at 18W for 1 min (Harrick Plasma, model PDC-32G, Ithaca, NY) and placed in a vacuum desiccator with 40 μL of

perfluorooctyl silane. Vacuum was applied for approximately 5 min to allow silane vapor to fill the desiccator and then it was sealed for 20-30 min. This treatment reduced PDMS adhesion to the master. A secondary mold of the master was cast in PDMS by placing the master channel-side up in a larger mold form and covering it with PDMS to a 5-10 mm depth. The PDMS-filled mold form was placed in a vacuum desiccator with vacuum applied for 15-20 min to degas the PDMS. The mold was then cured for 30 min at 60 °C followed by 15 min at 95 °C. After cooling, the PDMS mold was removed from the mold form and separated from the master, and the edges were trimmed with a razor blade.

The PDMS secondary mold was silanized in the same manner as the glass master, but with a shorter 5 s plasma treatment step. The PDMS layer of the microfluidic chip was made by pouring ~4 mL of PDMS into the mold, degassing under vacuum, placing a glass slide over the top of the mold to push out excess PDMS and to give the chip a reproducible thickness, and then curing at 95 °C for 15 min. The PDMS chip layer was then separated from the mold and trimmed with a razor blade. The silanization prevented the PDMS chip layer from adhering to the PDMS mold.

Access holes were made with a 3 mm diameter biopsy punch (Sklar Instruments, West Chester, PA) at the ends of each channel to form fluid reservoirs. The PDMS layer was irreversibly bonded to a glass microscope slide to give a completed PDMS/glass hybrid chip. Before bonding, PDMS layers were cleaned with isopropanol and dried with nitrogen. Microscope slides were cleaned with a 5% Contrad solution (Decon Labs, King of Prussia, PA), rinsed with DI water, and dried with nitrogen. Both layers were then plasma treated at 18 W for 12 s and irreversibly bonded by gently pressing the channel

side of the PDMS layer onto the glass slide. Bonded chips were allowed to stabilize at room temperature for at least 1 day before use.

An image of a chip, an SEM image of an FIB milled array, and a schematic of the cross section of a chip are shown in figure 2.1. The chip has 4 reagent reservoirs to introduce sample, secondary antibody, AF488, and wash buffer. Vacuum is applied to a fifth waste reservoir to effect fluid flow. The reagent reservoirs individually connect to the main channel that includes the microwell array followed by a serpentine path to the waste reservoir. The serpentine path has a large enough volume such that delivered reagents used during an assay will remain on-chip. This will prevent the chip reader (control instrument) from becoming contaminated with sample or other reagents. The reader instrument will use pinch valves to automate fluid handling on-chip. When actuated, the valves press on the PDMS above a channel, pinching it closed. Valving locations are shown in figure 2.1A. The assay development and limit of detection determination described in this chapter were performed without valves.

Chip Preparation

Prior to running an assay, the chip's microwell array was loaded with antibody-functionalized microspheres. The chip was first filled with buffer (PBS/PEG10k unless otherwise noted) by filling all 4 reagent reservoirs and applying vacuum to the waste reservoir. Then a slurry containing a mixture of different antibody-coupled microspheres was introduced into the array chamber by putting the bead mixture into the sample reservoir and applying vacuum to the waste. Once in the array chamber, beads were pushed into wells by applying pressure on the PDMS layer directly over the array, forcing beads into individual microwells. Pressure was applied by placing a thumb or

finger on the PDMS over the array and pressing down against the glass. The extent of array loading was monitored with a fluorescence microscope and pressure was applied repeatedly until the array was sufficiently loaded (usually to a 90% efficiency or better). Unloaded microspheres were washed away with buffer. The channels were then filled with fresh buffer (PBS/PEG10k unless otherwise noted), the reservoirs were sealed with PCR tape to prevent evaporation, and the chips were stored in the dark at 4°C for at least 1 hour before using for an assay.

Assay Procedure

The assay procedure was adapted from the fiber optic immunoassays developed at Tufts University.[23] Protein assays were performed with the following procedure unless otherwise noted. Reagent solutions were introduced onto the chip through all four reagent reservoirs because these assays were performed without valves. Each solution was added to the reservoirs just before it was delivered, and excess reagent was removed from the reservoirs (with vacuum) just before the next reagent was added. Sample solution (20 μL) containing cytokines diluted in PBS/PEG10k buffer was added to the reservoirs of the chip and delivered to the microarray. The array was incubated with the sample for 20 min. The secondary antibody solution, also diluted in PBS/PEG10k buffer, was introduced into the chip in the same manner as the sample followed by a 15 min incubation. AF488 was then added to the chip followed by a 10 min incubation. Finally, the wash buffer, TBS/Tween 20, was added to the chip and the array and channels were rinsed for 10 min by continuously flowing the wash buffer over the array. After rinsing, the top and bottom surfaces of the chip were cleaned with ethanol and the array was imaged. The chips were protected from light during the entire assay.

A schematic of the sandwich assay is shown in figure 2.2. During the sample incubation, the cytokines are captured by the antibodies attached to the beads. The biotinylated secondary antibodies then attach to the antigen-antibody complex on the beads during the secondary antibody incubation. During the AF488 incubation, the streptavidin in the AF488 forms a linkage with the biotin on the secondary antibodies and labels the antigen-antibody sandwich with a fluorescent tag. The final wash removes the excess AF488 and the AF488 bound to the antigen-antibody complex can be detected with fluorescence microscopy.

For experiments using saliva supernatant as samples, whole saliva was collected from healthy volunteers by having them drool into a clean centrifuge tube. The samples were centrifuged at 4000 rpm for 30 min. Aliquots of saliva supernatant were spiked with cytokine standards for limit of detection determinations.

Image Collection and Analysis

Arrays were imaged with a Nikon Eclipse Ti-U inverted microscope with a Nikon Intensilight C-HGFIE mercury light source (Melville, NY) and collected with a Cascade II 512 electron multiplying CCD (EMCCD) camera (Photometrics, Tucson, AZ). A custom optical filter cube (Chroma Technology Corp., Rockingham, VT) was used for fluorescence imaging of the europium encoding dye (λ_{ex}=365 nm, λ_{em}=605 nm) and a Nikon filter cube B-2E/C was used for collection of the AF488 signal (λ_{ex}=488 nm, λ_{em}=520 nm). Two images were acquired for each array: an encoding image (λ_{ex}=365 nm, 100 ms exposure), and an assay image (λ_{ex}=488 nm, 8 s exposure). Encoding and assay images were acquired using Micromanager[31] and analyzed using ImageJ[32]

(National Institutes of Health, USA), IgorPro (WaveMetrics, Inc., Lake Oswego, OR), and OriginPro (OriginLab Corp., Northampton, MA).

ImageJ was used to decode images and determine signal intensities. For both encoding and assay images, microsphere intensities are spread over ~4 pixels but only the intensity of the brightest pixel is used. Encoding images were used to identify microsphere types so that individual cytokine signal intensities could be determined from the assay images. For each array, signal intensities from microspheres of the same type were averaged to obtain the raw signal. Values not within 2.5 standard deviations from the mean were discarded and the remaining values were averaged to obtain the corrected signal. This is a technique commonly used with clinical chemistry data to eliminate false positives and negatives and other outliers, although outliers can easily inflate the standard deviation to the point that they are not discarded.[33] A microsphere type for which no analyte was present was used as a control to determine non-specific binding. The net signal for a given cytokine was calculated by subtracting the corrected control bead signal from the corrected target analyte bead signal. Noise values were calculated in IgorPro by finding the standard deviation of the pixel intensities in an area of the background outside the array. The net signal is divided by the noise to calculate the signal to noise ratio (S/N). A set of encoding and assay images from a VEGF assay is shown in figure 2.3, with selected VEGF and control (IL-8) beads circled in both images. Limit of detection data were fit to a 4-parameter logistics equation using OriginPro. Theoretical limits of detection were based on a S/N of 3.

2.3 Results and Discussion

Surface Passivation

The surface of PDMS is hydrophobic, making it prone to nonspecific adsorption of biomolecules such as proteins.[3, 34-38] Surface passivation of both the PDMS and glass surfaces is essential to ensure compatibility with the biological sample matrix and assay reagents. Many strategies to prevent protein adsorption and increase biocompatibility of these surfaces have been described.[36-41] Both static and dynamic surface coatings were investigated to reduce non-specific adsorption to the channel walls during assays, but dynamic coatings were favored due to their simplicity and faster chip preparation times. Dynamic coatings are buffer additives that are thought to reduce non-specific adsorption by preferentially adsorbing to the surface instead of the protein.[42]

Eight different dynamic coatings and a static silane coating were evaluated: four commercial blocking buffers (10% Blocker BSA, SuperBlock, Protein Free, and SEA Block), PBS with 0.1% BSA, PBS with 0.1% PVP, PBS with 0.1% PEG 200, PBS/PEG10k, and a PEG-silane coating. One chip was used to test each coating. For these experiments, the buffer used for chip preparation and during the assay was the buffer containing the dynamic coating listed above instead of the PBS/PEG10k described in section 2.2. The PEG-silane coated chip was prepared following the procedure described by Sui, et. al.[38] Briefly, after the chip was bonded, a 5:1:1 mixture of $H_2O/H_2O_2/HCl$ was continuously washed through the channels for 5 min, the channels were rinsed with DI water and dried with air, the channels were filled with neat PEG-silane and incubated for 30 min at room temperature, and then the channels were rinsed with DI water again and dried with air. PBS with 0.1% BSA was used as the buffer for

the PEG-silane coated chip. After bead loading, all channels were filled with the appropriate buffer and incubated for at least 1 h at 4 °C. Reagent solutions were prepared with each of the buffers using VEGF as a model analyte. 500 pg/mL VEGF, 3 μg/mL anti-VEGF, and 20 μg/mL AF488 were used. The assay was performed at room temperature with a 1 h sample incubation, 30 min secondary antibody incubation, 10 min AF488 incubation, 10 min wash with assay buffer, and a 10 min wash with TBS/Tween 20.

The results of these assays are shown in figure 2.4. PBS/PEG10k buffer was found to be the best of all the coatings tested, and therefore was used for all future experiments. The S/N was 2.1 times higher than that for the SEA block dynamic coating, which had the second highest S/N, and 5.9 times higher than that for the static PEG-silane coating. The PBS with PEG 200 and PEG 10k buffers were found to result in the lowest noise values and were among the assays with the lowest control signals. The chips using other blocking buffers had higher control bead signal intensities and higher noise values. This combination led to lower S/N ratios compared to that from the PBS/PEG10k blocking buffer.

Incubation Temperature

The effect of incubation temperature on assay performance was also investigated. According to Ekins' ambient analyte theory of immunoassay behavior, only a small fraction of the analyte molecules in solution are captured by their complementary antibodies for immunoassays in a microarray format.[43, 44] It has also been found that most microarray immunoassays exhibit kinetic limitations and are diffusion limited.[45] Some of the ways to overcome diffusional limitations in microarrays are to incorporate

stirring into the assay design, to decrease the size of the microspots, and to change the reaction conditions in order to increase the diffusion coefficients of the sample and reagents.[45] Since the size of the microspots for our assay is the size of the microspheres, decreasing their size is not an optimal solution. Many mixer designs have been developed for microfluidic chips, but incorporating a mixer would add complexity to the device in both design and operation.[46, 47] Changing the reaction conditions to affect the diffusion coefficient is much more easily done. The diffusion coefficient is directly proportional to temperature.[48] Performing the incubations at an elevated temperature should increase the diffusion coefficients and may produce increased signals if the immunoassay is diffusion limited.

Two different incubation temperatures were evaluated: room temperature (~25 °C) and 37 °C. 37 °C was evaluated because it is the normal human body temperature. Four chips were used to test each incubation temperature. For incubations at 37 °C, the chips were placed in a 37 °C oven. Wash steps were performed at room temperature for all of the chips. Reagent solutions were prepared in PBS/PEG10k buffer using VEGF as a model analyte. 500 pg/mL VEGF, 3 μg/mL anti-VEGF, and 20 μg/mL AF488 were used for this assay. The assay was performed with a 1 h sample incubation, 30 min secondary antibody incubation, 10 min AF488 incubation, 10 min wash with PBS/PEG10k buffer, and a 10 min wash with TBS/Tween 20. The average S/N for VEGF assays with incubations at 37 °C was ~33% higher than that for assays with incubations at room temperature. All future experiments used an incubation temperature of 37 °C.

Assay Step Elimination

Assay time is an important consideration for a POC device. If results are acquired while the patient is still at the doctor's office and treatment decisions based on those results can be made without the need for a follow-up visit, patient outcomes will improve for population groups that often do not return for their test results.[49-51] In order to decrease the total assay time and the complexity of the chip design, eliminating the first buffer wash with PBS/PEG10k was tested. VEGF was again used as the model analyte with all reagent concentrations and assay steps the same as above.

Eliminating the first buffer wash resulted in an ~98% increase in S/N over the original procedure. The increase may be due to less time for the antibody-antigen interactions to dissociate. The reactions between antibodies and antigens are in equilibrium, so if a complex dissociates during a wash step, it will not remain nearby and be recaptured by the antibody. Due to the increase in S/N from the elimination of the first wash step, it was eliminated from all future assays.

Incubation Time

Secondary antibody, sample, and AF488 incubation times were optimized individually with VEGF as the model analyte. Ideally, assay conditions would be optimized for each individual analyte. However, for the multiplexed bead array format, it is necessary to have a single incubation time for all analytes. It would not be possible to use a 30 min sample incubation for one analyte and a 60 min sample incubation for another analyte if the analytes are simultaneously measured with the same microarray. In this instance, VEGF was chosen as the cytokine for optimizing these parameters. Reagent concentrations of 500 pg/mL VEGF, 3 μg/mL anti-VEGF, and 20 μg/mL

AF488, and an incubation temperature of 37 °C were used for all incubation time optimization experiments. One chip was used to test each incubation time.

For secondary antibody incubation time optimization, the secondary antibody incubation time was varied from 1 to 60 min. A 1 h sample incubation, 10 min AF488 incubation, and 10 min wash with TBS/Tween 20 were used. The results are shown in figure 2.5A. As expected, an increase in S/N was observed with increasing incubation times, but without much improvement beyond 20 min. In addition to improving the overall results, the goal for the incubation time optimizations was to limit the total assay time to less than 1 h. In the interest of balancing sensitivity with total assay time, a 15 min secondary antibody incubation was used for all future assays. Although an assay was not performed with a 15 min incubation time, this was expected to deliver results nearly as high as the 20 min incubation time while allowing more time for the sample and AF488 incubations.

For sample incubation time optimization, the sample incubation time was varied from 1 to 120 min. A 15 min secondary antibody incubation, 10 min AF488 incubation, and a 10 min wash with TBS/Tween 20 were used. The results are shown in figure 2.5B. As expected, an increase in S/N was observed with increasing incubation times, but with less dramatic increases when the incubation time was longer than 20 min. With an increase from 10 min to 20 min the S/N increased 35%, but with an increase from 20 to 30 min the S/N only increased 13%. Although a large increase was observed at the 60 min incubation time, it was not present at 120 min. In order to balance the overall assay time with assay sensitivity, a 20 min sample incubation was used for all future assays.

For AF488, the incubation time was varied from 1 min up to 20 min, with a 20 min sample incubation, 15 min secondary antibody incubation, and a 10 min wash with TBS/Tween 20. Despite repeated attempts, no consistent trend in the S/N relative to AF488 incubation time was observed. For future assays the incubation time was therefore left at 10 min, the optimal AF488 incubation time found for the microspheres at Tufts University. These incubation time optimizations, along with the elimination of the first wash step, resulted in a reduction of total assay time from 2 h down to 55 min, less than half the original length of time.

Reagent Concentration

Secondary antibody and AF488 concentrations were optimized individually with VEGF as the model analyte. The secondary antibody concentration should be optimized individually for each analyte, but, as with incubation times, the same concentration of AF488 must be used by all analytes measured in the same bead array. The reagent concentration optimization assays were performed with a 20 min sample incubation, 15 min secondary antibody incubation, 10 min AF488 incubation, and a 10 min TBS/Tween 20 wash, an incubation temperature of 37 °C, and a sample concentration of 500 pg/mL VEGF. One chip was used to test each reagent concentration.

For secondary antibody concentration optimization, 0.5, 1, 2, 3, and 4 μg/mL anti-VEGF solutions were tested. An AF488 concentration of 20 μg/mL was used. The results are shown in figure 2.6A. An initial increase in S/N is observed as the secondary antibody concentration is increased from 0.5 μg/mL to 2 μg/mL with no clear trend at higher concentrations, indicating that the greatest binding of secondary antibody to the antibody-antigen complex occurs at relatively low concentrations. Since significant

increases in background signal or noise were not seen at high concentrations, the secondary antibody concentration was left at 3 μg/mL for future assays in case larger antigen concentrations should require more secondary antibody.

For AF488 optimization, the AF488 concentration was varied from 0.5 μg/mL up to 40 μg/mL. A secondary antibody concentration of 3 μg/mL was used. The results are shown in figure 2.6B. As expected, the S/N increases with increasing AF488 concentration. As the concentration of AF488 increases, the likelihood of non-specific binding of the dye also increases, increasing background signal and noise. The error was also much greater for the assay at the highest concentration, 40 μg/mL, so the AF488 concentration was left at 20 μg/mL for future assays.

Limit of Detection

Limits of detection (LOD) were determined for VEGF and IL-8 in buffer and saliva supernatant solutions using the optimized conditions listed in table 2.1. The range of sample concentrations for the studies was 1 pg/mL up to 500 pg/mL. Each concentration was tested with one chip. The S/N results were fit to the following 4-parameter logistics equation[11] where y is the S/N and x is the analyte concentration. This

$$y = d + \frac{a - d}{1 + \left(x/c\right)^b}$$

equation was then used to find the theoretical LOD at a S/N of 3. The results for VEGF in buffer are shown in figure 2.7.

The results of the LOD studies are shown in table 2.2. The LOD for VEGF and IL-8 in buffer were found to be 0.3 and 2.5 pg/mL, or 15 and 150 fM, respectively. The LODs were 1.2 and 3.9 pg/mL, or 130 and 500 fM, for VEGF and IL-8 respectively in

saliva supernatant. The higher LODs in saliva supernatant are probably due to increased non-specific binding seen with the saliva samples, likely from the presence of mucins and other glycoproteins in the saliva matrix. For VEGF, ELISA kits can be purchased with ranges extending down to ~100 fM (Thermo Scientific, Rockford, IL). Reported concentrations of VEGF in saliva range from 10-100 pM for healthy individuals to 5-170 pM in asthmatic patients.[29, 52] The theoretical LOD for VEGF using this assay is well below that, even in saliva supernatant. For IL-8, ELISA kits can be purchased with ranges extending down to ~3 pM (Thermo Scientific, Rockford, IL). Reported concentrations of IL-8 in saliva vary from 29-125 pM for healthy individuals, 85-390 pM for oral cancer patients, and 20-130 pM for patients with burning mouth syndrome.[7, 53-55] The theoretical LOD for IL-8 in saliva supernatant using this assay is well below those ranges. Since the LODs for VEGF and IL-8 are well below physiological levels, the decreased incubation times used to keep the total assay time under 1 h do not need to be increased.

2.4 Conclusions and Future Directions

The microsphere-based multiplexed immunoassay developed by the Walt group has been incorporated onto a microfluidic device that is easily fabricated and disposable. This is the first step in making a POC device to detect protein biomarkers in saliva samples. The microfluidic chips were designed with automation in mind, through a reader being developed by Ahura Scientific. Compatibility with a reader instrument led to the incorporation of separate reagent reservoirs, channels long enough to accommodate valves, and a long waste channel to prevent reader contamination. The chips were fabricated out of PDMS because it is optically transparent for fluorescence detection,

inexpensive compared to chips made of glass or silicon, and its flexibility means microspheres can be easily loaded into an array and the channels can be easily pinched closed for valving. Assay optimization was performed with VEGF as a model analyte, and LODs in buffer and saliva supernatant were found for both VEGF and another cytokine, IL-8.

Although my work on this microfluidic immunoassay chip did not continue any further, Patty Dennis, a postdoctoral associate in the Ramsey group, continued the work. One of her experiments investigated the shelf life of chips loaded with microspheres, another consideration for using the chips in a clinical setting. Chips were successfully stored for 48 days, so clinicians may be able to keep more than a month's supply of chips on hand. A new molding strategy has also been developed that uses deep reactive-ion etching (DRIE) to etch silicon wafers to make the master molds. This eliminates the need to FIB mill the microwell arrays and to make complementary PDMS molds, greatly simplifying the chip fabrication.

One of the biggest problems with the continuing development of this chip has been the antibody-coupled microspheres used to make the microarray. The batch of microspheres used for the experiments described in this chapter was exhausted soon after the experiments were completed. Subsequent batches produced results greatly inferior to those seen with the original batch, even after reoptimizing the assay conditions. Work eventually continued with microspheres that do not perform as well, but are the best available. Chips are currently being sent to Tufts University for testing with the reader instrument and to be loaded with beads and sent on to clinicians for real-world testing.

The Walt group has successfully used the chips to perform a multiplexed immunoassay with 8 analytes (data not published).

2.5 Tables and Figures

Table 2.1. Optimized conditions for microfluidic bead-based immunoassays.

Condition	Optimized Value
Incubation Temperature	37 °C
Sample Incubation Time	20 min
Secondary Antibody Concentration	3 μg/mL
Secondary Antibody Incubation Time	15 min
AF488 Concentration	20 μg/mL
AF488 Incubation Time	10 min
TBS/Tween 20 Wash Time	10 min

Table 2.2. Theoretical limits of detection for individual cytokines in buffer and saliva. Assays were performed using the optimized assay conditions listed in table 2.1.

Cytokine	Limit of detection in buffer		Limit of detection in saliva supernatant	
	pg/mL	fM	pg/mL	fM
VEGF	0.3	15	2.5	130
IL-8	1.2	150	3.9	500

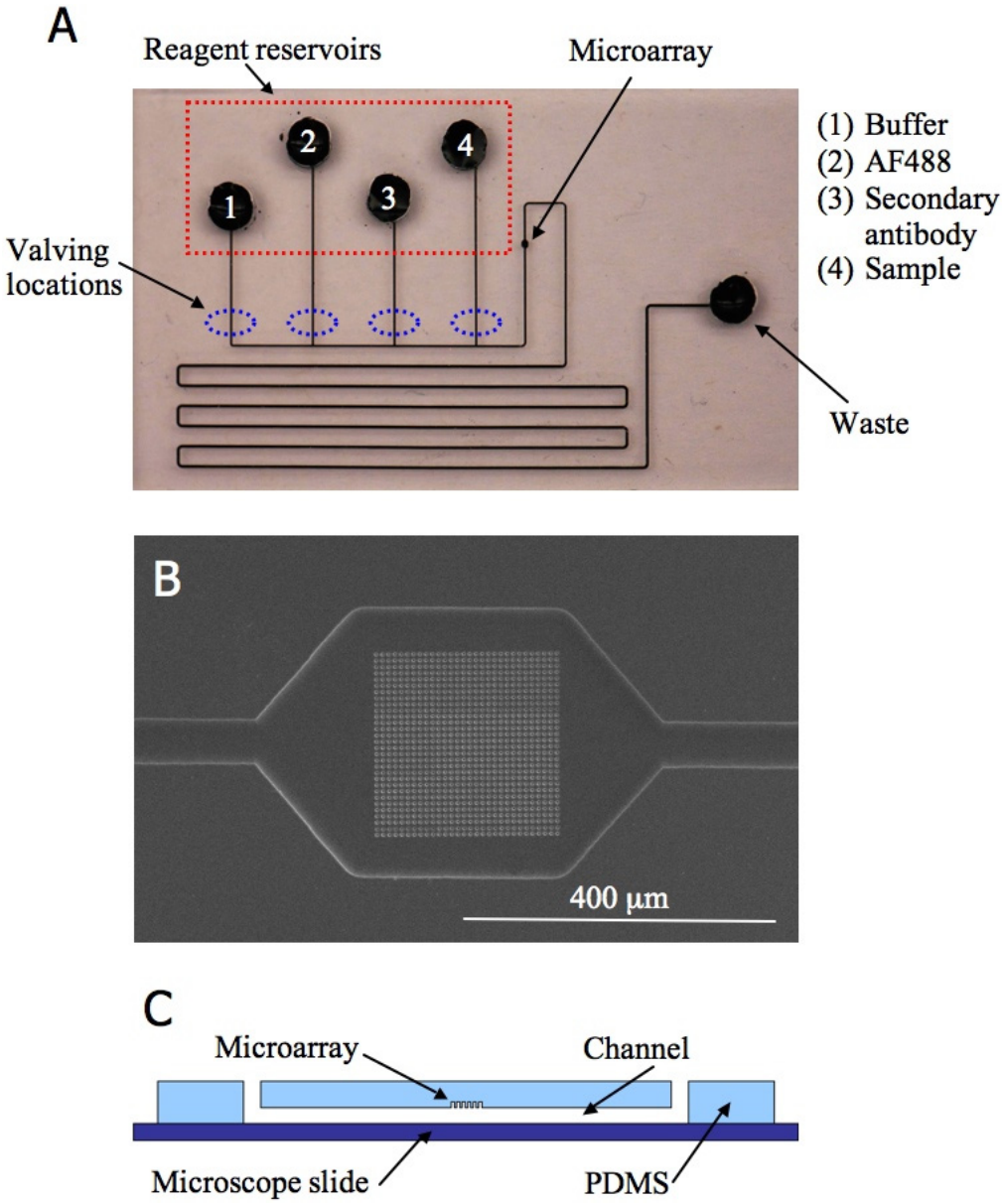

Figure 2.1. An image of the immunoassay chip (A), an SEM image of an FIB milled array (B), and a schematic of the cross-section of a chip (C). The reservoirs in (A) are 3 mm in diameter. The schematic (C) is not to scale.

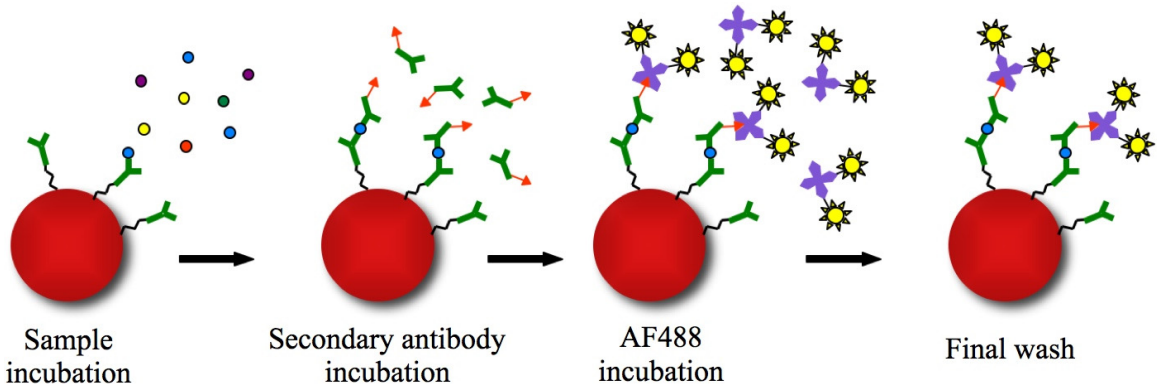

Figure 2.2. Schematic of the sandwich assay used with the Walt group microspheres. The antibody-functionalized microspheres are incubated with sample and the antibodies on the beads capture the target analytes. Biotinylated secondary antibodies bind to the antigen-antibody complex, forming a sandwich. The streptavidin in the AF488 binds to the biotin on the secondary antibodies, fluorescently labeling the sandwich. The excess AF488 is then washed away and the signal can be measured with fluorescence detection.

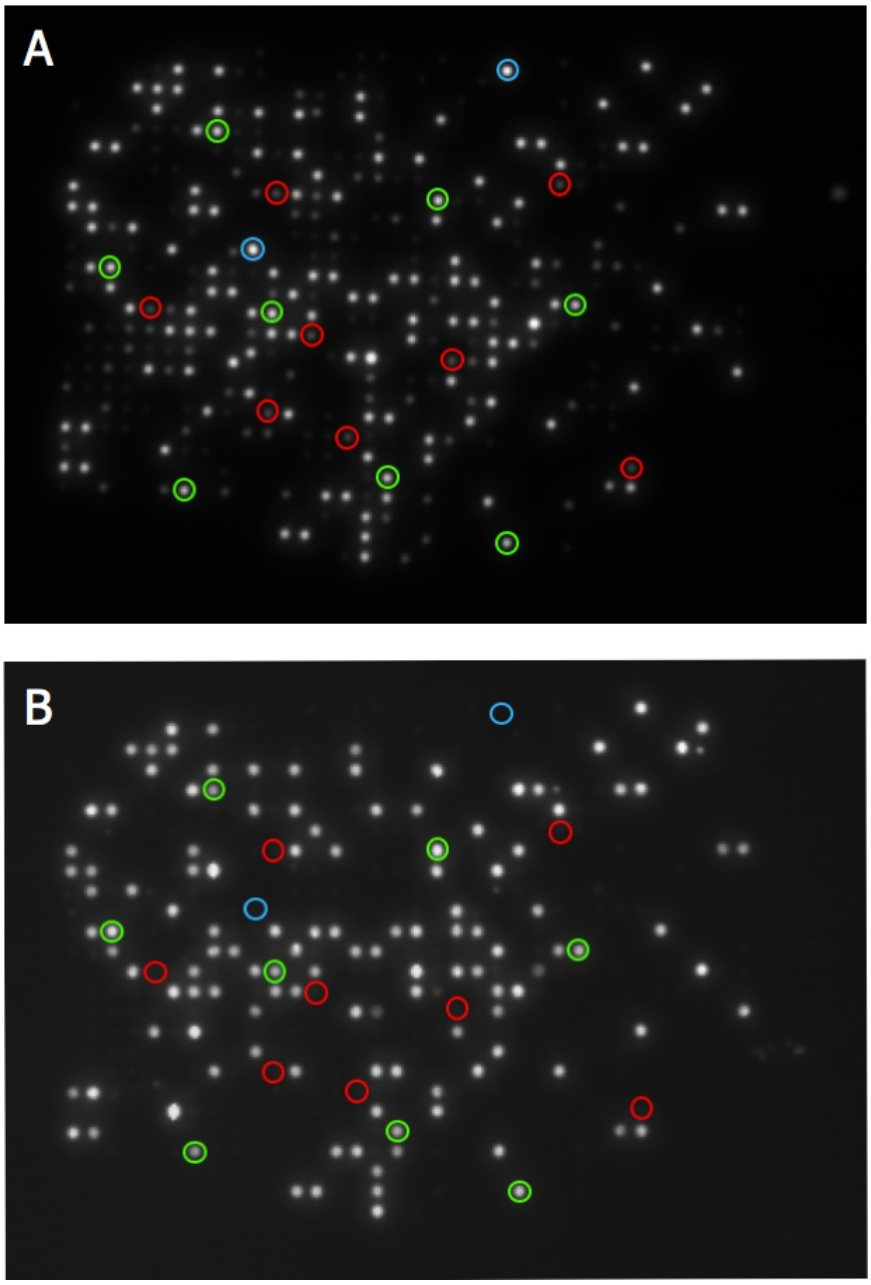

Figure 2.3. Example (A) encoding and (B) assay images from a VEGF assay. Selected VEGF microspheres are circled in green, selected IL-8 microspheres are circled in red, and two false negative VEGF microspheres are circled in blue.

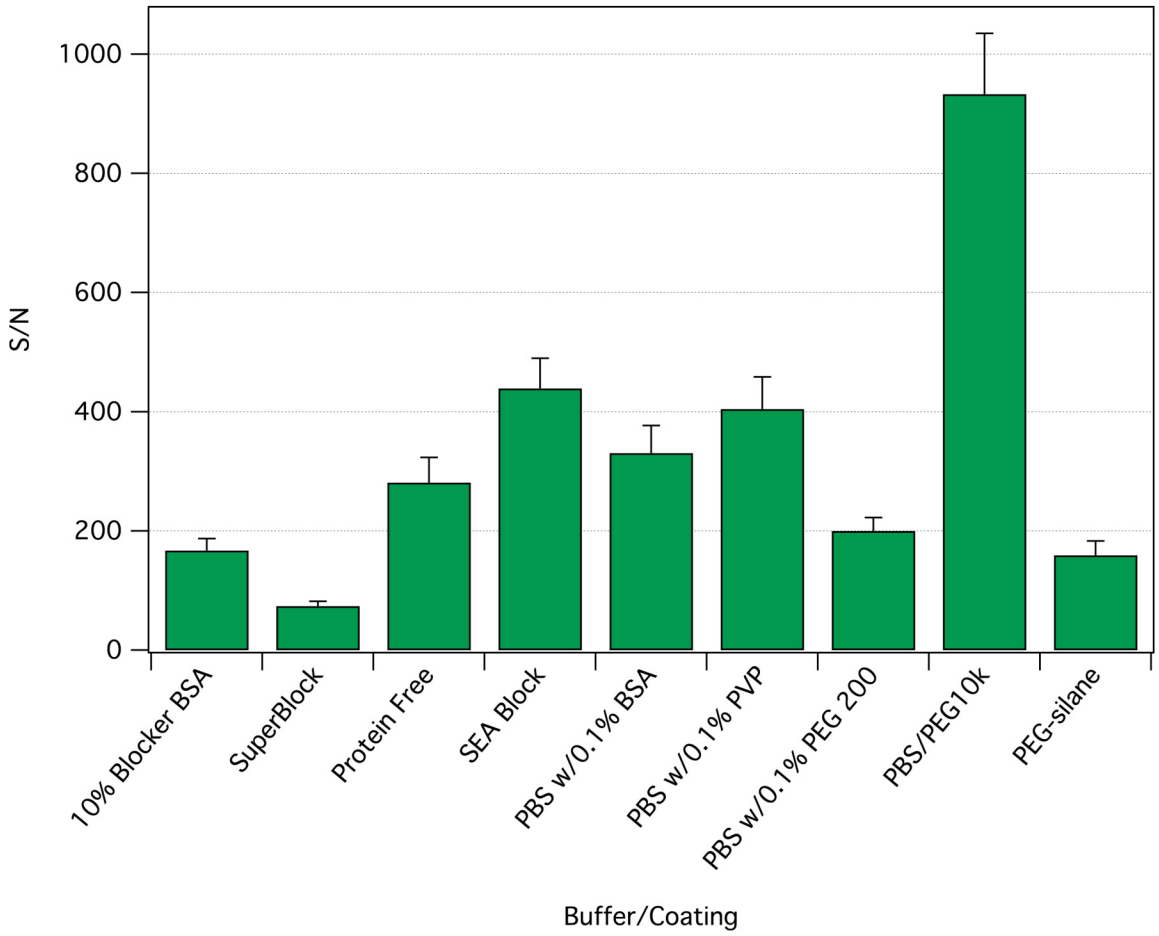

Figure 2.4. Results of assays comparing eight different dynamic coatings and a silane coating. The superior performance of PBS/PEG10k led to it being used for all future assays. Error bars indicate the bead-to-bead variation within an array.

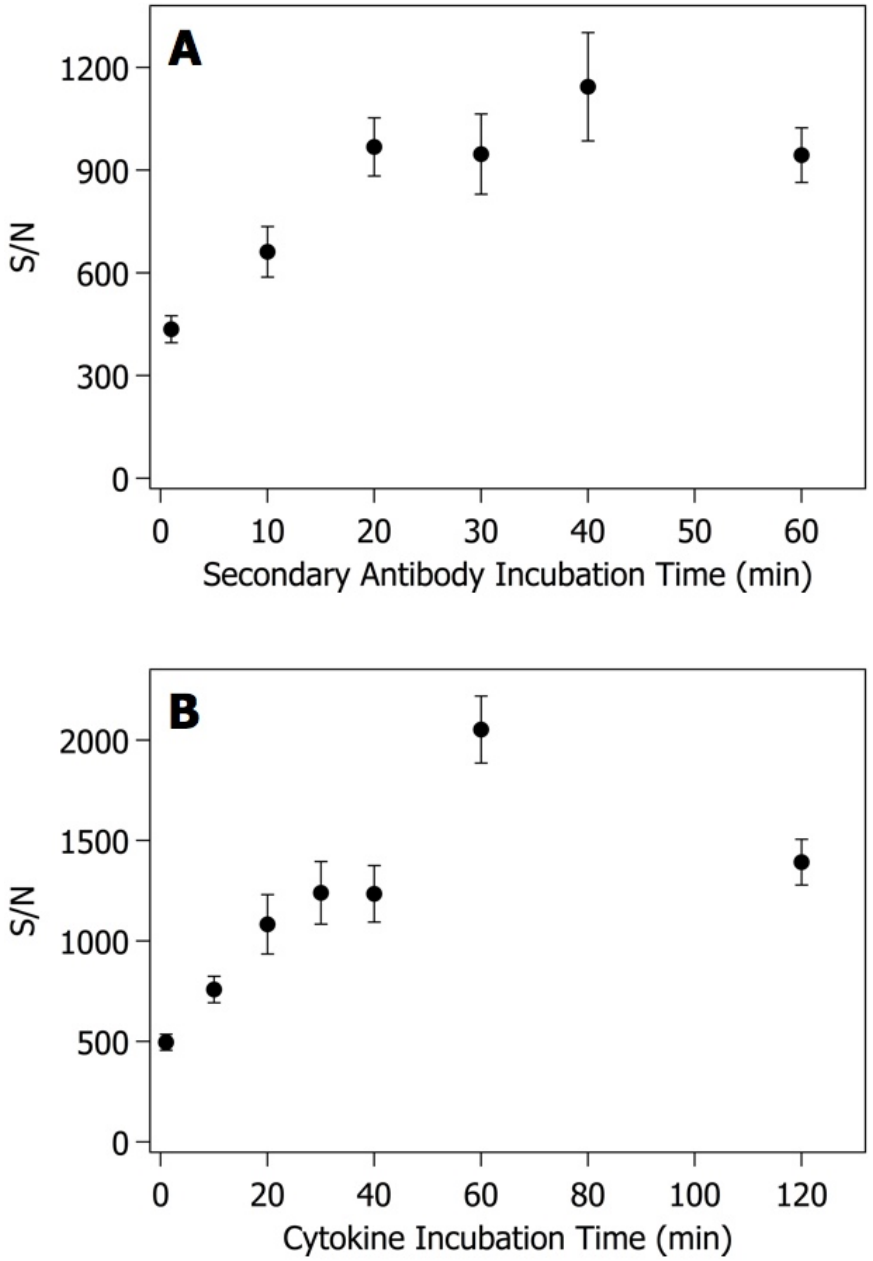

Figure 2.5. Results of (A) secondary antibody and (B) cytokine incubation time optimization for VEGF. Based on these results, a 15 min secondary antibody incubation and 20 min sample incubation time were used for all future assays. Error bars indicate bead-to-bead variation within an array.

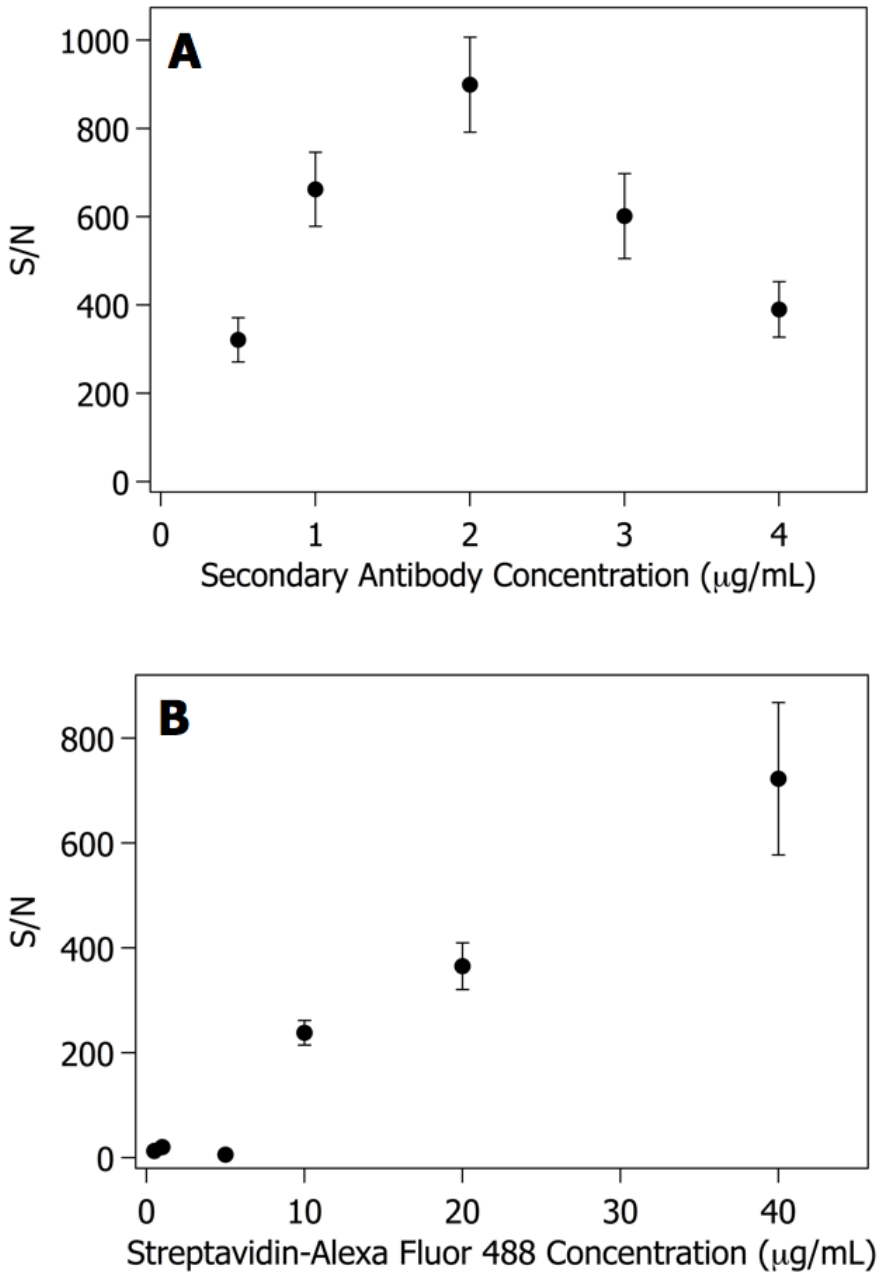

Figure 2.6. Results of (A) secondary antibody and (B) AF488 concentration optimization for VEGF. Based on these results, 3 μg/mL secondary antibody and 20 μg/mL AF488 solutions were used for all future assays. Error bars indicate bead-to-bead variation within an array.

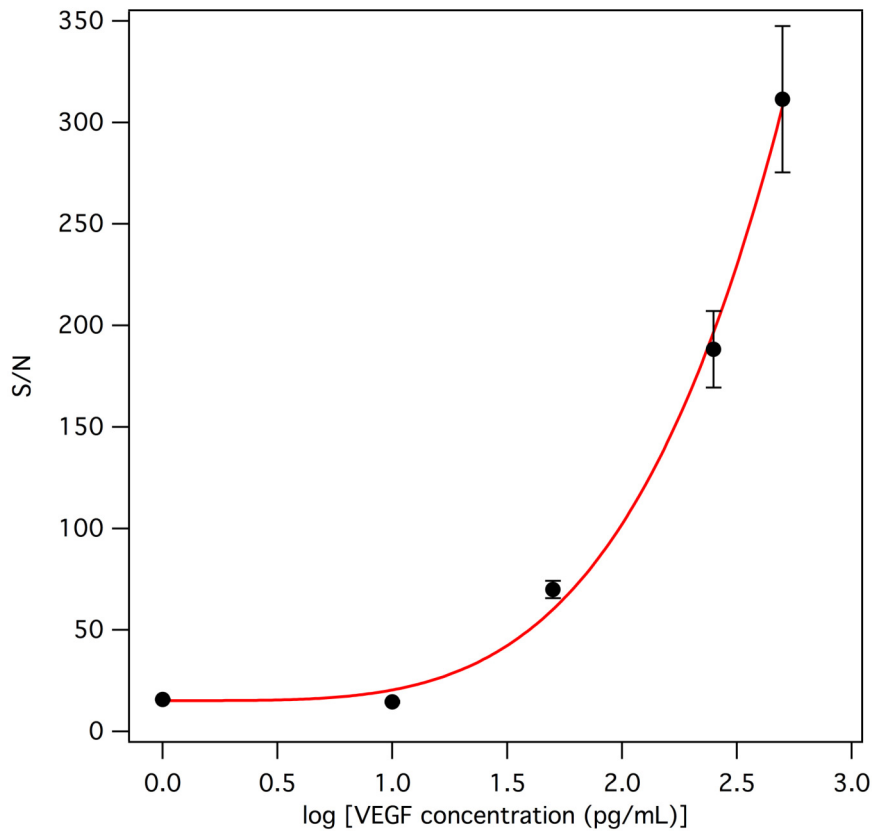

Figure 2.7. Results of the limit of detection determination for VEGF in buffer. The theoretical limit of detection is 15 fM. The limits of detection for VEGF in saliva supernatant as well as those for IL-8 in buffer and saliva supernatant are shown in table 2.3. Error bars indicate bead-to-bead variation within an array.

2.6 References

1. Bange, A.; Halsall, H. B.; Heineman, W. R., Microfluidic immunosensor systems. *Biosensors & Bioelectronics* 2005, *20*, (12), 2488-2503.

2. Henares, T. G.; Mizutani, F.; Hisamoto, H., Current development in microfluidic immunosensing chip. *Analytica Chimica Acta* 2008, *611*, (1), 17-30.

3. Sia, S. K.; Whitesides, G. M., Microfluidic devices fabricated in poly(dimethylsiloxane) for biological studies. *Electrophoresis* 2003, *24*, (21), 3563-3576.

4. Kricka, L. J.; Wild, D., Lab-on-a-chip, Micro-, and Nanoscale Immunoassay Systems. In *The Immunoassay Handbook*, 3rd ed.; Wild, D., Ed. Elsevier: New York, NY, 2005; pp 294-309.

5. Spisák, S.; Guttman, A., Biomedical Applications of Protein Microarrays. *Current Medicinal Chemistry* 2009, *16*, (22), 2806-2815.

6. Kricka, L. J.; Wild, D., Signal Generation and Detection Systems (Excluding Homogeneous Assays). In *The Immunoassay Handbook*, 3rd ed.; Wild, D., Ed. New York, NY: 2005; pp 192-211.

7. Tan, W.; Sabet, L.; Li, Y.; Yu, T.; Klokkevold, P. R.; Wong, D. T.; Ho, C.-M., Optical protein sensor for detecting cancer markers in saliva. *Biosensors & Bioelectronics* 2008, *24*, (2), 266-271.

8. Liu, C.; Qiu, X.; Ongagna, S.; Chen, D.; Chen, Z.; Abrams, W. R.; Malamud, D.; Corstjens, P. L. A. M.; Bau, H. H., A timer-actuated immunoassay cassette for detecting molecular markers in oral fluids. *Lab on a Chip* 2009, *9*, (6), 768-776.

9. MacBeath, G., Protein microarrays and proteomics. *Nature Genetics* 2002, *32*, (4S), 526-532.

10. Urbanowska, T.; Mangialaio, S.; Zickler, C.; Cheevapruk, S.; Hasler, P.; Regenass, S.; Legay, F., Protein microarray platform for the multiplex analysis of biomarkers in human sera. *Journal of Immunological Methods* 2006, *316*, (1-2), 1-7.

11. Derveaux, S.; Stubbe, B. G.; Roelant, C.; Leblans, M.; De Geest, B. G.; Demeester, J.; De Smedt, S. C., Layer-by-Layer Coated Digitally Encoded Microcarriers for Quantification of Proteins in Serum and Plasma. *Analytical Chemistry* 2008, *80*, (1), 85-94.

12. Hartmann, M.; Schrenk, M.; Döttinger, A.; Nagel, S.; Roeraade, J.; Joos, T. O.; Templin, M. F., Expanding Assay Dynamics: A Combined Competitive and Direct Assay System for the Quantification of Proteins in Multiplexed Immunoassays. *Clinical Chemistry* 2008, *54*, (6), 956-963.

13. Silzel, J. W.; Cercek, B.; Dodson, C.; Tsay, T.; Obremski, R. J., Mass-sensing, multianalyte microarray immunoassay with imaging detection. *Clinical Chemistry* 1998, *44*, (9), 2036-2043.

14. Wolf, M.; Juncker, D.; Michel, B.; Hunziker, P.; Delamarche, E., Simultaneous detection of C-reactive protein and other cardiac markers in human plasma using micromosaic immunoassays and self-regulating microfluidic networks. *Biosensors & Bioelectronics* 2004, *19*, (10), 1193-1202.

15. Derveaux, S.; Stubbe, B. G.; Braeckmans, K.; Roelant, C.; Sato, K.; Demeester, J.; De Smedt, S. C., Synergism between particle-based multiplexing and microfluidics technologies may bring diagnostics closer to the patient. *Analytical and Bioanalytical Chemistry* 2008, *391*, (7), 2453-2467.

16. Rissin, D. M.; Walt, D. R., Duplexed sandwich immunoassays on a fiber-optic microarray. *Analytica Chimica Acta* 2006, *564*, (1), 34-39.

17. Szurdoki, F.; Michael, K. L.; Walt, D. R., A duplexed microsphere-based fluorescent immunoassay. *Analytical Biochemistry* 2001, *291*, (2), 219-228.

18. Barbee, K. D.; Hsiao, A. P.; Roller, E. E.; Huang, X., Multiplexed protein detection using antibody-conjugated microbead arrays in a microfabricated electrophoretic device. *Lab on a Chip* 2010, *10*, (22), 3084-3093.

19. Thompson, J. A.; Du, X.; Grogan, J. M.; Schrlau, M. G.; Bau, H. H., Polymeric microbead arrays for microfluidic applications. *Journal of Micromechanics and Microengineering* 2010, *20*, (11), 115017.

20. Thompson, J. A.; Bau, H. H., Microfluidic, bead-based assay: Theory and experiments. *Journal of Chromatography B* 2010, *878*, (2), 228-236.

21. Diercks, A. H.; Ozinsky, A.; Hansen, C. L.; Spotts, J. M.; Rodriguez, D. J.; Aderem, A., A microfluidic device for multiplexed protein detection in nano-liter volumes. *Analytical Biochemistry* 2009, *386*, (1), 30-35.

22. Christodoulides, N.; Mohanty, S.; Miller, C. S.; Langub, M. C.; Floriano, P. N.; Dharshan, P.; Ali, M. F.; Bernard, B.; Romanovicz, D.; Anslyn, E.; Fox, P. C.; McDevitt, J. T., Application of microchip assay system for the measurement of C-reactive protein in human saliva. *Lab on a Chip* 2005, *5*, (3), 261-269.

23. Blicharz, T. M.; Siqueira, W. L.; Helmerhorst, E. J.; Oppenheim, F. G.; Wexler, P. J.; Little, F. F.; Walt, D. R., Fiber-Optic Microsphere-Based Antibody Array for the Analysis of Inflammatory Cytokines in Saliva. *Analytical Chemistry* 2009, *81*, (6), 2106-2114.

24. Deiss, F.; LaFratta, C. N.; Symer, M.; Blicharz, T. M.; Sojic, N.; Walt, D. R., Multiplexed Sandwich Immunoassays Using Electrochemiluminescence Imaging

Resolved at the Single Bead Level. *Journal of the American Chemical Society* 2009, *131*, (17), 6088-6089.

25. Epstein, J. R.; Walt, D. R., Fluorescence-based fibre optic arrays: a universal platform for sensing. *Chemical Society Reviews* 2003, *32*, (4), 203-214.

26. Ahn, S.; Walt, D. R., Detection of *Salmonella* spp. Using Microsphere-Based, Fiber-Optic DNA Microarrays. *Analytical Chemistry* 2005, *77*, (15), 5041-5047.

27. Konry, T.; Hayman, R. B.; Walt, D. R., Microsphere-Based Rolling Circle Amplification Microarray for the Detection of DNA and Proteins in a Single Assay. *Analytical Chemistry* 2009, *81*, (14), 5777-5782.

28. Walt, D. R., Bead-based fiber-optic arrays. *Science* 2000, *287*, (5452), 451-452.

29. Walt, D. R.; Blicharz, T. M.; Hayman, R. B.; Rissin, D. M.; Bowden, M.; Siqueira, W. L.; Helmerhorst, E. J.; Grand-Pierre, N.; Oppenheim, F. G.; Bhatia, J. S.; Little, F. F.; Brody, J. S., Microsensor arrays for saliva diagnostics. *Annals of the New York Academy of Sciences* 2007, *1098*, 389-400.

30. Henley, W. H.; Dennis, P. J.; Ramsey, J. M., Fabrication of Microfluidic Devices Containing Patterned Microwell Arrays. *Analytical Chemistry* 2012, *84*, (3), 1776-1780.

31. Edelstein, A.; Amodaj, N.; Hoover, K.; Vale, R.; Stuurman, N., Computer Control of Microscopes Using µManager. In *Current Protocols in Molecular Biology*, John Wiley & Sons, Inc.: 2001.

32. Rasband, W. S. ImageJ, U.S. National Institutes of Health, Bethesda, MD, USA. http://imagej.nih.gov/ij/, 1997-2011

33. Healy, M. J. R., Outliers in Clinical Chemistry Quality-Control Schemes. *Clinical Chemistry* 1979, *25*, (5), 675-677.

34. Bélanger, M.-C.; Marois, Y., Hemocompatibility, Biocompatibility, Inflammatory and *in Vivo* Studies of Primary Reference Materials Low-Density Polyethylene and Polydimethylsiloxane: A Review. *Journal of Biomedical Materials Research* 2001, *58*, (5), 467-477.

35. Brunner, C.; Ernst, K.-H.; Hess, H.; Vogel, V., Lifetime of biomolecules in polymer-based hybrid nanodevices. *Nanotechnology* 2004, *15*, (10), S540-S548.

36. Séguin, C.; McLachlan, J. M.; Norton, P. R.; Lagugné-Labarthet, F., Surface modification of poly(dimethylsiloxane) for microfluidic assay applications. *Applied Surface Science* 2010, *256*, (8), 2524-2531.

37. Sibarani, J.; Takai, M.; Ishihara, K., Surface modification on microfluidic devices with 2-methacryloyloxyethyl phosphorylcholine polymers for reducing

unfavorable protein adsorption. *Colloids and Surfaces B-Biointerfaces* 2007, *54*, (1), 88-93.

38. Sui, G.; Wang, J.; Lee, C.-C.; Lu, W.; Lee, S. P.; Leyton, J. V.; Wu, A. M.; Tseng, H.-R., Solution-phase surface modification in intact poly(dimethylsiloxane) microfluidic channels. *Analytical Chemistry* 2006, *78*, (15), 5543-5551.

39. Giordano, B. C.; Copeland, E. R.; Landers, J. P., Towards dynamic coating of glass microchip chambers for amplifying DNA via the polymerase chain reaction. *Electrophoresis* 2001, *22*, (2), 334-340.

40. McDonald, J. C.; Duffy, D. C.; Anderson, J. R.; Chiu, D. T.; Wu, H. K.; Schueller, O. J. A.; Whitesides, G. M., Fabrication of microfluidic systems in poly(dimethylsiloxane). *Electrophoresis* 2000, *21*, (1), 27-40.

41. Shin, Y. S.; Cho, K.; Lim, S. H.; Chung, S.; Park, S.-J.; Chung, C.; Han, D.-C.; Chang, J. K., PDMS-based micro PCR chip with parylene coating. *Journal of Micromechanics and Microengineering* 2003, *13*, (5), 768-774.

42. Kricka, L. J.; Wilding, P., Microchip PCR. *Analytical and Bioanalytical Chemistry* 2003, *377*, (5), 820-825.

43. Ekins, R. P., Ligand assays: from electrophoresis to miniaturized microarrays. *Clinical Chemistry* 1998, *44*, (9), 2015-2030.

44. Saviranta, P.; Okon, R.; Brinker, A.; Warashina, M.; Eppinger, J.; Geierstanger, B. H., Evaluating sandwich immunoassays in microarray format in terms of the ambient analyte regime. *Clinical chemistry* 2004, *50*, (10), 1907-1920.

45. Kusnezow, W.; Syagailo, Y. V.; Rüffer, S.; Baudenstiel, N.; Gauer, C.; Hoheisel, J. D.; Wild, D.; Goychuk, I., Optimal Design of Microarray Immunoassays to Compensate for Kinetic Limitations. *Molecular & Cellular Proteomics* 2006, *5*, (9), 1681-1696.

46. Reyes, D. R.; Iossifidis, D.; Auroux, P.-A.; Manz, A., Micro Total Analysis Systems. 1. Introduction, Theory, and Technology. *Analytical Chemistry* 2002, *74*, (12), 2623-2636.

47. Vilkner, T.; Janasek, D.; Manz, A., Micro Total Analysis Systems. Recent Developments. *Analytical Chemistry* 2004, *76*, (12), 3373-3386.

48. Berg, O. G.; von Hippel, P. H., Diffusion-Controlled Macromolecular Interactions. *Annual Review of Biophysics and Biophysical Chemistry* 1985, *14*, 131-160.

49. Hart, R. W.; Mauk, M. G.; Liu, C.; Qiu, X.; Thompson, J. A.; Chen, D.; Malamud, D.; Abrams, W. R.; Bau, H. H., Point-of-care oral-based diagnostics. *Oral Diseases* 2011, *17*, (8), 745-752.

50. Lee-Lewandrowski, E.; Lewandrowski, K., Perspectives on Cost and Outcomes for Point-of-Care Testing. *Clinics in Laboratory Medicine* 2009, *29*, (3), 479-489.

51. Pothier, K.; Kirtland, M.; Gupta, S., Has Point-of-Care Come of Age? *Point of Care* 2010, *9*, (3), 147-150.

52. Taichman, N. S.; Cruchley, A. T.; Fletcher, L. M.; Hagi-Pavli, E. P.; Paleolog, E. M.; Abrams, W. R.; Booth, V.; Edwards, R. M.; Malamud, D., Vascular Endothelial Growth Factor in Normal Human Salivary Glands and Saliva: A Possible Role in the Maintenance of Mucosal Homeostasis. *Laboratory Investigation* 1998, *78*, (7), 869-875.

53. Arellano-Garcia, M. E.; Hu, S.; Wang, J.; Henson, B.; Zhou, H.; Chia, D.; Wong, D. T., Multiplexed immunobead-based assay for detection of oral cancer protein biomarkers in saliva. *Oral Diseases* 2008, *14*, (8), 705-712.

54. St. John, M. A. R.; Li, Y.; Zhou, X.; Denny, P.; Ho, C.-M.; Montemagno, C.; Shi, W.; Qi, F.; Wu, B.; Sinha, U.; Jordan, R.; Wolinsky, L.; Park, N.-H.; Liu, H.; Abemayor, E.; Wong, D. T. W., Interleukin 6 and interleukin 8 as Potential Biomarkers for Oral Cavity and Oropharyngeal Squamous Cell Carcinoma. *Archives of Otolaryngology - Head & Neck Surgery* 2004, *130*, (8), 929-935.

55. Suh, K.-I.; Kim, Y.-K.; Kho, H.-S., Salivary levels of IL-1β, IL-6, IL-8, and TNF-α in patients with burning mouth syndrome. *Archives of Oral Biology* 2009, *54*, (9), 797-802.

CHAPTER 3

MICROFLUIDIC PCR CHIP INCORPORATING DNA EXTRACTION

3.1 Introduction

Many different microfluidic devices to perform PCR amplification have been developed. The level of integration of the microfluidic device affects which substrate materials are used. For example, if a capillary electrophoresis (CE) separation is to be integrated on-chip then the materials need to be CE compatible. If optical detection will be used, than the chip materials, at least in the detection region, need to be optically transparent. Materials, including silicon, glass, PDMS, polycarbonate, and other polymers have been reported, though some are better suited to PCR than others.[1, 2] Silicon has a high thermal conductivity that makes rapid thermocycling possible; however, its opacity limits detection options in a fully integrated system.[2, 3] The optical transparency of glass makes highly sensitive fluorescence detection possible, and its electrical insulation properties allow coupling to a CE separation step for analysis of the PCR products.[2, 3] However, both silicon and native glass surfaces can inhibit PCR.[2-4] Additionally, glass and silicon devices can be expensive to manufacture, often making disposable chips produced from these materials impractical.[3, 5-7] Polymeric devices have consequently become more common.[6, 7] PDMS chips are easily fabricated on a prototype scale, are optically transparent, and are more compatible with PCR than silicon or glass.[3, 7] Lower fabrication costs make PDMS chips readily disposable, reducing cross-

contamination risks.[6] Hybrid devices, containing two or more materials, are often used to exploit the benefits of one material and to offset the drawbacks of another.[8-11]

The level of integration will also affect the degree of interaction a user has with the device. For a true sample-in answer-out microfluidic device, the sample preparation and reagent delivery steps must be integrated onto the device.[5, 12-14] For a PCR device, a critical step in the sample preparation is extracting DNA from the sample.[15, 16] Many chip designs have been described that integrate sample preparation and PCR onto the same device. Sample preparation steps usually include both cell lysis to release the DNA from the nucleus of the cell and DNA extraction to separate the DNA from sample components that may inhibit PCR. Some chip designs only integrate cell lysis with PCR and perform amplification without the extraction step.[17-19] This is sufficient for samples with no PCR inhibitors, but most clinical samples, including saliva, contain a wide variety of PCR inhibitors such as proteases and DNase and require an extraction step.[20] In another strategy, antibody-functionalized beads were used to capture target cells and separate them from the rest of the sample.[21] Cell lysis was then performed in the PCR chamber without a DNA extraction step. This may sufficiently remove PCR inhibitors for some samples, but analysis for more than one species would require antibody-functionalized beads for each target, making the addition of new species difficult. Several chip designs have been described that use silica-based separations or magnetic beads for extraction.[22-26] Silica and some magnetic beads are strong PCR inhibitors, so the DNA must be eluted before downstream amplification, often with ethanol, another strong PCR inhibitor.[15, 27-30]

Aluminum oxide membranes (AOMs) are an alternative to silica and magnetic beads for DNA extraction. AOMs are rigid membranes made of a highly ordered alumina matrix with porosities of 25-50%. They are commercially available with highly monodisperse pore sizes of either 20, 100, or 200 nm. They have previously been used to extract λ-DNA, gDNA from lysed whole human blood samples, gDNA from lysed bacteria cells grown in culture, and viral DNA from cerebrospinal fluid samples.[27, 28, 31-34] Unlike silica-based DNA extractions, PCR of extracted DNA has been performed directly on AOMs with no need for an elution step.[27, 31, 33] This is possible because PCR master mixes have a basic pH and are able to release the DNA bound to the membrane, freeing it for amplification.[28] Polymerase will adsorb to the surface of the AOM, and so devices with large regions of exposed AOM may require the addition of BSA and additional *Taq* polymerase to the reaction mixture to minimize inhibition.[33]

In this chapter the development of a microfluidic device to perform DNA extraction and PCR of bacterial DNA targets for POC diagnosis of respiratory infections is described. The DNA extraction is performed with AOMs integrated into a PDMS/glass hybrid chip with polypropylene reservoirs to form PCR chambers. Both the extraction and amplification steps were initially developed off-chip in PCR tubes and later integrated and tested on-chip with purified DNA. The amplification step was first developed using λ-DNA and then bacterial gDNA. *Haemophilus influenzae, Staphylococcus aureus, Streptococcus mitis, Streptococcus mutans, Streptococcus pneumoniae,* and *Streptococcus salivarius* were used as model organisms.

The initial goal of this work was to multiplex the PCR and simultaneously test for many different organisms by using broad range primers. Standard PCR primers are

specific to their intended target, so multiplexing with standard primers requires a unique primer set for each organism or gene. Performing multiplex PCR with many sets of unique primers in the same reaction is difficult. Overlapping primers can produce dimers, reducing target amplification, other non-specific interactions between primers can also prevent amplification, and incompatible cycling temperatures can result in amplification failure for one or more of the targets.[35, 36] In contrast, broad-range PCR primers are for highly conserved sequences of DNA, usually in genes that encode for essential molecules.[37, 38] The conserved sequences are the same across multiple species, but the amplicons include highly variable regions that can be used to identify bacterial species.[37, 39, 40] The presence of target organisms can then be determined through DNA hybridization assays targeting these variable regions.

Successful detection of the broad-range PCR amplicons was to be achieved using an array of oligonucleotide-functionalized microspheres similar to the array of antibody-functionalized microspheres described in Chapter 2. The Walt group has developed encoded microspheres functionalized with oligonucleotide probes that can be used to capture amplicons from PCR.[41-48] The PCR products are hybridized to the oligonucleotide array and detected via fluorescence. Biotinylated primers and AF488 can be used to take advantage of the biotin-streptavidin linkage for detection as in Chapter 2, or the primers can be directly labeled with fluorescent tags to generate labeled amplicons and decrease the complexity of the hybridization assay.

3.2 Materials and Methods

Materials and Reagents

PCR tubes (200 μL) were obtained from Eppendorf (Hauppauge, NY). AOMs (13 mm diameter, 60 μm thickness, and 0.2 μm pores) were obtained from Whatman (Piscataway, NJ). Luer Lok syringes (5 mL) were obtained from BD (Franklin Lakes, NJ). O-rings (7/32" inner diameter, 11/32" outer diameter) were purchased from Parker Nitrile (Cleveland, OH). Biopsy punches with 1 and 3 mm diameters were obtained from Miltex (York, PA) and Sklar Instruments (West Chester, PA), respectively. Sylgard 184 (PDMS) was obtained from Dow Corning (Midland, MI). PDMS was prepared following the manufacturer's recommendation with a 10:1 polymer to cross-linker ratio. Silicon wafers were purchased from Silicon Quest International (San Jose, CA). ELIMINase cleaner was obtained from Decon Labs, Inc. (King of Prussia, PA). HotStarTaq polymerase, PCR buffer, and $MgCl_2$ were purchased from Qiagen Sciences, Inc. (Germantown, MD). dNTPs were purchased from Stratagene (Cedar Creek, TX). Purified λ-DNA was purchased from Promega (Madison, WI). Red food coloring was purchased from Market Pantry, Target Corp. (Minneapolis, MN). Purified gDNA from *H. influenzae* (ATCC 51907), *S. aureus* (ATCC 25923), *S. mitis* (ATCC 49456), *S. mutans* (ATCC 25175), *S. pneumoniae* (ATCC 33400), *S. salivarius* (ATCC 9759), *Actinomyces naeslundii* (ATCC 12104), *Capnocytophaga gingivalis* (ATCC 33624), *Prevotella melaninogenica* (ATCC 25845), and *Veillonella parvula* (ATCC 10790) was purchased from ATCC (Manassas, VA). Custom primers for λ-DNA and bacterial targets, 20x RNase free Tris-EDTA (TE) buffer, streptavidin-Alexa Fluor® 488 (AF488) conjugate, and a ULYSIS® Alexa Fluor® 488 nucleic acid labeling kit were purchased

from Invitrogen (Carlsbad, CA). Purified gDNA and custom primers were resuspended following the instructions provided by their respective manufacturers. Resistance temperature detectors (RTDs) with 100 Ω resistance (F3102) were purchased from Omega Engineering, Inc. (Stamford, CT). PEG with an average molecular weight of 10,000 g/mol (PEG 10k) was obtained from Alfa Aesar (Ward Hill, MA). DNase, RNase, and protease free water, PVP with an average molecular weight of 10,000 g/mol, saline sodium citrate (SSC) buffer (20x concentrate), and 20% sodium dodecyl sulfate solution (SDS) were purchased from Sigma-Aldrich (St. Louis, MO). Microcentrifuge tubes (0.6 mL), sodium chloride (NaCl), glass cover slips (20 mm x 35 mm, 150 μm thick), isopropanol, Blocker BSA (10%) in PBS, DNase and RNase free mineral oil, Lyse-N-Go PCR reagent, PBS Starting Block blocking buffer, TBS Starting Block blocking buffer, and 1% (w/v) blocker casein in TBS were purchased from Thermo Fisher Scientific (Waltham, MA). Unless otherwise noted, dilutions were performed using DNase, RNase, and protease free water.

Tube-Mounted AOMs

Tube-mounted AOMs were used for initial DNA extraction experiments. They were made by cutting the bottom 2-3 mm off of a 200 μL PCR tube, heating an AOM on a hotplate to 185 °C, and then pressing the cut end of the PCR tube onto the AOM for 10-20 s until they were hermetically bonded. Excess AOM was trimmed away after bonding. Each 13 mm AOM could be used to make 3 or 4 tube-mounted AOMs. An image of a tube-mounted AOM is shown in figure 3.1.

DNA extraction experiments were performed by filtering DNA solutions through tube-mounted AOMs. An empty 5 mL syringe fitted with a suction cup was used to

apply pressure to the top of the tube-mounted AOM and push sample solutions through into a larger 0.6 mL microcentrifuge tube. The DNA concentration of each solution was measured using a NanoDrop 2000 micro-volume UV/Vis Spectrophotometer (NanoDrop Technologies, Wilmington, DE) before and after filtration. The default double-stranded DNA settings were used for measurements, reporting a nucleic acid concentration based on absorbance at 260 nm and the Beer-Lambert equation. The average of three measurements was used to calculate the DNA concentration. The amount of DNA captured on the AOM was calculated from the difference between the concentrations measured before and after filtration.

Some samples were forced through the AOM using centrifugation or vacuum. For centrifuge filtration, the tube-mounted AOM was put into a 0.6 mL microcentrifuge tube, the sample solution was added, and the nested tubes were centrifuged for 5 min at 900 rpm. For vacuum filtration, an o-ring was fitted around the top rim of the tube-mounted AOM and it was nested into a 0.6 mL microcentrifuge tube with an access hole in the side for applying vacuum. After sample addition into the tube-mounted AOM, vacuum was applied to the microcentrifuge tube, filtering the sample through the AOM.

The feasibility of preloading primers onto the AOM prior to DNA capture was tested using fluorescently labeled primers and a tube-mounted AOM. The primers were labeled with a ULYSIS labeling kit according to the kit instructions. The concentration of primers in solution after the labeling reaction was measured with the NanoDrop as before, but with the default settings for single-stranded DNA.

PCR Chip Design and Fabrication

The microfluidic chip consisted of three main parts: wells to hold sample and PCR solutions, the AOM to extract DNA, and a microfluidic channel and AOM support structure for fluid flow through the AOM. A variety of designs for the wells were tested. An image and schematic of the final design using sections of PCR tubes to form three reaction wells are shown in figure 3.2. The microfluidic chip base was composed of a PDMS layer with a channel bonded to a 150 μm thick glass cover slip. An 11 mm diameter region of microposts that supported the AOM for fluid flow was situated on the top of the PDMS layer. A 1 mm biopsy punch was used to make a hole through this 11 mm region and connect the micropost region to the fluidic channel underneath. A thin layer of PDMS (~0.5 mm thick) containing three holes, each made with a 3 mm biopsy punch, was affixed over the AOM using uncured PDMS. Sections of PCR tubes were also attached with uncured PDMS and positioned over the 3 mm holes atop the AOM to create the reaction wells.

A double-sided molding strategy was used to make the microfluidic base of the chip. To make the AOM supporting microposts, 15 arrays of approximately 75 μm diameter, 18 μm deep holes were etched into a silicon wafer using DRIE (Alcatel AMS 100 DRIE) with a low-roughness Bosch process. A secondary mold was cast in PDMS from this wafer and subsequently used to make a tertiary mold, also in PDMS, for chip manufacture. The tertiary mold was necessary because one side of the double-sided mold must be flexible for demolding of the chips. Another silicon wafer was etched to give 15 channels that were 300 μm wide, 1.6 cm long, and 30 μm high. Uncured PDMS (~10 mL) was spin-coated (Spincoater Model P6700, Specialty Coating Systems, Inc.,

Indianapolis, IN) onto this wafer at 750 rpm for 1 min, degassed under vacuum, and cured for 5 min at 150 °C. An additional 10 mL of uncured PDMS was spun onto the tertiary PDMS mold of the microposts at 550 rpm for 1 min and the micropost mold was mated to the PDMS layer on the silicon channel mold with the post regions aligned to the ends of the channels. The PDMS layer in the mold sandwich was degassed under vacuum and then cured for 15 min at 150 °C.

The casting was demolded, cut into individual chips with one channel and micropost region each, and excess PDMS was trimmed away. To connect the post region to the fluidic channel, 1 mm holes were punched, and 3 mm access holes for the waste reservoirs were also punched. The chips were washed on both sides with isopropanol and dried with N_2 gas. The glass cover slips were cleaned with ELIMINase and dried with N_2 gas prior to bonding. The chip was bonded to the cover slip by exposing both to atmospheric plasma for 12 s at 18 W in a Harrick plasma cleaner (model PDC-32G, Pleasantville, NY) and then pressing the two together with the channel side of the chip facing down onto the glass. After bonding, an AOM was placed over the micropost region. The underside of an ~15 mm diameter circle of ~0.5 mm thick PDMS with three 3 mm diameter holes was coated with a thin layer of uncured PDMS and placed over the AOM. PCR tubes with the bottoms and tops trimmed off, making hollow conical cylinders 8-9 mm high, were used as reservoirs. The larger ends of reservoirs were dipped in uncured PDMS and positioned over each of the holes in the PDMS layer above the AOM and above the waste access hole. The cover slip-PDMS-AOM-PDMS-reservoir sandwiches were heated to 95 °C for 15 min to cure the interstitial PDMS and complete chip fabrication. Chips were stored dry and at room temperature.

PCR Development

For on-chip DNA extraction, 20 μL of sample solution was added to each well and vacuum was applied to the waste reservoir until the entire sample had been pulled through the AOM, usually 5-10 min. Then 10 μL of PCR master mix containing 1x PCR buffer, 5 units HotStarTaq DNA polymerase, 3.5 mM $MgCl_2$, 200 μM of each dNTP, and 0.75% Blocker BSA, as well as 0.4 μM of each primer was added to each well. The PCR solution in each well and the waste reservoir was then covered with 25 μL of mineral oil. The master mix contained DNase, RNase, and protease free water dyed red with a small amount of food coloring to make the location and any evaporation of the PCR solution in the chip apparent. The chip was thermocycled using an Eppendorf Mastercycler Personal (Eppendorf, Hauppauge, NY) benchtop thermocycler with an aluminum plate made in-house to fit the thermocycler. The heated lid was not used for on-chip PCR. Prior to performing any on-chip PCR experiments, the temperature cycling of the aluminum plate was monitored with an RTD to verify that the thermocycling temperature profile. An image of the plate and a plot of a few temperature cycles are shown in figure 3.3. The thermocycling program used for on-chip experiments with bacterial gDNA was 15 min at 95 °C, 30 cycles of 45 s at 94 °C, 45 s at 56 °C, and 45 s at 72 °C, with a final extension step of 10 min at 72 °C. The PCR products were collected after thermocycling and stored in clean PCR tubes at 4 °C until analysis using an Agilent 2100 Bioanalyzer with DNA 1000 kits (Santa Clara, CA). The Bioanalyzer performs capillary gel electrophoretic separations of the PCR products to determine the size and concentration of the amplicons for up to twelve samples. PCR chips were discarded after thermocycling, and a new chip was used for each experiment.

PCR in tubes was performed using the Eppendorf thermocycler with the heated lid set to 105 °C. For bacterial gDNA experiments, the master mix and thermocycling program described above were used. For PCR of λ-DNA, the master mix consisted of 1x PCR buffer, 2.5 units HotStarTaq DNA polymerase, 2.0 mM $MgCl_2$, and 200 μM of each dNTP, as well as 0.2 μM of each primer. The thermocycling program was 15 min at 95 °C, 30 cycles of 30 s at 95 °C, 30 s at 54 °C, and 45 s at 72 °C, with a final extension step of 10 min at 72 °C. These PCR products were also analyzed with the Bioanalyzer.

λ-DNA was used for initial PCR development. Primers for a 294 bp region were designed using the OligoPerfect™ tool on the Invitrogen website and the λ-DNA sequence obtained from NCBI's GenBank (accession number J02459.1). Six species of bacteria were used as model organisms for PCR development. *H. influenzae, S. aureus,* and *S. pneumoniae* are all pathogenic bacteria while *S. mitis, S. mutans,* and *S. salivarius* are control organisms commonly found in the human mouth. Broad-range primers described by Roth, et. al., for an ~300 bp region of the *gyrB* gene that encodes for DNA gyrase, a protein that introduces negative supercoils in DNA, were used with bacterial gDNA.[37] The *gyrB* gene is highly conserved in the regions the primers are designed for, while more variable regions are found between the primers. Sequences for the λ-DNA and *gyrB* primers are listed in Table 3.1.

Microarray Hybridization Assays

Hybridization assays were performed with oligonucleotide probe-functionalized microspheres provided by the Walt group at Tufts University. A schematic of the microsphere-based hybridization assay is shown in figure 3.4 and the primer and probe sequences are listed in table 3.2. Chips similar to those developed for protein assays in

Chapter 2 were used. The microspheres average 4.5 μm in diameter so microarrays with 6 mm diameter wells were used to accommodate the larger beads. Chips were loaded with beads in the same manner described in Chapter 2, using PBS buffer with 0.1% PEG 10k. The probes on the beads targeted four model control organisms: *P. melaninogenica, C. gingivalis, A. naeslundii,* and *V. parvula*. The primers designed by the Walt group were biotinylated so that PCR products could be readily detected in the oligonucleotide array after reacting with fluorescently labeled streptavidin. The biotinylated amplicons hybridize to probes on the microspheres and a stringency wash removes nonspecifically bound DNA. Then AF488 forms a linkage with the biotin during a staining step. A final wash removes excess AF488, and the amplicons hybridized to the microspheres can be detected. PCR products for hybridization assays were generated with 50 μL tube-based PCR with 1 ng of purified gDNA as the template, 1x PCR buffer, 2.5 units HotStarTaq DNA polymerase, 1.5 mM $MgCl_2$, 200 μM of each dNTP, and 0.2 μM each of the appropriate forward and reverse primers with the following thermocycling program: 15 min at 95 °C, 35 cycles of 30 s at 95 °C, 30 s at 55 °C, and 30 s at 72 °C, with a final extension step of 10 min at 72 °C.

The Walt group hybridization assay protocol was adapted for use on a microfluidic chip. The PCR products were first denatured by incubating for 5 min at 95 °C and then chilled on ice for 1 min. All other steps in the hybridization assay were performed at room temperature. The denatured products were delivered to the bead arrays and incubated for 30 min. The arrays were next rinsed with the stringency wash solution (2x SSC, 0.2% SDS) for 2 min and then the general wash solution (0.5x SSC) for 1 min. The arrays were then incubated with blocking solution (1% blocker casein in

TBS) for 5 min followed by staining solution (2 μg/mL AF488 in blocker casein) for 10 min. The array was then rinsed with the general wash solution again for 1 min, dried with vacuum, and imaged using the same microscope setup, filters, and exposure times as described for the protein microarrays. The images were also analyzed in the same way.

3.3 Results and Discussion

DNA Extraction

DNA extraction by AOM was investigated using tube-mounted AOMs. Solutions of three different concentrations of λ-DNA (80 μg/mL, 40 μg/mL, and 20 μg/mL) were filtered through tube-mounted AOMs using pressure from a syringe. The sample size was 25 μL. Three replicates were performed at each concentration, as well as three blanks using water. The concentration of λ-DNA in the solutions before and after filtration through the AOM was measured, and the difference was used to calculate the amount of DNA captured. A greater percentage of DNA was captured from the samples with lower concentrations, but the total DNA captured at all three concentrations was similar (table 3.3). This suggests that the amounts of DNA used in this experiment exceeded the maximum amount of DNA that could be captured by the tube-mounted AOMs under these conditions. Due to variations in the fabrication, the exposed area of AOM will be slightly different for each AOM. This is likely the reason for deviations in the total amount of DNA captured.

Another experiment investigated the effect of the method used to effect fluid flow through the AOM on the amount of DNA captured. On a microfluidic chip, vacuum will be used to pull solutions through the AOM, so experiments using either a centrifuge or vacuum were undertaken. These techniques are more complex than the syringe method,

but it was important to verify that results from experiments with the syringe method would still be applicable to on-chip DNA extraction. Sample solutions of 40 μg/mL λ-DNA (25 μL each) were filtered through each AOM. Centrifugation was compared to the syringe method on one day and vacuum was compared to the syringe method on a second day. On each day, three replicates were performed for each filtration technique as well as three blanks. On the first day centrifugation was used with the blanks while on the second day the syringe method was used.

The results of these experiments are shown in table 3.4. Similar amounts of DNA were captured with the vacuum filtration method as with the syringe method, with no discernable difference observed between using the vacuum or the syringe. With a 10% greater percentage of DNA captured, the syringe method was found to be slightly better than using the centrifuge. It is unclear why there was a decrease in the amount of DNA captured for the centrifuge method. One possibility is that the forces in the centrifuge caused small cracks in the AOMs, allowing solutions to pass through the cracks instead of through the pores, therefore reducing the amount of DNA captured. There is also a great difference between the amounts of DNA captured with the syringe method between the two days. This may be due to the AOMs used on the first day (comparing syringe with centrifuge) being fabricated with a larger area of AOM exposed for filtration, day-to-day variations with the NanoDrop, or DNase contamination on the first day resulting in lower post-filtration DNA concentrations measured by the NanoDrop.

Kim and Gale have also described DNA extraction with AOMs and found that the amount of DNA captured increased with increasing NaCl concentration.[28] This effect was confirmed by performing a DNA capture experiment with 25 μL samples of 20

μg/mL λ-DNA solutions containing 0 mM, 100 mM, 300 mM, or 500 mM NaCl. Three replicates were performed at each concentration along with three blanks containing no DNA and 0 mM NaCl. The syringe method was used to filter solutions through the AOM. The results are shown in table 3.5. There was 100% DNA capture from the solutions containing additional NaCl while only 31% of the DNA was captured from the 0 mM solution. The 0 mM solution is the same as the 20 μg/mL λ-DNA solution used in the first DNA capture experiment described and as expected the results are similar, although lower. These results agree with those found by Kim and Gale who offered two explanations for the increase.[28] In high salt conditions the DNA may be able to form a salt bridge with the AOM, which would increase binding. The salt may also neutralize the charge on the DNA eventually resulting in DNA aggregation to the point that the aggregates may not be able to pass through the pores in the AOM. Kim and Gale thought the second explanation had a greater effect with membranes that have smaller pore diameters than the size used for this work. No matter which mechanism is behind the increased DNA capture, adding NaCl to samples can be used to improve DNA extraction efficiency if necessary for later experiments. Just 1 ng of DNA is often more than enough for successful PCR, and that amount is easily captured without adding NaCl to the sample solution. However, if the target DNA is a very small percentage of the total DNA in solution, NaCl could be added to capture enough total DNA to get a sufficient amount of target DNA for PCR.

The effect of buffer concentration was also investigated by performing a DNA capture experiment using λ-DNA samples with different buffer concentrations. The concentrated λ-DNA is supplied in TE buffer, but the sample solutions prior to this

experiment were diluted only with water. For this experiment the sample solutions all contained 20 μg/mL λ-DNA in either 0 mM, 10 mM, 50 mM, or 150 mM additional TE buffer. Three replicates were performed at each concentration along with three blanks containing no DNA and 0 mM additional buffer. The syringe method was used to filter solutions through the AOM. The results are shown in table 3.6. With the exception of the 10 mM samples, the results showed a decreasing amount of DNA captured with increasing buffer concentration, the opposite effect seen from increasing NaCl concentration. For unknown reasons, repeated NanoDrop measurements for the 10 mM samples found a greater amount of DNA after filtration through the AOM than before, resulting in negative values for the amount of DNA captured. The background measurements for those samples, taken with a solution containing 10 mM additional TE buffer but no DNA, were lower than usual, resulting in the apparent increase in DNA after filtration. This may be a poor buffer for use with the NanoDrop, or there may have been some problem with this background solution causing the lower absorbance. The experiment was not repeated since the trend in the rest of the samples indicated that increasing the TE buffer concentration did not facilitate DNA capture. Kim and Gale found that cationic buffers are the best elution buffers to release DNA from AOMs,[28] which, since Tris buffers are cationic, would explain the poor DNA extraction with increasing concentrations of buffer. If the DNA is easily dissolved in the buffer, it may not bind to the surface of the AOM. For future experiments, dilutions of DNA for sample solutions continued to be made with only water.

Primer Spotting on AOMs

With the success of DNA capture experiments, the potential to preload primers for PCR on the AOM was also investigated. For the POC application, the same sample will be used for all reaction wells on a chip but there would be different primer sets in each well. This would lower the level of multiplexing required of the reaction in each well. Since all the PCR reagents other than the primers are identical for all wells, a way to store the primers on-chip in the appropriate wells would simplify chip operation for the end user. For this experiment *gyrB* primers were labeled with Alexa Fluor 488 using a ULYSIS labeling kit. First, a tube-mounted AOM was imaged with a fluorescence microscope to obtain a background image (figure 3.5A). Next, 10 pmol of primers were spotted onto the AOM and allowed to dry. The AOM was then imaged again (figure 3.5B). The AOM was finally washed with 25 μL of water and imaged a final time (figure 3.5C). All of the images were taken with a 4 s exposure. The regions of different fluorescence intensity seen in figure 3.5B are due to the majority of the primer solution being delivered to one side of the AOM. As seen in the images, the fluorescence present after primer spotting does not disappear after the AOM is washed. The primers remain on the AOM so pre-spotting different primers to reaction wells at the point of manufacturing appears feasible.

PCR of Captured DNA

With the success of the DNA extraction and primer spotting experiments, the next step was to determine if the DNA captured by the AOM could be amplified by PCR. First, 25 μL samples of a 40 μg/mL solution of λ-DNA (1 μg of DNA in each sample) were filtered through each of six tube-mounted AOMs using the syringe method. Three

tube-mounted AOMs were run as blanks with DNase, RNase, and protease free water used in place of the λ-DNA. After DNA capture, the dry AOMs were punched out into clean 200 μL PCR tubes using 1000 μL pipette tips. PCR master mix (as described above for PCR of λ-DNA in tubes), including forward and reverse primers for a 294 bp region of λ-DNA, was added to each tube to a total volume of 50 μL. The reactions were then thermocycled with the temperature program described above for λ-DNA in tubes. Two positive controls, each containing 5 ng of λ-DNA added in solution, and one negative control that did not contain AOM were thermocycled alongside the other reactions. After PCR, the solutions were analyzed on the Bioanalyzer to determine if successful PCR amplification occurred. Figure 3.6 shows a gel representation of the Bioanalyzer results for this experiment. The bands at ~300 bp indicate product was present in those samples. Amplification was successful for all tubes containing DNA, and no amplification was seen for any of the blanks. Since the experiment was successful for DNA captured on the AOMs, DNA extracted with AOMs can be used for PCR without any need for a separate elution step.

Pre-spotting primers for amplification of DNA captured on the AOM was then tested. Nine tube-mounted AOMs were spotted with 30 pmol each of forward and reverse λ-DNA primers (~3x the amount of primers used in the previous 50 μL PCR reactions to allow for some loss of primers during the DNA extraction step). DNA extraction was performed using the syringe method with 25 μL of a 20 μg/mL λ-DNA solution (500 ng of DNA in each tube). The previous experiment was performed before determining that 40 μg/mL solutions of λ-DNA contain more DNA than can be captured on a tube-mounted AOM. In this experiment, the concentration of λ-DNA was decreased

to the lowest concentration tested for DNA capture. After extraction, the AOMs were punched out into clean PCR tubes and PCR master mix without primers was added to each tube to a final volume of 50 μL. One negative and two positive controls were included as described for the previous experiment with λ-DNA and primers added in solution (10 pmol each of forward and reverse primers). The reactions were then thermocycled and the products analyzed on the Bioanalyzer. The results are shown in figure 3.7. Amplification was successful for all wells except the blanks, so the primers can be loaded onto the AOM before DNA extraction and will still be available to amplify the target DNA.

Initial Development of a PCR Chip

After successful amplification of DNA captured with tube-mounted AOMs, integration of the AOM onto a microfluidic PCR chip was explored. Initial chip designs were similar to that shown in figure 3.2 but without the micropost region to support the AOM. Instead, access holes at both ends of the microfluidic channel were made with a 3 mm punch and a reservoir was placed above the hole at one end to make a single reaction well. The first reservoirs tested were made out of PDMS and could contain a 50 μL PCR reaction overlaid with 50 μL of mineral oil. An image of one of these chips is shown in figure 3.8A. This reaction well design had a tendency to leak and PCR with these chips was not successful. Another reservoir design used a solid block of PDMS (~7.5 mm thick) molded with the lower channel layer to ensure that the reservoirs would be completely sealed. An image of one of these chips is shown in figure 3.8B. This design did eliminate the leaking problem, but PCR was not successful, possibly due to the thermal mass of the PDMS preventing accurate thermocycling. Eventually, the reservoir

design using sections of PCR tubes described in section 3.2 was tested. The reaction volume (10 μL) was smaller than before, and although leaking and evaporation were no longer problems, PCR was still not successful.

In addition to evaluating different reservoir designs, larger access holes were also tested to expose more of the AOM surface. With the larger holes, the AOM had a tendency to flex downward and touch the glass surface when vacuum was applied. This sealed the channel and prevented fluid flow. The AOM's brittleness and its flexing under vacuum occasionally resulted in cracking. The micropost region was developed to allow access to a greater AOM surface area while still providing support to prevent flexing under vacuum. The microposts also increased flexibility in reservoir placement and allowed multiple reaction reservoirs on the same chip. Without the microposts, the reaction reservoir had to be located directly above the channel access hole. If the reservoir was misaligned, solutions could not be transported through the AOM. With the microposts, multiple reservoirs can be located throughout the micropost region and still allow solutions to be filtered through the membrane. The microposts also make it possible to reduce the diameter of the access hole at the end of the channel under the membrane to 1 mm, reducing the dead volume beneath the AOM.

PCR Inhibition from AOMs

After on-chip PCR failure for multiple reservoir designs, an investigation of on-chip conditions was undertaken to achieve successful amplification. A major difference between PCR in tubes and on-chip is the surfaces the solution is in contact with. Many materials used to make microfluidic devices will inhibit PCR.[4] While the PCR tubes used to make the reservoirs do not inhibit PCR, the solutions are also in contact with

PDMS and the AOM. PDMS is not known to be a major PCR inhibitor[4] and this was confirmed by performing PCR in tubes with pieces of PDMS. Although the previous experiments with tube-mounted AOMs did not indicate that AOMs would inhibit PCR, the amount of AOM in those experiments was very small relative to the reaction volume. A much larger surface area was exposed on-chip and the reaction volume was decreased to 10 μL. Therefore, the surface area-to-volume ratio was much greater on-chip. Since the degree of PCR inhibition is positively correlated to surface area-to-volume ratio,[4] the effect of a larger area of AOM was investigated.

Different amounts of AOM were placed into PCR tubes. The mass of AOM added to each tube was assumed to correlate to exposed surface area. PCR in these tubes was performed with either 5 or 25 ng of λ-DNA template in a 50 μL reaction volume. The reactions were thermocycled and the products were analyzed with the Bioanalyzer. A plot of PCR product concentration vs. mass of AOM added to the reaction is shown in figure 3.9. The concentration of PCR products decreased as the amount of AOM increased, confirming that the AOM inhibits PCR when the surface area-to-volume ratio is large. Inhibition from the AOM was probably not the cause of PCR failure for the initial reservoir designs since they used 50 μL reaction volumes and the surface area of the exposed AOM would correlate to ~0.25-1 mg. Failure in those designs was probably due to the leakage problems and inaccurate thermocycling temperatures. However, inhibition from the AOM was most likely the cause of failure for the chip designs with greater than 3 mm diameter access holes and for the initial test of the final reservoir design with a 10 μL reaction volume.

PCR inhibitors generally cause one or more of three possible problems with a reaction: they interfere with cell lysis and the release of template DNA, they degrade or otherwise make nucleic acids unavailable, or they inhibit polymerase activity.[20] The previous failed reactions used purified DNA, so cell lysis was not an issue, and figure 3.9 shows that the initial amount of template had no noticeable effect on product concentration. Inhibition of polymerase activity was therefore evaluated as the mechanism for PCR failure, since the AOM could bind *Taq* polymerase. Adding additional polymerase to the reaction is one possible solution, but *Taq* polymerase is one of the most expensive reagents used for PCR. Another possible solution is to add a blocking agent, like BSA, to the master mix to prevent adsorption. Both of these solutions were tested. PCR was performed with 5 ng of λ-DNA, a 50 μL reaction volume, and 4-5 mg of AOM added to each tube except for two positive controls containing no AOM. Qiagen recommends 2.5 units of *Taq* polymerase per reaction, and this was the amount used for previous experiments. Adding up to 2.5 additional units, in 0.5 unit increments, was tested with duplicates at each concentration. Adding BSA to a final concentration of 1% without additional polymerase was also tested. A plot of PCR product concentration vs. *Taq* polymerase concentration is shown in figure 3.10. Increasing the amount of *Taq* led to small increases in product concentration, while the addition of BSA led to product concentrations much closer to that of the controls. This confirms that the AOM was inhibiting the activity of the polymerase, and that a blocking agent added to the master mix can reduce the inhibition.

While PCR in the presence of AOM with 1% BSA resulted in product concentrations similar to those of the controls, the high BSA concentration led to gelation

of the solutions upon heating. Gelation would likely clog a microfluidic chip, preventing downstream analysis of the PCR products. Duplicate reactions were performed to test six other potential blocking agents: Lyse-N-Go (a PCR compatible lysis reagent), 1% PEG 10k, 1% PVP, 0.75% BSA, PBS Starting Block, and TBS Starting Block. The results are shown in figure 3.11A. While none of the blocking agents worked as well as 1% BSA, acceptable results without gelation were obtained with 0.75% BSA, PBS Starting Block, TBS Starting Block, and Lyse-N-Go.

In a POC device with saliva samples, other factors can negatively affect PCR efficiency, such as PCR inhibitors from the sample. While the blocking agents produced acceptable results under the nearly ideal conditions in tubes, eliminating as much of the effect of the AOM as possible will reduce the chances of PCR failing on the POC device. Lyse-N-Go, 0.75% BSA, and PBS Starting Block were tested with additional *Taq* polymerase, with 2.5, 4.0, and 5.0 total units of *Taq* polymerase per reaction. Duplicate reactions were performed for each blocking buffer at each concentration of Taq polymerase. These results are shown in figure 3.11B. The reactions with 0.75% BSA and 5.0 units of *Taq* polymerase had a product concentration closest to that of the controls, so these conditions were used to prevent inhibition from the AOM in future on-chip PCR experiments.

On-Chip DNA Extraction and PCR

With the addition of 0.75% BSA to the master mix to prevent polymerase adsorption to the AOM, on-chip PCR with 10 μL reaction volumes was retested. The test was performed with *gyrB* primers and bacterial gDNA from *S. pneumoniae* and *S. aureus*. Master mix and template DNA in solution were pipetted into the reaction

wells and then overlaid with mineral oil. Mineral oil was also added to the waste reservoir to prevent evaporation through the waste channel. Three chips with three reaction wells each were thermocycled. One chip contained 1 ng of *S. pneumoniae* gDNA as the template in each well, one chip contained 1 ng of *S. aureus* gDNA in each well, and the final chip was a blank with no template in any of the wells. Three control reactions, a positive control for each target and one negative control, were run in PCR tubes. The products were analyzed using the Bioanalyzer, and the results are shown in figure 3.12. On-chip PCR was successful for both *S. pneumoniae* and *S. aureus* gDNA. This was repeated with gDNA from the other species of bacteria. The results from *H. influenzae* and *S. salivarius* are shown in figure 3.13 and the results from *S. mutans* and *S. mitis* are shown in figure 3.14. While the *H. influenzae* and *S. salivarius* samples worked as well as *S. pneumoniae* and *S. aureus*, only very small amounts of product were seen from *S. mutans*, and no product was seen in the *S. mitis* samples. The *S. mitis* positive control also did not work as well as the other positive controls, indicating that even under ideal conditions, PCR efficiency for *S. mitis* was decreased. Although optimization might have improved results for *S. mitis* and *S. mutans*, it was not performed, and they were dropped from the group of target organisms.

PCR with preloaded primers and DNA capture was then evaluated on-chip. As with the tube-mounted AOM primer spotting experiment, 30 pmol each of the forward and reverse primers, triple the usual amounts, was preloaded onto the AOM at the bottom of each reaction well. Solutions of gDNA with concentrations of 50 ng/mL were made for each of the four remaining target organisms. Samples of 20 μL were added to each well and filtered through the AOM, then 10 μL of master mix and 25 μL of mineral oil

were added to each well, and the chip was thermocycled. Control reactions, with primers and DNA added in solution, were performed in PCR tubes. The results for *S. pneumoniae* and *S. aureus* are shown in figure 3.15 and the results for *H. influenzae* and *S. salivarius* are shown in figure 3.16. Successful amplification was seen for all of the species, but the results for *S. aureus* were both the most consistent and had the greatest amount of product. For the other species, there are one or more wells for which only a small amount of product was detected. While some additional optimization of the on-chip PCR is needed, the chip was successfully used to extract bacterial gDNA from a sample and amplify the target with PCR.

Microarray Hybridization Assay

Since the amplicons from the *gyrB* primers are approximately the same size (~300 bp) for all of the bacterial targets, the Bioanalyzer cannot be used to determine the success of multiplexed PCR experiments. Hybridization assays using a microarray of oligonucleotide-functionalized beads can be used instead, with a different bead type for each product. The Walt group at Tufts University supplied oligonucleotide-functionalized microspheres, but was not able to test probes and produce beads for the *gyrB* amplicons. As an alternative, beads with probes for *P. melaninogenica, C. gingivalis, A. naeslundii,* and *V. parvula* were used to test an on-chip hybridization assay. The Walt group designed a separate primer set for each of these organisms that could be multiplexed in a single reaction. PCR with biotinylated primers for each of the four organisms was performed with bacterial gDNA in tubes with 50 μL reaction volumes to generate amplicons to use as samples for the hybridization assays. Results of the Bioanalyzer analysis of products from PCR with multiplexed primers, including two

reactions with simultaneous amplification of both *P. melaninogenica* and *V. parvula*, are shown in figure 3.17. In the reactions with two types of template DNA, the concentration of *P. melaninogenica* products is decreased due to competition with *V. parvula*. Because of the effects of PCR competition, the hybridization assays were tested with products from reactions with only one set of primers and one type of template DNA.

An initial hybridization assay test with three bead types and their matching PCR products was performed following the adapted Walt group protocol. The arrays were imaged with an EMCCD on an epifluorescence microscope with 8 s exposures. The results of the assay are shown in table 3.7. S/N values were low because raw signals from the target beads were low and the signal from the control beads was very close to the signal from the target beads. The S/N for *C. gingivalis* was lower than that for the blank, although the values are not completely comparable since the signal from the blank was measured off of the *V. parvula* beads. The S/N for *V. parvula* was approximately double that of the blank, less than expected for such a concentrated sample. The S/N for *P. melaninogenica* was the greatest, which was unexpected since its sample concentration was the lowest. Optimization would most likely improve the signal from the target beads, and non-specific binding probably caused the relatively high control bead signal. The casein used as the blocking solution to prevent the dye from adsorbing to the channel and array surfaces is known to contain variable amounts of biotin. Since the assay takes advantage of biotin-streptavidin binding to label the biotinylated PCR products with a streptavidin conjugated fluorescent dye, surfaces coated with biotin from the blocking step will be labeled with AF488 during the staining step.

An experiment was performed to compare three other blocking solutions, 1% BSA in PBS, PBS SuperBlock blocking buffer, and TBS Starting Block blocking buffer, with casein. The blocking solutions were also used to make the AF488 staining solutions. The assays were performed with the same protocol used in the previous experiment. The results of the assays are shown in table 3.8. For all of the blocking buffers tested, the result from the blank array was indistinguishable from the arrays incubated with PCR products. This may indicate that there are additional problems with the assay other than non-specific binding. Low signal from the target beads, probably due to poor hybridization, is the other possible reason for the S/N being the same for the blanks and the positive arrays. Assay optimization could probably improve the signal, most likely by increasing the 30 min hybridization step in which the array is incubated with denatured PCR products to a longer duration. Hybridization assays are commonly performed with long incubations, from 5 hrs to overnight.[37, 48, 49] Shorter incubations have been successfully used, from 1 hr to less than 15 min,[41, 44, 50] but do not seem to work with this particular array design and probe set. Since the thermocycling for on-chip PCR already takes ~2 hrs and the hybridization assay takes ~1 hr, increasing the length of the hybridization step is undesirable if the assay time is to be kept within reasonable limits. In the interest of minimizing the total PCR assay time, real-time PCR detection was pursued as an alternative to hybridization assays.

3.4 Conclusions

We have developed a microfluidic chip to extract DNA from samples and perform PCR of the extracted DNA. By using a PCR-compatible AOM for DNA extraction, we integrated an important sample preparation step onto the chip without requiring complex

architecture to move DNA from a sample preparation region to an amplification region. The extraction procedure is very fast and is exceedingly simple, only requiring sample addition followed by filtration through the AOM. Unlike other DNA extraction procedures, no centrifugation or washing steps are required. This is considerably faster than other methods, including commercial kits, which, even with an elution step, can sometimes result in downstream inhibition of PCR.[51] This uncomplicated extraction procedure means that on-chip DNA extraction could be fully automated with a reader device capable of reagent dispensing. Primers can also be preloaded on the AOM before DNA extraction and used for PCR amplification. Primer spotting helps make automation possible by allowing the same reagents to be dispensed onto a specific chip regardless of the target organisms. Since the template DNA is extracted from the sample and the primers are preloaded onto the chip, only a single reagent solution (PCR master mix) needs to be delivered, irrespective of the bacterial targets.

We found that higher NaCl concentrations and lower TE buffer concentrations increase the amount of DNA captured on the AOM. The effect of other salts and buffers, and the effect of pH on DNA extraction were not investigated. If greater extraction efficiency is needed for samples in the future, other sample additives and buffers could be explored. We also did not extensively investigate the release of DNA from the AOM. Previous work has found that cationic buffers and a basic pH, like PCR buffer, will release DNA from the membrane.[28] Since no problems with DNA release were observed in these experiments, DNA elution was not examined. While the AOM worked well for DNA capture, at large surface area-to-volume ratios it was found to inhibit PCR through adsorption of the *Taq* polymerase. The addition of 0.75% BSA and extra polymerase to

the master mix reduced the inhibition effects to the point where PCR amplification was possible. The inhibition could be further reduced by using 1% BSA, but gelation of those solutions during thermocycling was incompatible with a chip design requiring downstream analysis of the PCR products.

The microfluidic chip was made out of PDMS and polypropylene PCR tubes. The chips were made with PDMS because of its ease of laboratory-scale fabrication as well as its ability to seal the AOM and PCR tube reservoirs onto the chip. The micropost design incorporated onto the chip was a major improvement since the number of reservoirs could be expanded while still using a single, unbranched channel for fluid flow. A microfluidic device incorporating an AOM for DNA extraction has been previously described in the literature, but consisted of only one reaction chamber rather than the three in our design. Although in these experiments all three reaction wells used the same primers, targeting multiple analytes by preloading different primers is possible and is described in Chapter 4 of this work. Successful PCR of bacterial gDNA extracted onto the membrane, including primer spotting before DNA capture, was demonstrated on this device with gDNA from 5 species of bacteria.

Currently the PCR products are detected off-chip using the Bioanalyzer. An on-chip detection scheme using oligonucleotide-functionalized microspheres was tested, but the results were disappointing. The S/N values for assays with large amounts of PCR products were indistinguishable from blank assays with samples containing no PCR products. Optimization of the assay, in particular increasing the length of the hybridization step, could probably improve these results, but optimization was not performed. The hybridization assay tested already added an hour onto the 2 hr assay time

from DNA extraction and PCR. Since the purpose is to develop a POC device, real-time PCR, described in Chapter 4, was pursued as the detection strategy in place of the hybridization assay.

3.5 Tables and Figures

Table 3.1. Primer sequences for λ-DNA and *gyrB* targets. Sequences for *gyrB* were designed by Roth, et al.[37]

Organism/gene	Sequence
λ-DNA	294 bp product
forward	5′-GGATTTAGTGCGCTTTCTAC-3′
reverse	5′-GTGTGTGATACGAAACGAAG-3′
Bacterial *gyrB*	~300 bp product
forward	5′-CGTCCWGGKATGTAYATHGG-3′
reverse	5′-CCHACRCCRTGWAAWCCDCC-3′

Table 3.2. Primer and probe sequences for control organisms used with the hybridization array. Biotin is attached to the 5′ ends of reverse primers and probes with a C6 spacer arm. Sequences were designed by the Walt group at Tufts University.

Organism	Sequence
A. naeslundii	264 bp product
forward	5′-ATGAGACCAACCCCGACATC-3′
reverse	5′-/Biotin/TGTAGTAGGAGAAGGAGACGAAG-3′
probe	5′-/Biotin/CGCCAACTACGCCTTCGGAGACCTC-3′
C. gingivalis	227 bp product
forward	5′-AGAGTTTGATCCTGGCTCAG-3′
reverse	5′-/Biotin/GGACGCATGCCCATCCTTTCACCACCGC-3′
probe	5′-/Biotin/GCGTATGCAACCTACCTTTCACA-3′
P. melaninogenica	281 bp product
forward	5′-TCTGGAGAGGATGCTTATTAGTTG-3′
reverse	5′-/Biotin/CAGTCTTGCTTGTGTCAATATGTC-3′
probe	5′-/Biotin/CCTTATCCTCCACCACTGCTGTTCTATGCT-3′
V. parvula	232 bp product
forward	5′-CTGTAGATAATGGCGAATACTATGAAG-3′
reverse	5′-/Biotin/CCAGGCAAGAAACCAGGAAC-3′
probe	5′-/Biotin/GCTGGTTGCTTGGACATTAACGCTTCTGA-3′

Table 3.3. Effect of λ-DNA concentration on the amount of DNA captured with a tube-mounted AOM.

Sample	Captured DNA (ng)	% DNA Captured
Blank	-2.5 ± 10	-
20 μg/mL	200 ± 47	53 ± 12
40 μg/mL	120 ± 14	18 ± 1.9
80 μg/mL	140 ± 21	8.5 ± 1.2

Table 3.4. Effect of the method used to move solutions through the AOM on the amount of DNA captured. Sample solutions contained 40 μg/mL λ-DNA.

Method	Captured DNA (ng)	% DNA Captured
Blanks (day 1)	7.9 ±0.6	-
Syringe (day 1)	260 ± 41	31 ± 5.0
Centrifuge (day 1)	170 ± 27	20 ± 3.3
Blanks (day 2)	-9.7 ±10	-
Syringe (day 2)	92 ± 27	13 ± 4.0
Vacuum (day 2)	110 ± 14	17 ± 2.0

Table 3.5. Effect of NaCl concentration on DNA capture with tube-mounted AOMs. Sample solutions contained 20 μg/mL λ-DNA.

Concentration of NaCl	Captured DNA (ng)	% DNA Captured
Blanks	-51 ± 67	-
0 mM	110 ± 4.6	31 ± 1.3
100 mM	320 ± 4.9	110 ± 1.6
300 mM	280 ± 31	100 ± 11
500 mM	300 ± 3.9	110 ± 1.4

Table 3.6. Effect of buffer concentration on DNA capture with tube-mounted AOMs. Sample solutions contained 20 μg/mL λ-DNA.

Concentration of Additional TE buffer	Captured DNA (ng)	% DNA Captured
Blanks	-7.2 ± 6.8	-
0 mM	130 ± 56	34 ± 15
10 mM	-58 ± 78	-15 ± 21
50 mM	32 ± 21	7.0 ± 4.6
150 mM	14 ± 4.1	2.5 ± 0.7

Table 3.7. Results of the initial test of the hybridization assay with oligonucleotide functionalized microspheres.

Target beads for	Sample	Sample Concentration (ng/μL)	S/N
V. parvula	Blank	0	48 ± 2.3
V. parvula	*V. parvula* PCR products	22.52	89 ± 5.7
P. melaninogenica	*P. melaninogenica* PCR products	13.30	280 ± 12
C. gingivalis	*C. gingivalis* PCR products	29.11	9.7 ± 0.26

Table 3.8. Results of hybridization assays comparing four different blocking solutions. Assays were for *V. parvula* and the sample concentration was 17.32 ng/μL *V. parvula* PCR products.

Blocking Solution	Sample	S/N
1% Blocker Casein in TBS	Blank	58 ± 4.0
	PCR products	44 ± 7.4
1% BSA in PBS	Blank	120 ± 20
	PCR products	120 ± 38
PBS SuperBlock	Blank	51 ± 5.4
	PCR products	49 ± 13
TBS Starting Block	Blank	54 ± 3.8
	PCR products	51 ± 6.9

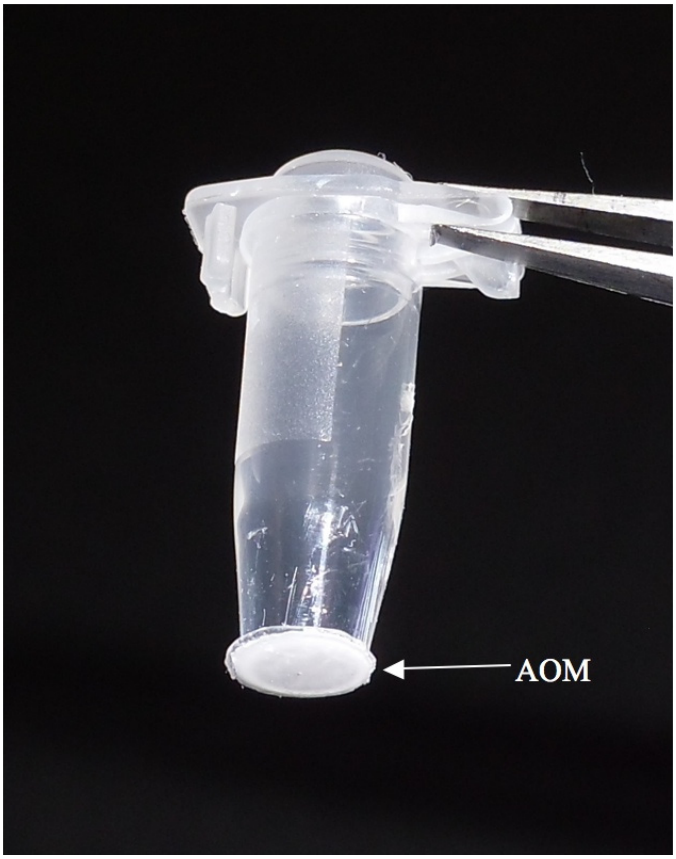

Figure 3.1. An image of a tube-mounted AOM used to test DNA extraction efficiency. The bottom 2-3 mm is trimmed off of a 200 μL PCR tube and an AOM is hermetically sealed to the cut end.

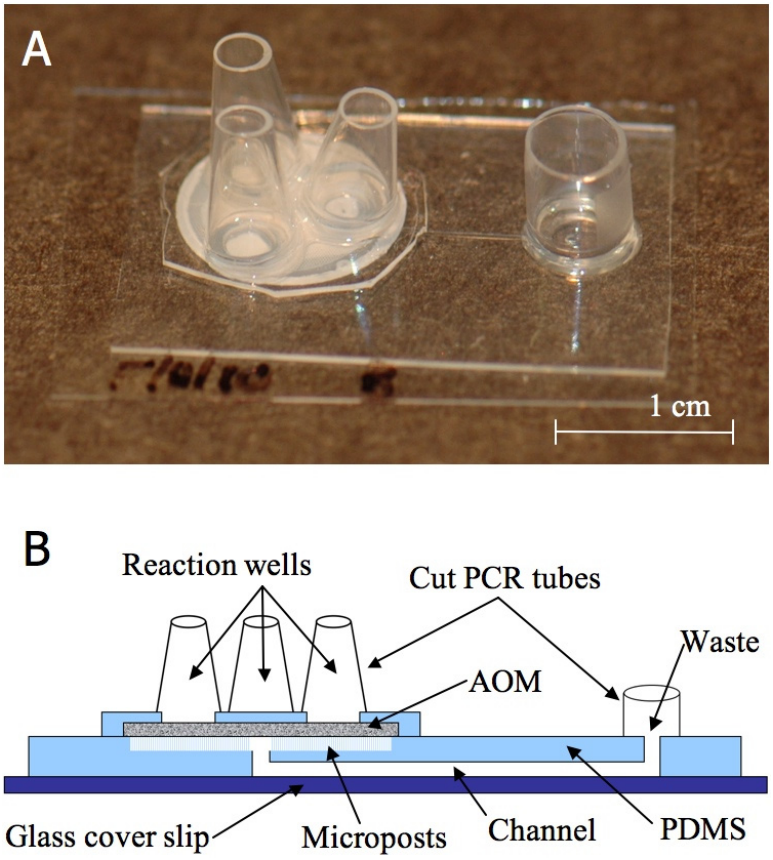

Figure 3.2. An image of the PCR chip (A) and a schematic of its cross-section (B). Pieces of PCR tubes are used to form reaction wells. The schematic is not to scale.

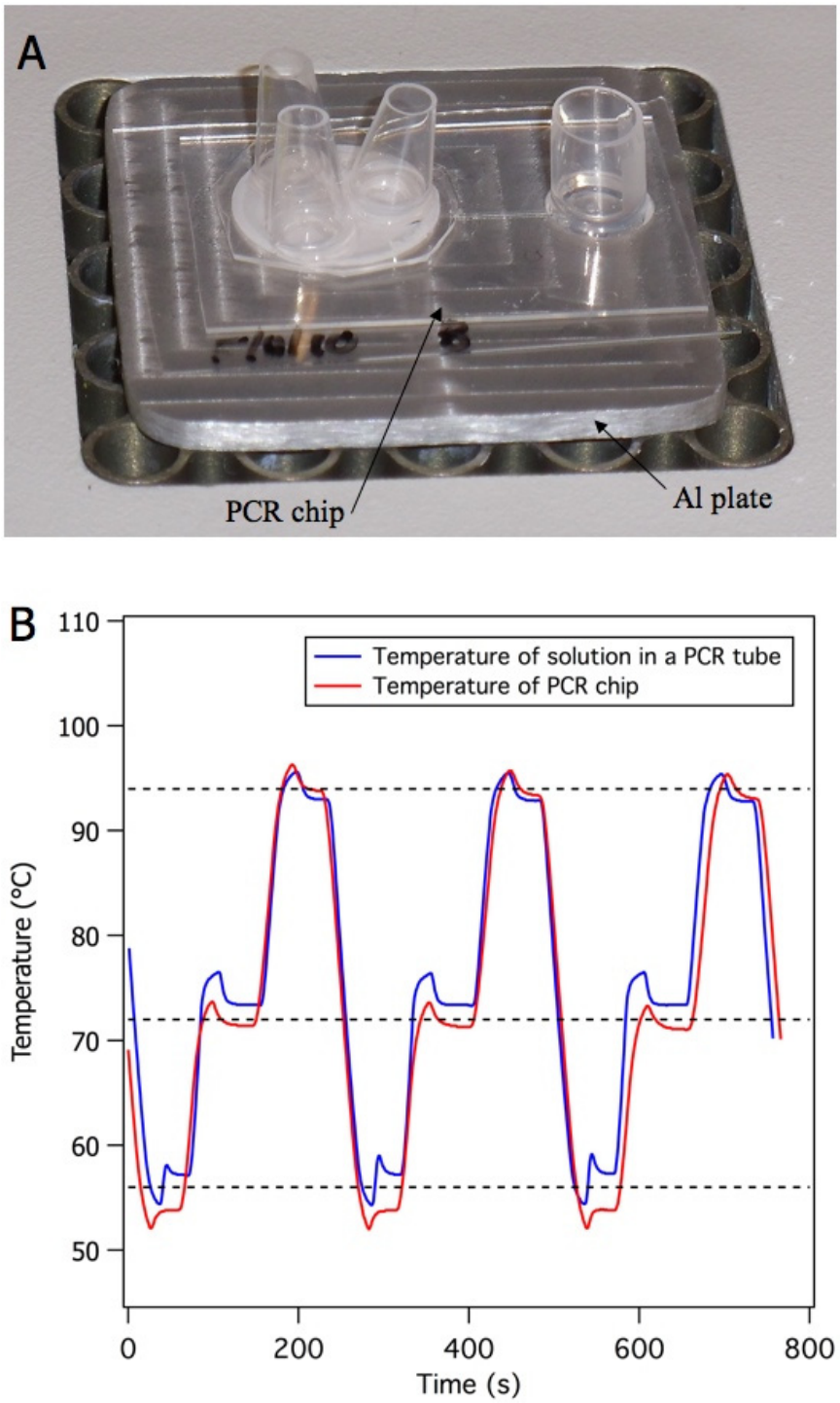

Figure 3.3. An image of the aluminum plate used to thermocycle the PCR chips (A) and a plot of the temperatures measured during thermocycling in a tube and on a chip (B). The plate has posts on the bottom that fit into holes in the thermal block of a commercial thermocycler. The plate is shown inserted into the thermocycler with a PCR chip on top. The target PCR temperatures of 94 °C, 72 °C, and 56 °C are shown with dashed lines on the temperature plot.

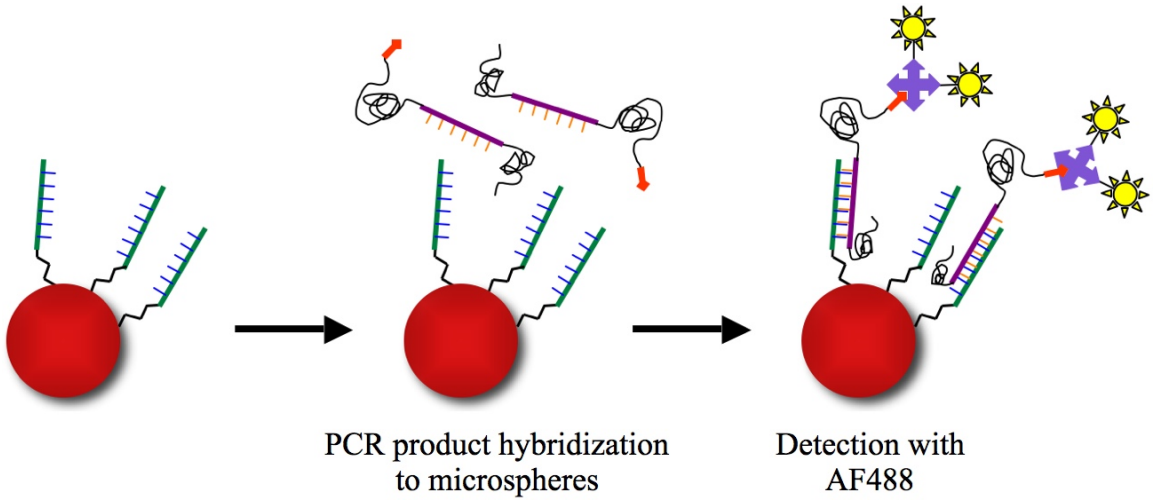

Figure 3.4. Schematic of the hybridization assay for detecting PCR products. Biotinylated PCR products hybridize to oligonucleotide probes on the microspheres and are detected with streptavidin-conjugated Alexa Fluor 488.

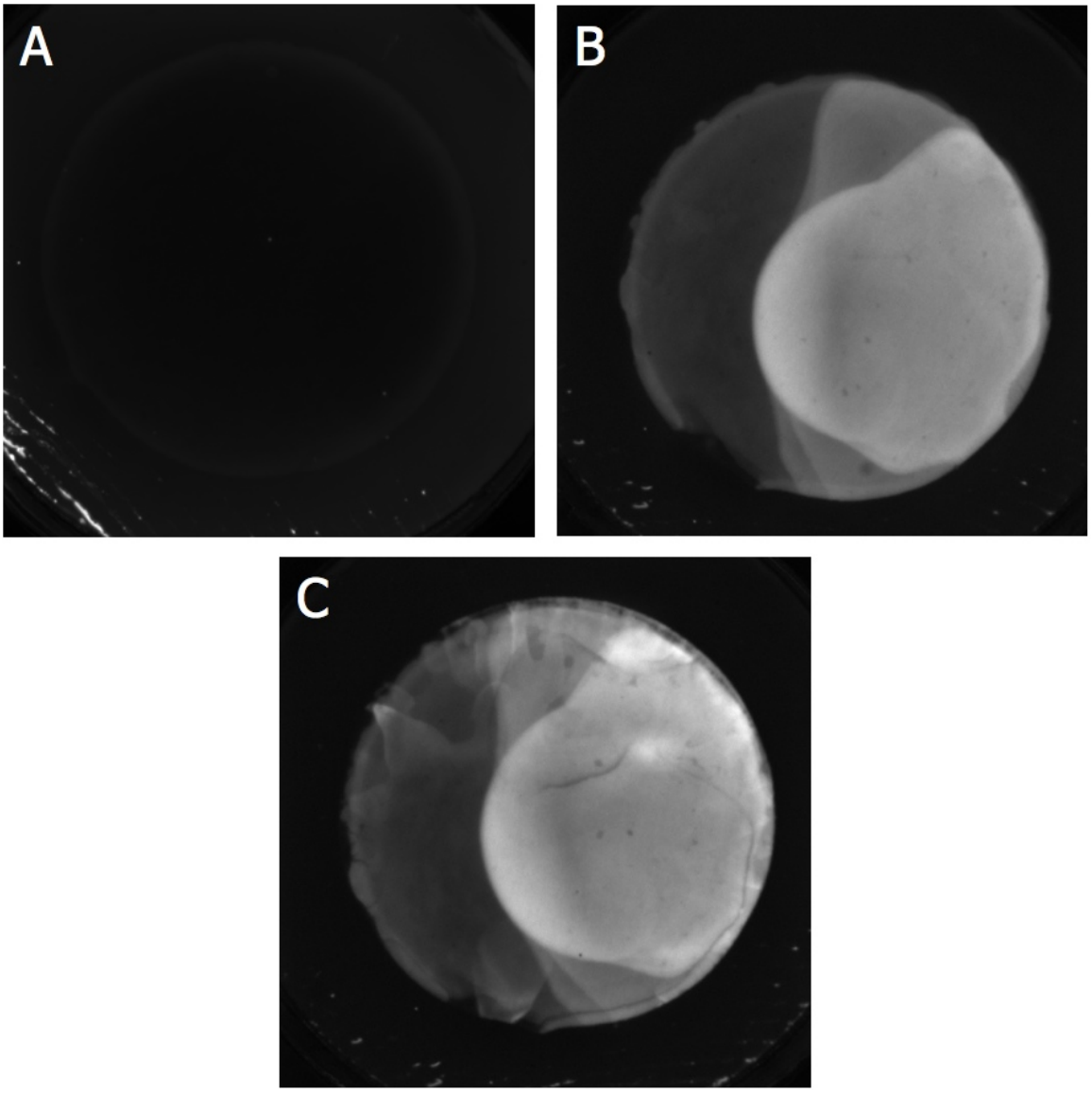

Figure 3.5. Fluorescence images of an AOM before primer spotting (A), after primer spotting (B), and after washing with 25 μL of water (C). The primers were covalently labeled with Alexa Flour 488 for visualization. All of the images were taken with a 4 s exposure and the brightness and contrast settings are identical for all three images.

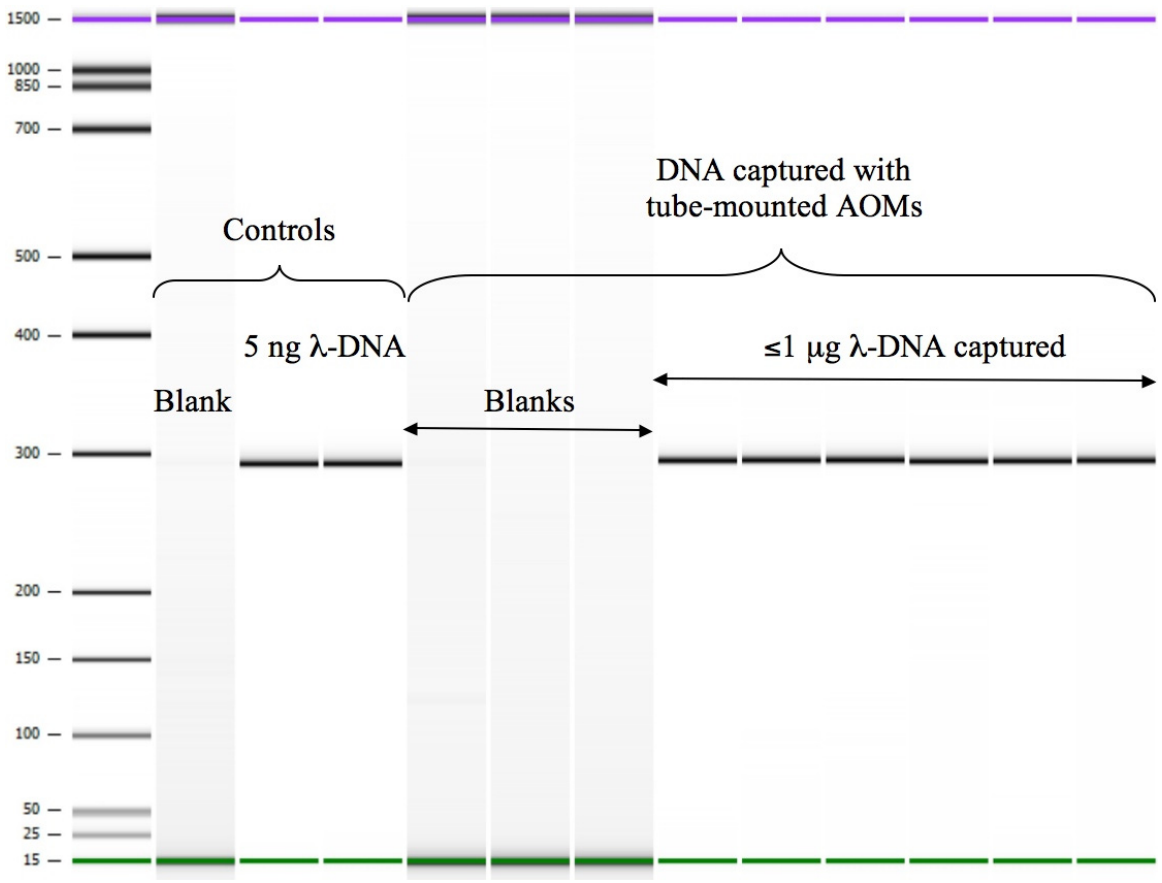

Figure 3.6. Results of PCR of λ-DNA captured on a tube-mounted AOM. For the reactions with DNA captured on tube-mounted AOMs, no additional DNA was added to the PCR solution. The expected size of the PCR products for the λ-DNA primer set is 294 bp.

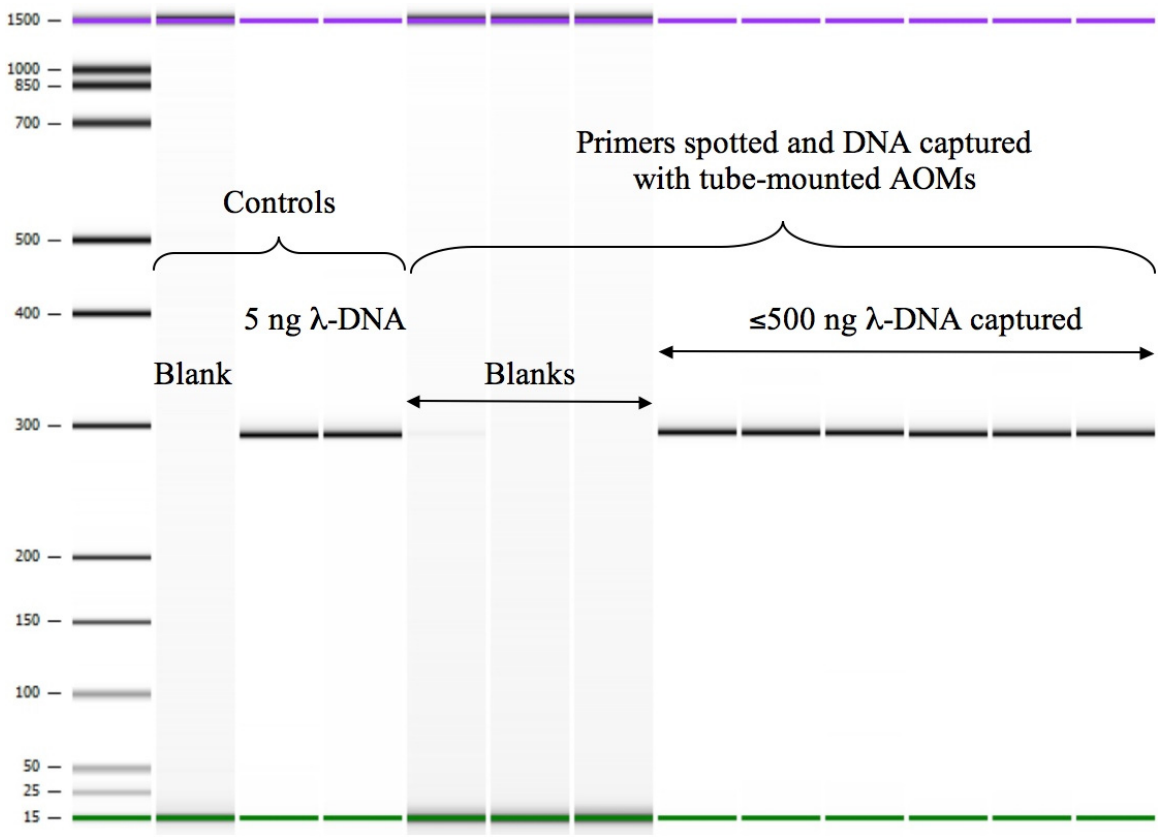

Figure 3.7. Results of PCR of λ-DNA captured on a tube-mounted AOM with pre-spotted primers. For the reactions using tube-mounted AOMs, no additional primers or DNA were added to the PCR solution. The expected size of the PCR products for the λ-DNA primer set is 294 bp.

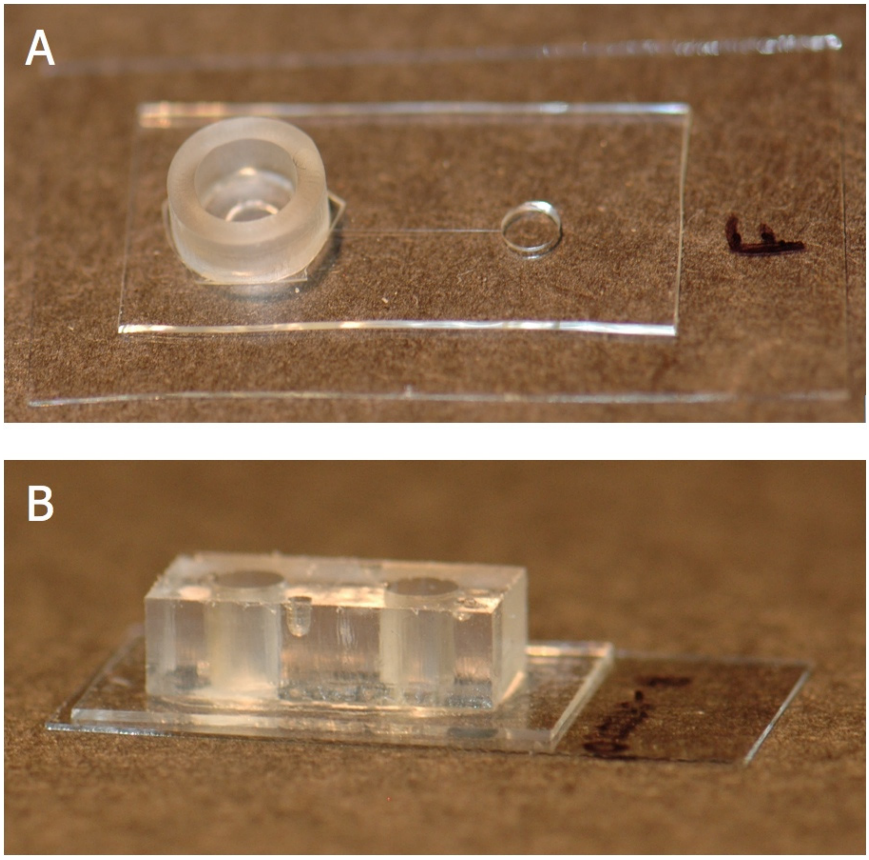

Figure 3.8. Images of two prototype PCR chips. (A) has a reservoir with an ~100 μL volume, but these reservoirs had a tendency to leak. (B) was made as a solid block of PDMS, eliminating leaking, but PCR was still not successful.

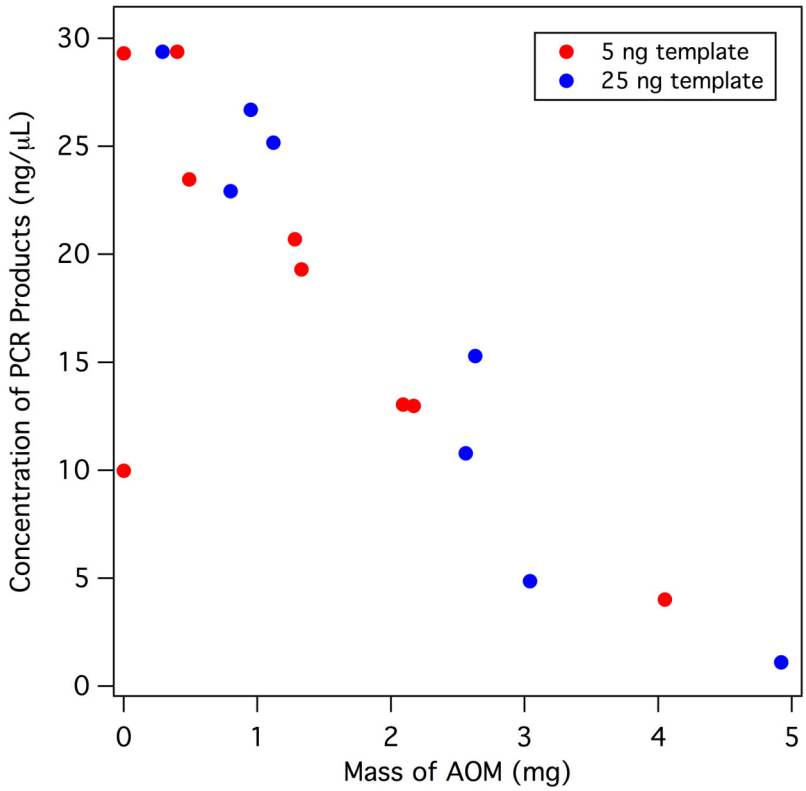

Figure 3.9. Plot of the concentration of PCR products vs. the mass of AOM added to the reaction for 5 ng and 25 ng of template λ-DNA. As the mass of AOM in the reaction mixture increases, the concentration of PCR products decreases. An outlier is seen at 0 mg AOM with 10 ng/μL PCR products.

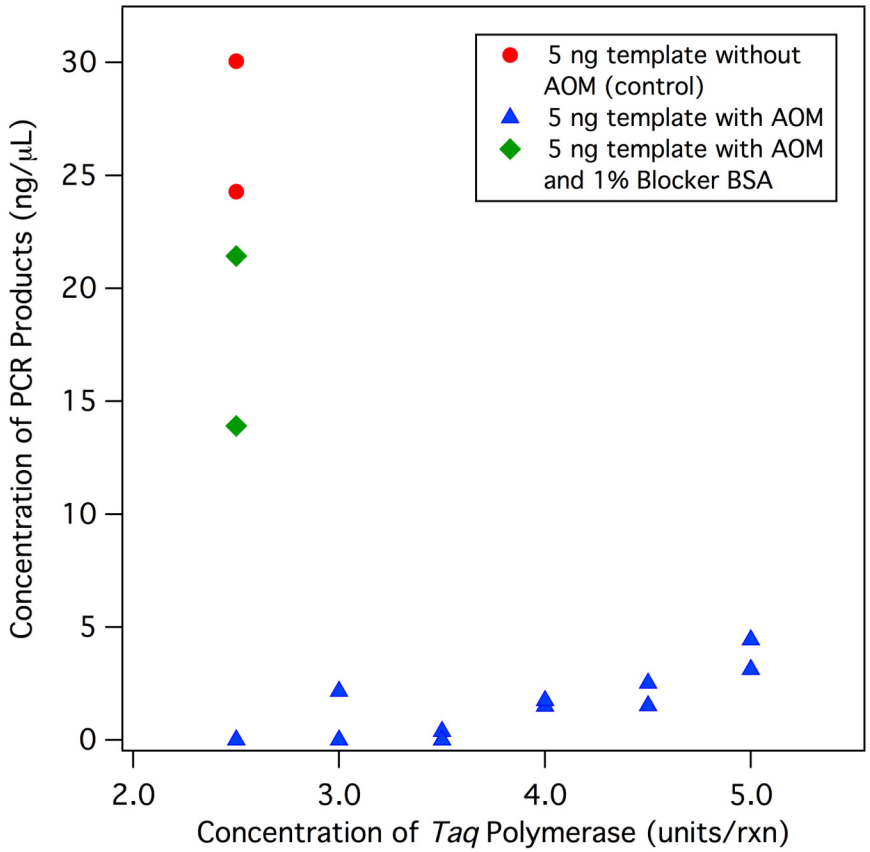

Figure 3.10. Plot of the concentration of PCR products vs. the concentration of *Taq* polymerase. All solutions except the controls contained 4-5 mg of AOM, and 1% BSA was added to two solutions without adding additional *Taq* polymerase. The addition of BSA or extra *Taq* polymerase resulted in an increased concentration of PCR products, but the addition of BSA resulted in a much more dramatic increase.

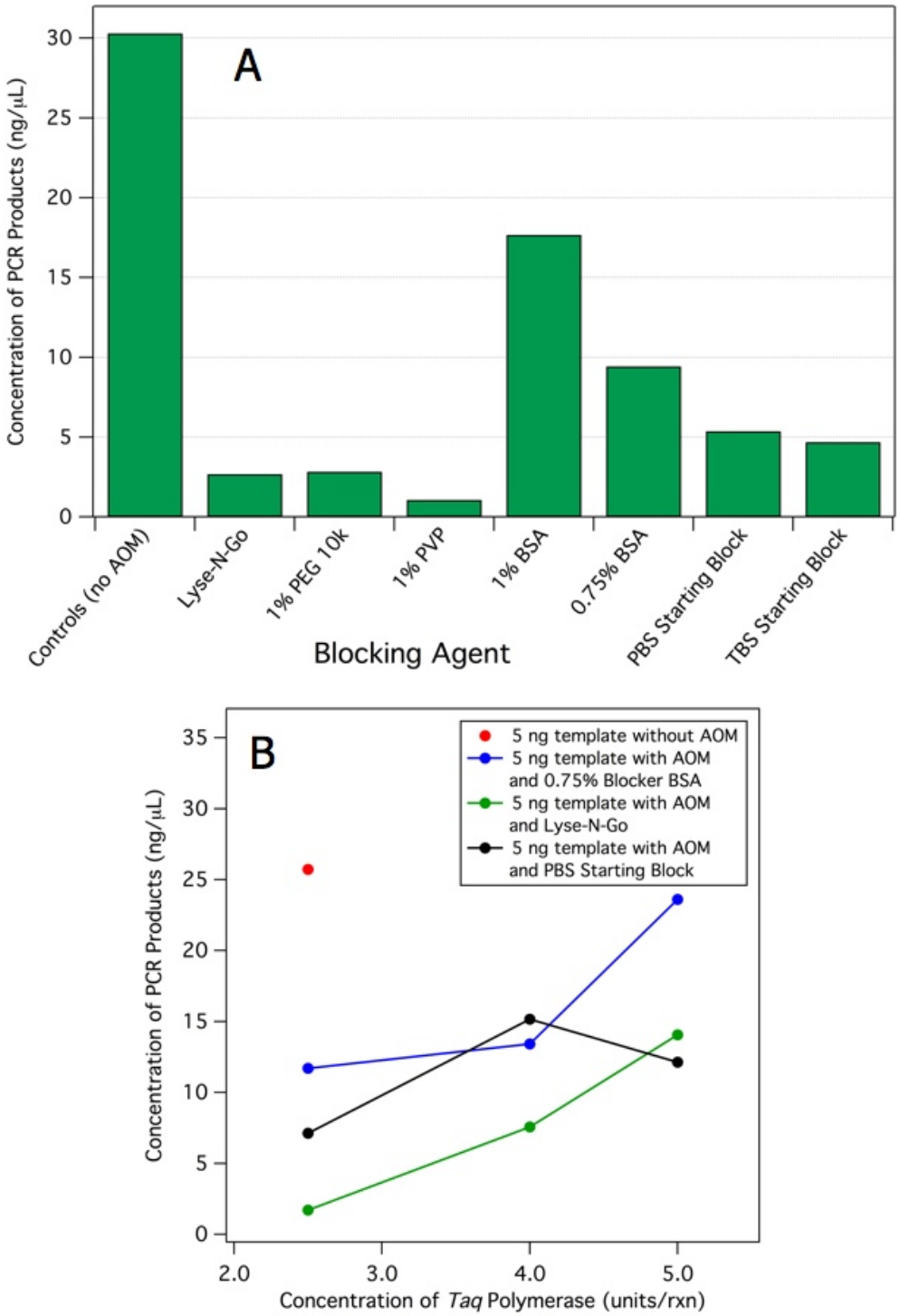

Figure 3.11. Results of PCR comparing seven different blocking agents to prevent PCR inhibition from AOMs (A) and testing three of the best blocking agents with additional *Taq* polymerase (B). For both A and B, all reactions except the controls contained 4-5 mg of AOM. While 1% BSA was the best blocking agent tested, it caused gelation of the PCR reagents. Using 0.75% BSA with 5 units of *Taq* polymerase gave nearly the same concentration of PCR products as the control.

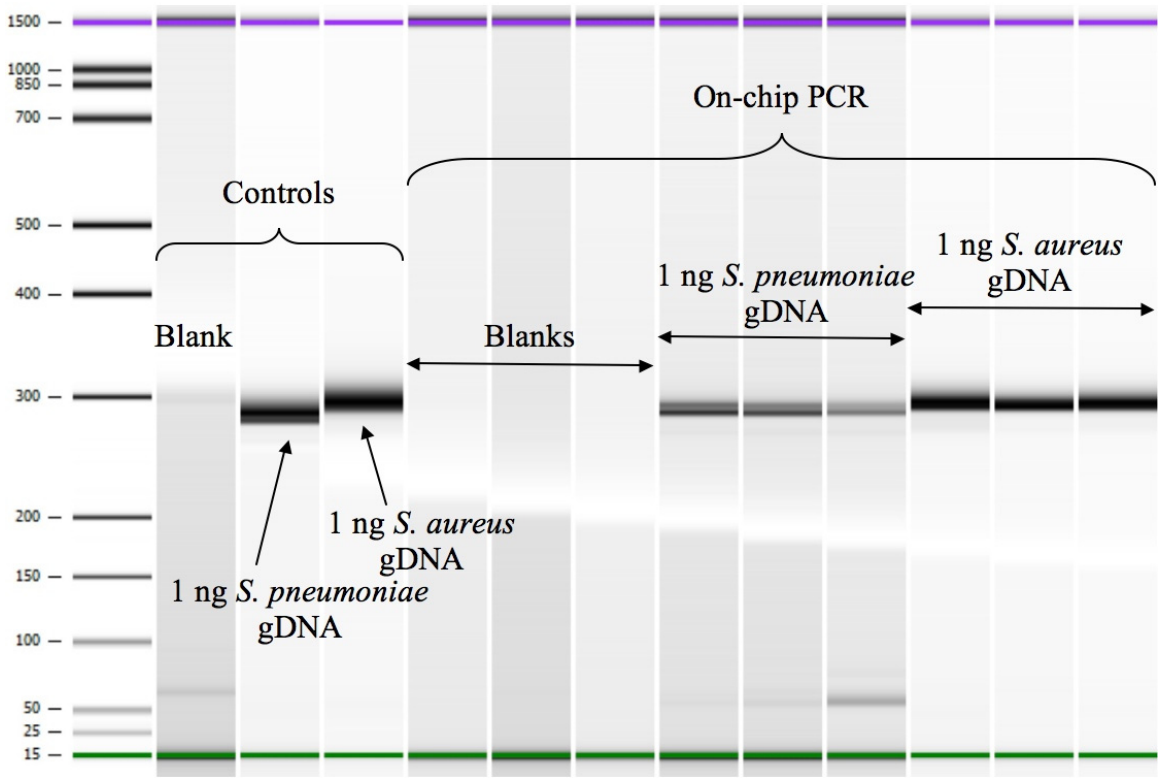

Figure 3.12. Results of on-chip PCR of gDNA from *S. pneumoniae* and *S. aureus*. The expected product size for the *gyrB* primers is ~300 bp. The weak bands at ~60 bp were likely due to primer dimers.

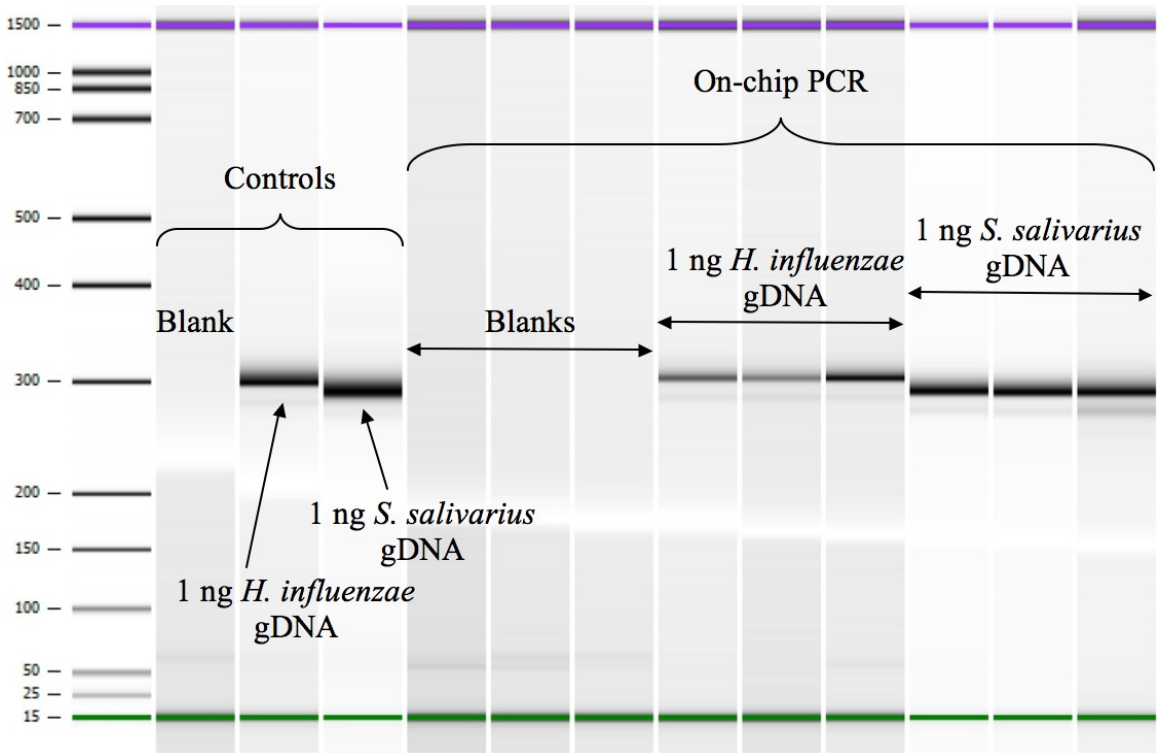

Figure 3.13. Results of on-chip PCR of gDNA from *H. influenzae* and *S. salivarius*. The expected product size for the *gyrB* primers is ~300 bp.

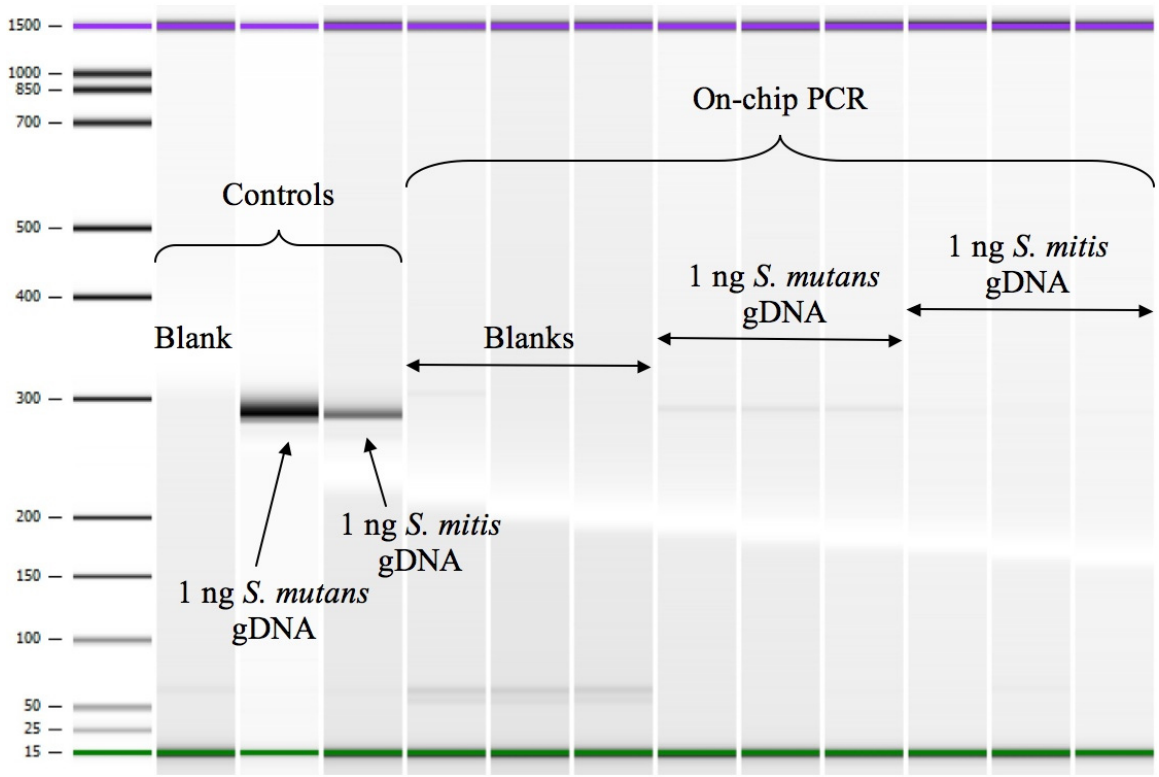

Figure 3.14. Results of on-chip PCR of gDNA from *S. mutans* and *S. mitis*. The expected product size for the *gyrB* primers is ~300 bp. Only very weak product bands were seen for *S. mutans* and no product was seen from *S. mitis*. Annealing temperature optimization could probably increase the product yields for both of these species, but since *S. mutans* and *S. mitis* are both control organisms, they were simply dropped from the group of target organisms. The weak bands at ~60 bp were likely due to primer dimers.

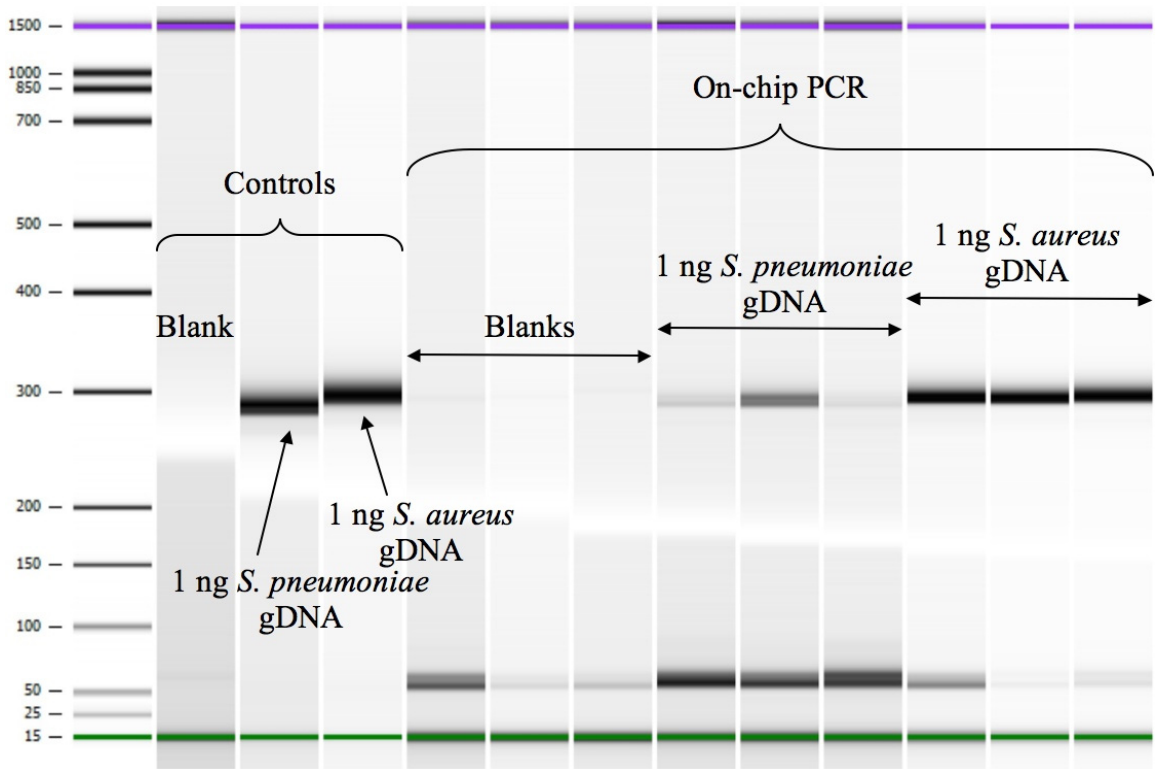

Figure 3.15. Results of on-chip nucleic acid extraction and PCR of gDNA from *S. pneumoniae* and *S. aureus* with primers pre-spotted into the reaction wells. The expected product size for the *gyrB* primers is ~300 bp. The bands at ~60 bp were likely due to primer dimers.

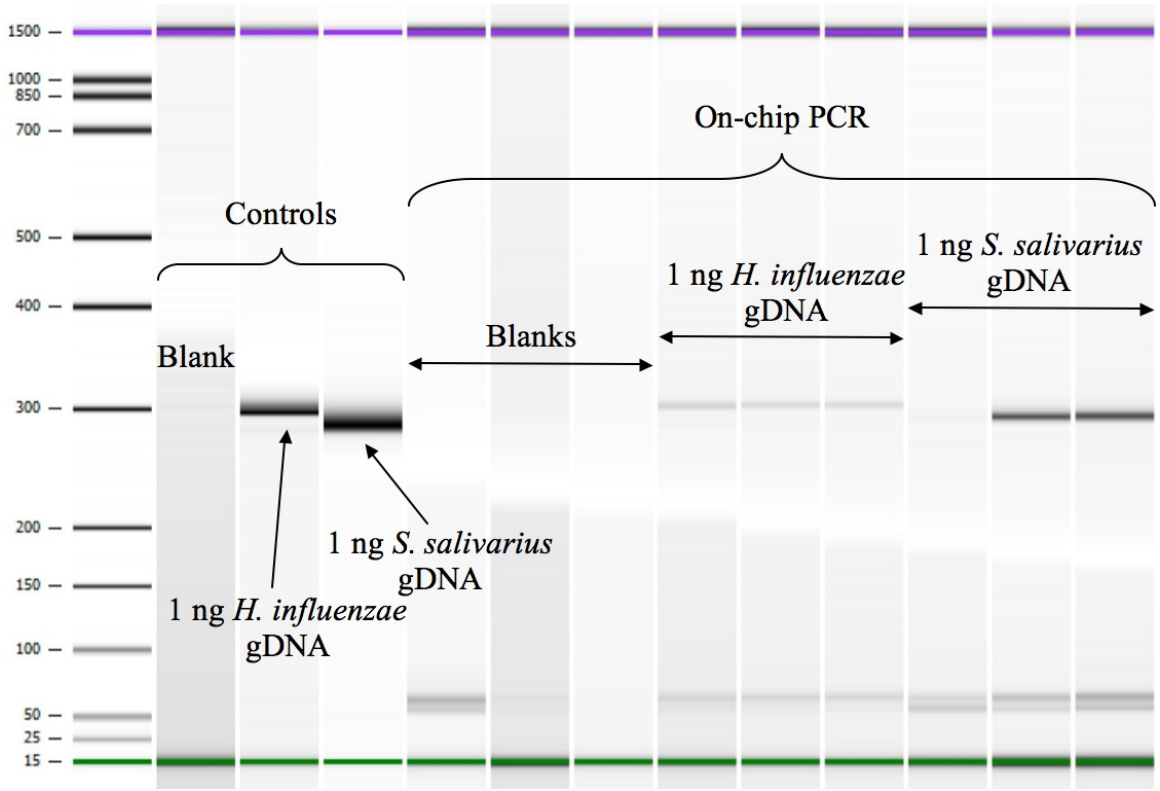

Figure 3.16. Results of on-chip nucleic acid extraction and PCR of gDNA from *H. influenzae* and *S. salivarius* with primers pre-spotted into the reaction wells. The expected product size for the *gyrB* primers is ~300 bp. The first *S. salivarius* replicate contains only a very weak product band. This is probably due to a bubble forming in that reaction well and preventing the reaction mixture from accurately thermocycling. Optimization is needed to increase the amount of product for *H. influenzae*. The weak bands at ~60 bp were likely due to primer dimers.

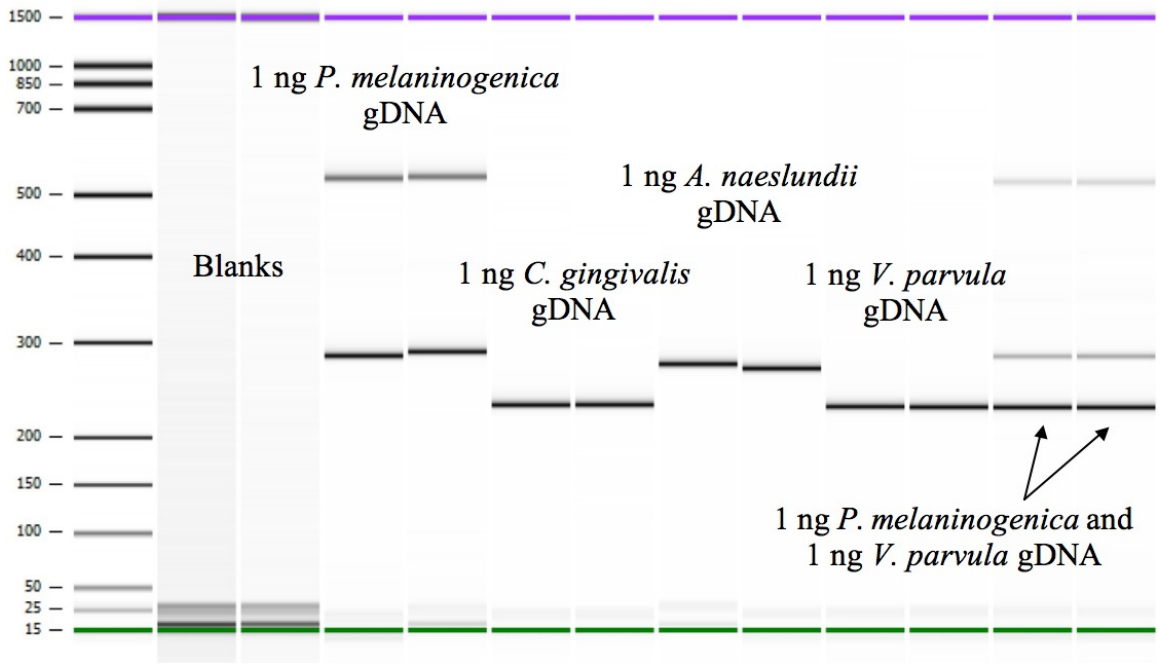

Figure 3.17. Results of PCR with multiplexed primers for control organisms. All reactions contained primers for all four control organisms. The last two lanes are the results from reactions that contained gDNA from both *P. melaninogenica* and *V. parvula*. The decrease in *P. melaninogenica* products from those reactions is due to competition with *V. parvula*.

3.6 References

1. Kricka, L. J.; Wilding, P., Microchip PCR. *Analytical and Bioanalytical Chemistry* 2003, *377*, (5), 820-825.

2. Zhang, C. S.; Xu, J. L.; Ma, W. L.; Zheng, W. L., PCR microfluidic devices for DNA amplification. *Biotechnology Advances* 2006, *24*, (3), 243-284.

3. Zhang, C. S.; Xing, D., Miniaturized PCR chips for nucleic acid amplification and analysis: latest advances and future trends. *Nucleic Acids Research* 2007, *35*, (13), 4223-4237.

4. Kolari, K.; Satokari, R.; Kataja, K.; Stenman, J.; Hokkanen, A., Real-time analysis of PCR inhibition on microfluidic materials. *Sensors and Actuators B-Chemical* 2008, *128*, (2), 442-449.

5. Liu, P.; Mathies, R. A., Integrated microfluidic systems for high-performance genetic analysis. *Trends in Biotechnology* 2009, *27*, (10), 572-581.

6. Mairhofer, J.; Roppert, K.; Ertl, P., Microfluidic Systems for Pathogen Sensing: A Review. *Sensors* 2009, *9*, (6), 4804-4823.

7. Park, S.; Zhang, Y.; Lin, S.; Wang, T.-H.; Yang, S., Advances in microfluidic PCR for point-of-care infectious disease diagnostics. *Biotechnology Advances* 2011, *29*, (6), 830-839.

8. Fukuba, T.; Yamamoto, T.; Naganuma, T.; Fujii, T., Microfabricated flow-through device for DNA amplification - towards in situ gene analysis. *Chemical Engineering Journal* 2004, *101*, (1-3), 151-156.

9. Kim, J. A.; Lee, J. Y.; Seong, S.; Cha, S. H.; Lee, S. H.; Kim, J. J.; Park, T. H., Fabrication and characterization of a PDMS-glass hybrid continuous-flow PCR chip. *Biochemical engineering journal* 2006, *29*, (1-2), 91-97.

10. Ramalingam, N.; Liu, H.-B.; Dai, C.-C.; Jiang, Y.; Wang, H.; Wang, Q.; Hui, K. M.; Gong, H.-Q., Real-time PCR array chip with capillary-driven sample loading and reactor sealing for point-of-care applications. *Biomedical Microdevices* 2009, *11*, (5), 1007-1020.

11. Shin, Y. S.; Cho, K.; Lim, S. H.; Chung, S.; Park, S.-J.; Chung, C.; Han, D.-C.; Chang, J. K., PDMS-based micro PCR chip with parylene coating. *Journal of Micromechanics and Microengineering* 2003, *13*, (5), 768-774.

12. Chen, L.; Manz, A.; Day, P. J. R., Total nucleic acid analysis integrated on microfluidic devices. *Lab on a Chip* 2007, *7*, (11), 1413-1423.

13. Mariella, R., Sample preparation: the weak link in microfluidics-based biodetection. *Biomedical Microdevices* 2008, *10*, (6), 777-784.

14. Schulze, H.; Giraud, G.; Crain, J.; Bachmann, T. T., Multiplexed optical pathogen detection with lab-on-a-chip devices. *Journal of Biophotonics* 2009, *2*, (4), 199-211.

15. Kim, J.; Johnson, M.; Hill, P.; Gale, B. K., Microfluidic sample preparation: cell lysis and nucleic acid purification. *Integrative Biology* 2009, *1*, (10), 574-586.

16. Price, C. W.; Leslie, D. C.; Landers, J. P., Nucleic acid extraction techniques and application to the microchip. *Lab on a Chip* 2009, *9*, (17), 2484-2494.

17. Lee, C.-Y.; Lee, G.-B.; Lin, J.-L.; Huang, F.-C.; Liao, C.-S., Integrated microfluidic systems for cell lysis, mixing/pumping and DNA amplification. *Journal of Micromechanics and Microengineering* 2005, *15*, (6), 1215-1223.

18. Thaitrong, N.; Toriello, N. M.; Del Bueno, N.; Mathies, R. A., Polymerase Chain Reaction-Capillary Electrophoresis Genetic Analysis Microdevice with In-Line Affinity Capture Sample Injection. *Analytical Chemistry* 2009, *81*, (4), 1371-1377.

19. Waters, L. C.; Jacobson, S. C.; Kroutchinina, N.; Khandurina, J.; Foote, R. S.; Ramsey, J. M., Microchip device for cell lysis, multiplex PCR amplification, and electrophoretic sizing. *Analytical Chemistry* 1998, *70*, (1), 158-162.

20. Wilson, I. G., Inhibition and Facilitation of Nucleic Acid Amplification. *Applied and Environmental Microbiology* 1997, *63*, (10), 3741-3751.

21. Liu, R. H.; Yang, J.; Lenigk, R.; Bonanno, J.; Grodzinski, P., Self-Contained, Fully Integrated Biochip for Sample Preparation, Polymerase Chain Reaction Amplification, and DNA Microarray Detection. *Analytical Chemistry* 2004, *76*, (7), 1824-1831.

22. Chen, D.; Mauk, M.; Qiu, X.; Liu, C.; Kim, J.; Ramprasad, S.; Ongagna, S.; Abrams, W.; Malamud, D.; Corstjens, P.; Bau, H., An integrated, self-contained microfluidic cassette for isolation, amplification, and detection of nucleic acids. *Biomedical Microdevices* 2010, *12*, (4), 705-719.

23. Easley, C. J.; Karlinsey, J. M.; Bienvenue, J. M.; Legendre, L. A.; Roper, M. G.; Feldman, S. H.; Hughes, M. A.; Hewlett, E. L.; Merkel, T. J.; Ferrance, J. P.; Landers, J. P., A fully integrated microfluidic genetic analysis system with sample-in-answer-out capability. *Proceedings of the National Academy of Sciences of the United States of America* 2006, *103*, (51), 19272-19277.

24. Lien, K.-Y.; Liu, C.-J.; Kuo, P.-L.; Lee, G.-B., Microfluidic System for Detection of α-Thalassemia-1 Deletion Using Saliva Samples. *Analytical Chemistry* 2009, *81*, (11), 4502-4509.

25. Sauer-Budge, A. F.; Mirer, P.; Chatterjee, A.; Klapperich, C. M.; Chargin, D.; Sharon, A., Low cost and manufacturable complete microTAS for detecting bacteria. *Lab on a Chip* 2009, *9*, (19), 2803-2810.

26. Yeung, S.-W.; Lee, T. M.-H.; Cai, H.; Hsing, I.-M., A DNA biochip for on-the-spot multiplexed pathogen identification. *Nucleic Acids Research* 2006, *34*, (18), e118.

27. Dames, S.; Bromley, L. K.; Herrmann, M.; Elgort, M.; Erali, M.; Smith, R.; Voelkerding, K. V., A single-tube nucleic acid extraction, amplification, and detection method using aluminum oxide. *Journal of Molecular Diagnostics* 2006, *8*, (1), 16-21.

28. Kim, J.; Gale, B. K., Quantitative and qualitative analysis of a microfluidic DNA extraction system using a nanoporous AlO_x membrane. *Lab on a Chip* 2008, *8*, (9), 1516-1523.

29. Saunders, G. C.; Rossi, J. M., DNA Extraction. In *Essentials of Nucleic Acid Analysis: A Robust Approach*, Keer, J. T.; Birch, L., Eds. Royal Society of Chemistry: Cambridge, UK, 2008; pp 59-82.

30. Wen, J.; Legendre, L. A.; Bienvenue, J. M.; Landers, J. P., Purification of nucleic acids in microfluidic devices. *Analytical Chemistry* 2008, *80*, (17), 6472-6479.

31. Elgort, M. G.; Herrmann, M. G.; Erali, M.; Durtschi, J. D.; Voelkerding, K. V.; Smith, R. E., Extraction and amplification of genomic DNA from human blood on nanoporous aluminum oxide membranes. *Clinical Chemistry* 2004, *50*, (10), 1817-1819.

32. Erali, M.; Durtschi, J. D.; Voelkerding, K. V.; Smith, R. E., Localization and imaging of nucleic acids on nanoporous aluminum oxide membranes. *Clinical Chemistry* 2004, *50*, (10), 1819-1821.

33. Kim, J.; Mauk, M.; Chen, D.; Qiu, X.; Kim, J.; Gale, B.; Bau, H. H., A PCR reactor with an integrated alumina membrane for nucleic acid isolation. *Analyst* 2010, *135*, (9), 2408-2414.

34. Kim, J.; Voelkerding, K. V.; Gale, B. K. In *Multi-DNA extraction chip based on an aluminum oxide membrane integrated into a PDMS microfluidic structure*, IEEE/EMBS Special Topic Conference on Microtechnology in Medicine and Biology, Kahuku, HI, United States, May 12-15, 2005, 2005; Institute of Electrical and Electronics Engineers: Kahuku, HI, United States, 2005; pp 5-7.

35. Birch, L.; Bailey, C. L.; Anderson, M. T., Multiplex PCR and Whole Genome Amplification. In *Essentials of Nucleic Acid Analysis: A Robust Approach*, Keer, J. T.; Birch, L., Eds. Royal Society of Chemistry: Cambridge, UK, 2008; pp 167-188.

36. SantaLucia, J., Jr., Physical Principles and Visual-OMP Software for Optimal PCR Design. In *PCR Primer Design*, Yuryev, A., Ed. Humana Press: Totowa, NJ, 2007; pp 3-33.

37. Roth, S. B.; Jalava, J.; Ruuskanen, O.; Ruohola, A.; Nikkari, S., Use of an oigonucleotide array for laboratory diagnosis of bacteria responsible for acute upper respiratory infections. *Journal of clinical microbiology* 2004, *42*, (9), 4268-4274.

38. Sontakke, S.; Cadenas, M. B.; Maggi, R. G.; Diniz, P. P. V. P.; Breitschwerdt, E. B., Use of broad range 16S rDNA PCR in clinical microbiology. *Journal of Microbiological Methods* 2009, *76*, (3), 217-225.

39. Itoh, Y.; Kawamura, Y.; Kasai, H.; Shah, M. M.; Nhung, P. H.; Yamada, M.; Sun, X.; Koyana, T.; Hayashi, M.; Ohkusu, K.; Ezaki, T., *dnaJ* and *gyrB* gene sequence relationship among species and strains of genus *Streptococcus*. *Systematic and Applied Microbiology* 2006, *29*, (5), 368-374.

40. Tabacchioni, S.; Ferri, L.; Manno, G.; Mentasti, M.; Cocchi, P.; Campana, S.; Ravenni, N.; Taccetti, G.; Dalmastri, C.; Chiarini, L.; Bevivino, A.; Fani, R., Use of the *gyrB* gene to discriminate among species of the *Burkholderia cepacia* complex. *Fems Microbiology Letters* 2008, *281*, (2), 175-182.

41. Ahn, S.; Walt, D. R., Detection of *Salmonella* spp. Using Microsphere-Based, Fiber-Optic DNA Microarrays. *Analytical Chemistry* 2005, *77*, (15), 5041-5047.

42. Bowden, M.; Song, L.; Walt, D. R., Development of a Microfluidic Platform with an Optical Imaging Microarray Capable of Attomolar Target DNA Detection. *Analytical Chemistry* 2005, *77*, (17), 5583-5588.

43. Epstein, J. R.; Biran, I.; Walt, D. R., Fluorescence-based nucleic acid detection and microarrays. *Analytica Chimica Acta* 2002, *469*, (1), 3-36.

44. Epstein, J. R.; Lee, M.; Walt, D. R., High-Density Fiber-Optic Genosensor Microsphere Array Capable of Zeptomole Detection Limits. *Analytical Chemistry* 2002, *74*, (8), 1836-1840.

45. Epstein, J. R.; Leung, A. P. K.; Lee, K.-H.; Walt, D. R., High-density, microsphere-based fiber optic DNA microarrays. *Biosensors & Bioelectronics* 2003, *18*, (5-6), 541-546.

46. Epstein, J. R.; Walt, D. R., Fluorescence-based fibre optic arrays: a universal platform for sensing. *Chemical Society Reviews* 2003, *32*, (4), 203-214.

47. Ferguson, J. A.; Steemers, F. J.; Walt, D. R., High-Density Fiber-Optic DNA Random Microsphere Array. *Analytical Chemistry* 2000, *72*, (22), 5618-5624.

48. Steemers, F. J.; Ferguson, J. A.; Walt, D. R., Screening unlabeled DNA targets with randomly ordered fiber-optic gene arrays. *Nature biotechnology* 2000, *18*, (1), 91-94.

49. Curran, T.; Coulter, W. A.; Fairley, D. J.; McManus, T.; Kidney, J.; Larkin, M.; Moore, J. E.; Coyle, P. V., Development of a novel DNA microarray to detect bacterial pathogens in patients with chronic obstructive pulmonary disease (COPD). *Journal of Microbiological Methods* 2010, *80*, (3), 257-261.

50. Zhang, H.; Xu, T.; Li, C.-W.; Yang, M., A microfluidic device with microbead array for sensitive virus detection and genotyping using quantum dots as fluorescence labels. *Biosensors & Bioelectronics* 2010, *25*, (11), 2402-2407.

51. van Tongeren, S. P.; Degener, J. E.; Harmsen, H. J. M., Comparison of three rapid and easy bacterial DNA extraction methods for use with quantitative real-time PCR. *European Journal of Clinical Microbiology & Infectious Diseases* 2011, *30*, (9), 1053-1061.

CHAPTER 4

MICROFLUIDIC CHIP FOR REAL-TIME PCR

4.1 Introduction

To fully integrate a PCR assay onto a POC device, the following steps are required: extraction of DNA from the sample, amplification via thermocycling, and amplicon detection.[1-5] Chapter 3 described the development of a device integrating DNA extraction with PCR amplification, but the hybridization assay intended for amplicon detection proved unsuccessful. Other analytical techniques like CE and electrochemical detection have been integrated with PCR on microfluidic devices for downstream detection of amplicons,[6-13] but real-time PCR (rt-PCR) can perform amplification and detection simultaneously. There are a number of detection strategies for rt-PCR, but all use a fluorescent reporter that causes an increase in fluorescent signal as the concentration of products grows.[14-17] The first rt-PCR assay was described by Higuchi, et al., and used ethidium bromide (EtBr) to detect double stranded DNA.[18] EtBr is an intercalating dye, so its fluorescence increases when it is inserted into double stranded DNA. Since the amount of double stranded DNA in a PCR solution increases as the reaction proceeds, the fluorescent signal will increase and can be used to monitor the course of the reaction.

Amplicon detection with an intercalating dye is very flexible since it can be used with any primer set, but it is not specific.[14, 19] The dye will detect any double-stranded DNA in the reaction, even undesired non-specific amplification, which can lead to false

positives.[20, 21] Due to the toxicity of EtBr, it has been replaced by another intercalating dye, SYBR Green.[14, 17, 21, 22] An alternative to detection with an intercalating dye is to use a 5′ nuclease assay, commonly called a TaqMan assay. Holland, et al., described an assay using radioactively labeled oligonucleotide probes specific to the intended template that were degraded by the 5′-3′ exonuclease activity of the *Taq* polymerase.[23] During amplification, the *Taq* polymerase cleaves 5′ terminal nucleotides of double-stranded DNA, so if a probe is hybridized to the template strand, the polymerase will break it up into smaller pieces.[19, 21, 23-25] If a fluorophore is attached to the 5′ end of the probe and a quencher is attached to the 3′ end, then the exonuclease will separate the fluorophore from the quencher resulting in an increase in signal.[14, 15, 25] TaqMan probes are specific to the template DNA, so unlike with intercalating dyes, only amplification from the desired template will be detected.[14, 21, 24] Other probe designs including Molecular Beacons, Scorpion primers, and Plexor primers have also been developed that are specific like the TaqMan probes but do not rely on the exonuclease activity of *Taq* polymerase.[14, 19, 22, 24]

In addition to integrating detection onto a POC microfluidic PCR device, it is also desirable to incorporate some degree of multiplexing to test for multiple organisms simultaneously. The broad range primers used for multiplexing in Chapter 3 are not suitable for rt-PCR. The product sizes of ~300 bp are longer than the ideal for rt-PCR which usually has products less than 200 bp long.[14, 26] Multiplexing with the broad range primers could still be attempted with TaqMan or other sequence specific probes by putting different fluorescent dyes onto the probe for each organism, but the degree of multiplexing would be limited by the fluorophores.[15, 16, 25] Due to spectral overlap, the

maximum number of fluorophores that can be simultaneously analyzed is approximately four.[27] In addition to limitations in the degree of multiplexing, a single one-pot multiplexed assay can have problems with competition between primers and probes, overlapping primers producing dimers, and other non-specific interactions between primers and probes that can reduce amplification efficiencies.[28, 29] An alternative to this is to make an array of reaction wells and use a different primer and probe set in each well.[30-33] This multiplexing in space uses the same fluorophore for all of the reactions with the number of reaction wells limiting the degree of multiplexing. Location is used to identify target organisms with fluorescence from a particular well denoting the presence of the target corresponding to the primer and probe set in that well. Multiplexing in space also simplifies the necessary optical detection instrumentation since only one filter set is needed.

In this chapter, the 3-well PCR chip from Chapter 3 was adapted for real-time detection. The three PCR tube reservoirs were replaced with a monolithic PDMS reservoir containing seven reaction wells. The development of the rt-PCR assay and demonstration of successful extraction, amplification, and detection of DNA from lysed bacteria in saliva is described. The real-time assay was designed using *S. mutans,* methicillin-susceptible *S. aureus* (MSSA), and methicillin-resistant *S. aureus* (MRSA) as model organisms.

4.2 Materials and Methods

Materials and Reagents

Sylgard 184 PDMS was obtained from Dow Corning (Midland, MI) and prepared following the manufacturer's recommendation with a 10:1 polymer to cross-linker ratio.

AOMs (13 mm diameter, 60 μm thickness, and 0.2 μm pores) were obtained from Whatman (Piscataway, NJ). Brass blanks (brass alloy 360) were purchased from McMaster Carr (Chicago, IL). Octyltrichlorosilane and DNase, RNase, and protease free water were purchased from Sigma Aldrich (St. Louis, MO). ELIMINase cleaner was obtained from Decon Labs, Inc. (King of Prussia, PA). Glass cover slips (20 mm x 35 mm, 150 μm thick), Blocker BSA (10%) in PBS, and DNase and RNase free mineral oil were purchased from Thermo Fisher Scientific (Waltham, MA). Platinum *Taq* DNA polymerase and 2x Platinum qPCR Supermix-UDG were purchased from Invitrogen (Carlsbad, CA). Custom PrimeTime assay primers and double quenched probes were purchased from Integrated DNA Technologies (Coralville, IA). Purified gDNA from *S. mutans* (ATCC 25175), MSSA (ATCC 25923), and MRSA (ATCC 700699) was purchased from ATCC (Manassas, VA). Custom primer and probe sets and purified gDNA were resuspended following the instructions provided by their respective manufacturers. Unless otherwise noted, all dilutions were performed using DNase, RNase, and protease free water.

Cell lysate from MSSA cultures (ATCC 25923) was provided by Ryan Hayman from the Walt group at Tufts University. The cultures were autoclaved to lyse the cells. The autoclaved cultures were stored at 4 °C, and the Walt group has successfully amplified DNA from similar lysate stored for more than 4 years under the same conditions (data not published). Whole saliva was collected from a healthy volunteer by drooling into a clean centrifuge tube. Samples were collected immediately prior to analysis and were discarded after the experiment. A new sample was collected for each experiment using saliva.

Chip Design and Fabrication

The microfluidic chip design consisted of three main parts: the wells used for sampling and PCR reactions, the AOM for DNA extraction, and the microfluidic channel and AOM support structure for fluid handling. An image of the device and a schematic of its cross-section are shown in figure 4.1. The design of the microfluidic base was identical to the 3-well chip described in Chapter 3. A monolithic PDMS casting formed a reservoir containing seven wells, with each well measuring 2.4 mm in diameter and 3.0 mm in height for a volume of ~13.5 μL.

Molds for the 7-well PDMS reservoir were designed using BobCAD-CAM software (Clearwater, FL) and fabricated in brass blanks using a MicroMill DSLS 3000 (MicroProto Systems, Chandler, AZ) computer numeric controlled (CNC) machine. A double-sided molding strategy shown in figure 4.2 was used to cast a flexible PDMS mold (B) that mated with a second brass master (C). The PDMS mold was pretreated with octyltrichlorosilane that acted as a mold release agent. The PDMS mold and the second brass master were filled with uncured PDMS and degassed under vacuum, mated together to form the double-sided mold, and the PDMS was cured at 150 °C for 15 min. The resulting 7-well PDMS reservoirs (figure 4.2D) were then demolded.

The microfluidic base of the chip was fabricated and bonded to a glass cover slip as described in Chapter 3. An AOM was again placed over the micropost region of the chip. A 7-well PDMS reservoir was cleaned with ELIMINase and dried with N_2 gas, its underside was coated with a thin layer of uncured PDMS, and it was placed over the AOM. The cover slip-PDMS-AOM-reservoir sandwich was heated to 95 °C for 15 min

to cure the PDMS and complete chip fabrication. Chips were stored dry at room temperature.

Instrument Set-Up and Detection

Figure 4.3 shows an image of the instrument set-up for rt-PCR. Fluorescence imaging was conducted using a modified AZ100 Multizoom microscope (Nikon Instruments Inc., Melville, NY) equipped with a Roper Scientific (Trenton, NJ) frame transfer camera (Model NTE/CCD-512-EBFT, GR-1). A filter cube with 470/40 nm excitation, 495 nm dichroic, and 525/50 nm emission (Model 49002 ET – GFP, Chroma Technology Corp., Bellows Falls, VT) filters was used for fluorescence imaging of the FAM labeled probes.

Thermocycling of the chip was performed using a 40 mm x 40 mm Peltier stage built in-house using a high temperature Peltier device (Model VT-127-1.4-1.15-71; TE Technology, Inc., Traverse City, MI) driven with a Wavelength Electronics, Inc. (Bozeman, MT) model MPT5000 controller. A 250 μm thick layer of silver was bonded to the top of the Peltier device to ensure even heat distribution across its surface. The bottom of the Peltier was mounted onto a custom temperature controlled heat sink held at 60 °C by a recirculating water bath. Custom software written in LabView (National Instruments, Austin, TX) using Automicromanager[34] and Micromanager[35] was used to coordinate fluorescence imaging with temperature cycling.

PCR Development

To use a chip, 10 μL of sample solution was added to each well and vacuum was applied to the waste reservoir until the entire sample had been pulled through the AOM, usually 5-10 min. Then 5 μL of PCR master mix containing 1x Platinum qPCR

Supermix-UDG, 0.28 units of additional Platinum *Taq* DNA polymerase, and 1% BSA, as well as 0.5 μM of each primer and 0.25 μM of probe was added to each well. Since no post-PCR analysis on-chip is needed with rt-PCR, gelation was not expected to be problematic and 1% BSA could be used instead of the 0.75% BSA used in Chapter 3. The PCR solution in the wells was overlaid with 5 μL of DNase/RNase free mineral oil, and a drop of uncured PDMS was placed in the waste reservoir to seal the channel and prevent evaporation during thermocycling. The chip was then placed on the Peltier stage with a layer of mineral oil between the chip and the Peltier device to ensure good thermal contact. The thermocycling program used for all experiments was 2 min at 50 °C, 2 min at 95 °C, 60 cycles of 30 s at 95 °C followed by 65 s at 66 °C, with a final extension step of 2 min at 66 °C. No optimization of the PCR was performed. Images were taken at the end of each amplification cycle with a 500 ms exposure time. Chips were discarded after thermocycling, and a new chip was used for each experiment.

Three bacterial targets were used as models for assay development: *S. mutans*, a control organism commonly found in the human mouth, MSSA, and MRSA. Real-time primers and double quenched probes were designed using the PrimerQuest PCR design tool on the IDT website and sequences obtained from NCBI's GenBank (accession numbers AE014133.1 for *S. mutans* and NC_002758.2 for *S. aureus*). The primer and probes sequences were checked for specificity using NCBI's Primer-BLAST (http://www.ncbi.nlm.nih.gov/tools/primer-blast). For *S. mutans* the primers target a 137 bp region of the *16S rRNA* gene that encodes for a subunit of the ribosomes that translate mRNA into proteins. For *S. aureus* the primers target a 180 bp region of the *nuc* gene that encodes for an extracellular thermostable nuclease. For MRSA the primers

target a 147 bp region of the *mecA* gene that encodes for an altered penicillin-binding protein (PBP-2a) that gives MRSA its antibiotic resistance. The *nuc* primers will amplify template DNA from both MSSA and MRSA, while the *mecA* primers are specific to the gene that gives MRSA its antibiotic resistance.[36-38] The primer and probe sequences are listed in table 4.1.

Images were analyzed using ImageJ[39] (National Institutes of Health, USA) and IgorPro (Wavemetrics, Lake Oswego, OR) to determine if successful amplification had occurred. The average fluorescent signal from each well (~300 pixels) was measured in each image and plotted against cycle number. An image taken 3-5 cycles before the start of amplification was used as the background and subtracted from all the other images.

4.3 Results and Discussion

Primer Testing and Sensitivity

The primer and probe set for each model organism was first tested for specificity. These tests were done with a simplified chip design without the lower PDMS base layer containing the microposts and microfluidic channel. AOMs and 7-well PDMS reservoirs were sealed directly onto glass cover slips with uncured PDMS. The wells were filled with master mix containing primers and probes, and gDNA in solution. The PCR solution was overlaid with mineral oil to prevent evaporation during thermocycling. Each primer and probe set was tested with purified gDNA from each of the three strains of bacteria and found to be specific to the species or strain for which it was designed. The rt-PCR results for the *S. mutans* primer and probe set against 1 ng of *S. mutans* gDNA and 1 ng of MSSA gDNA is shown in figure 4.4A. An increase in fluorescence indicating amplification was seen only from the wells containing *S. mutans* gDNA and

not from the wells containing MSSA gDNA or from the blank well. The test results for the *S. aureus mecA* primer and probe set with 1 pg of MRSA gDNA and 1 pg MSSA gDNA is shown in figure 4.4B. Amplification is only seen from the wells containing MRSA gDNA and not from the wells containing MSSA gDNA or the blank well.

A test of the limit of detection for the *S. aureus nuc* primer and probe set was also performed using a simplified chip. Wells contained 1 ng (3×10^5-4×10^5 copies), 1 pg (300-400 copies), 30 fg (8-12 copies), or no (blank) MSSA gDNA. The amplification plot is shown in figure 4.5. A cycle threshold (C_t) line, designating a signal level above the background fluorescence, is indicated by the dashed line on the plot. The cycle number when the fluorescence level crosses the C_t line (C_t value) is the cycle when amplification can first be detected and can be used to calculate the initial concentration of template in a reaction.[16, 20, 21, 25] Duplicate reactions shown in the plot have nearly identical C_t values. Amplification was seen in all wells containing template DNA, with amplification detected at earlier cycles for the wells containing greater amounts of DNA. Amplification was seen from as little as 8-12 copies of MSSA gDNA, which is thought to be sufficient for most clinical samples of interest such that further optimization was not deemed necessary.

Cross-Contamination Between Wells

In a diagnostic test, the sample (saliva from a patient) will be identical in all wells while the primer and probe sequences will vary. In this way, simultaneous testing for many species and strains of bacteria by multiplexing in space is possible. Since the same fluorophore is used for detection for all target sequences, it is critical that probes do not travel between wells, creating false positives. There are three possible routes that primers

and probes could use to travel into other wells and cause cross-contamination. The first is cross-contamination over the tops of the wells. The volume of mineral oil overlaid on each reaction and the lack of fluid connecting the wells at their tops makes this unlikely. The second route is for cross-contamination at the interface between the wells and the membrane. When the 7-well-reservoir is sealed to the AOM, uncured PDMS wicks into the pores of the AOM and is polymerized. This effectively seals the wells at the surface of the AOM and prevents fluid from flowing laterally through the AOM. Thus each well is fully isolated above the AOM. The third route is for cross-contamination underneath the AOM in the micropost region. Since the wells are not isolated from each other in this region, this is the most likely route of cross-contamination.

To test this cross-contamination scenario, 1 pg of MSSA gDNA was captured in all seven wells of a chip. This experiment also served to verify that the DNA capture described with the 3-well chip in chapter 3 would also be successful with this slightly altered chip design. Master mix and primers and probes were added after DNA capture. *S. aureus nuc* primers and probes were added to three of the wells, *S. aureus mecA* primers and probes were added to another three wells, and the remaining well had no primers or probes added. A diagram showing the identity of the primers and probes added to each well is shown in the upper left of figure 4.6A. The primers and probes were added such that adjacent wells did not contain identical primers or probes. The chip was then thermocycled. Figure 4.6A shows the images collected after amplification cycles 25, 35, and 45 with increases in fluorescence only from the three wells containing *S. aureus nuc* primers and probes. As shown in the amplification plot in figure 4.6B, the only wells showing amplification were those containing primers and probes for the *S.*

aureus nuc gene. This indicates that each well remains isolated from the others to the extent that any amount of primers or probes traveling between the wells is not sufficient to result in an increase in fluorescence. As future experiments were performed, no false positives were detected in any known negative wells. This gives further confirmation that no cross-contamination is occurring between wells and that any increases in fluorescence from a well can be attributed to the primers and probes initially added to that well.

Simultaneous Multi-Analyte Detection

With no cross-contamination observed, the simultaneous detection of two bacterial species mixed in various combinations was undertaken. The initial test sample solution contained gDNA from both MSSA and *S. mutans* with 1 pg of gDNA from each species captured in each well. Primers and probes for the *S. mutans 16S rRNA*, *S. aureus nuc*, and *S. aureus mecA* genes were added to two wells each while the center well was left blank with no primers or probes. Amplification was seen for the target *S. mutans 16S rRNA* and *S. aureus nuc* genes as shown in the amplification plot in figure 4.7A. No amplification was seen in the blank and *S. aureus mecA* wells. The results of the same experiment performed with a sample solution containing 1 pg of *S. mutans* gDNA and 1 pg MRSA gDNA is shown in figure 4.7B. Since both *S. aureus nuc* and *S. aureus mecA* primers will amplify DNA from MRSA, amplification was seen from all three primer sets.

Test of Cell Lysate

The next experiment used cell lysate as the sample to determine if the DNA extraction step would remove the PCR inhibitors present in real world samples. Ten μL

of cell lysate from autoclaved MSSA cultures provided by the Walt group was used as the sample for each well of a chip. Primers and probes for the *S. aureus nuc* gene were added to six of the wells and one well was left as a blank with no primers and probes. The amplification plot is shown in figure 4.8. Amplification was seen from all wells except the blank, so DNA extraction with the AOM effectively removed any PCR inhibitors from the cell lysate. The concentration of DNA in the cell lysate (or even the concentration of cells in the solution prior to autoclaving) was unknown. Without a calibration curve, it is not possible to calculate the initial amount of DNA in the sample. Since the amplification can be detected at an earlier cycle than what is usually seen for 1 pg samples of MSSA gDNA, the DNA was probably more concentrated than 100 pg/mL, the concentration of the sample solutions used in the previous experiments.

Detection of Bacteria in Saliva

With the success of the cell lysate experiment, the detection of bacteria from a whole saliva sample was used to simulate a clinical sample. Whole saliva sample was collected from a healthy volunteer and heated to 95 °C for 10-15 min to thermally lyse the cells. On-chip DNA extraction was performed using the lysed sample. Each of the three primer and probe sets (*S. mutans 16S rRNA*, *S. aureus nuc*, and *S. aureus mecA*) was added to two wells and the seventh well was left as a blank. The amplification plot in figure 4.9 shows that only the *S. mutans 16S rRNA* wells exhibited amplification. *S. mutans* was chosen as a control organism because it is commonly found in the human mouth,[40] so these results were as expected for a sample from a healthy individual.

To simulate saliva from an infected individual, purified MSSA gDNA was spiked into saliva from the same healthy volunteer prior to thermal lysis. The sample was spiked

with MSSA gDNA to a concentration of 10-12 copies/μL. A volume of 10 μL of spiked saliva was added to each well and on-chip DNA extraction was performed. The amplification plot is shown in figure 4.10A. Amplification was seen for the *S. mutans 16S rRNA* gene and *S. aureus nuc* gene while no amplification was seen from the *S. aureus mecA* and blank wells. This experiment was repeated with MRSA gDNA in place of the MSSA gDNA. The amplification plot is shown in figure 4.10B and, as expected, amplification was seen from all three primer and probe sets. Differences between the three saliva experiments in the shape of the traces and in the apparent C_t value for the wells containing *S. mutans 16S rRNA* primers and probes are likely due to the initial amount of DNA in the sample. The samples were collected on different days and at different times of day so variations in the concentration of a particular microorganism are to be expected. For all of the experiments, the level of *S. mutans* present in the saliva sample was easily detected.

4.4 Conclusions

We have developed a microfluidic device that can extract DNA from lysed samples of whole saliva and perform rt-PCR amplification of the extracted DNA. We have successfully used it to detect bacteria (*S. mutans*) and spiked pathogenic bacterial gDNA (from MSSA and MRSA) in a whole saliva sample. The analysis time to go from saliva sample collection to results was less than 2.5 hrs. As with the device in Chapter 3, the on-chip sample preparation is particularly fast and simple. Though it only took a few minutes, the DNA extraction step still captured sufficient gDNA to detect 100-125 copies spiked into a whole saliva sample. Again unchanged from the device in Chapter 3, the only actions the user must perform are pipetting reagents into the reaction wells and

applying vacuum to the waste reservoir. Pairing the device with automated reagent dispensing could make it suitable for use in a clinical setting. The use of rt-PCR to perform amplification and detection simultaneously was a timesaving improvement over the design in chapter 3 that required off-chip detection or a separate detection region on-chip for hybridization assays.

The majority of the analysis time (>2 hrs) was due to thermocycling. While that is slow for a microfluidic chip, the overall analysis time for this device is still much faster than receiving results for samples sent to a centralized lab. Slow thermocycling conditions were used to reduce any problems that could have been caused by poor thermal conductivity of the PDMS and glass substrates that make up the bulk of the chip. In addition, the chip is heated from below so that it can be imaged from above. The PCR solutions are located above the AOM, so the entire bulk of the chip must be heated and cooled to the target temperature before the reaction mixture will reach the desired temperature. Alternative and more efficient heating strategies, using more thermally conductive materials, and decreasing the volume of the wells would likely reduce the thermocycling time and allow more wells to fit on a chip, increasing the number of targets for which the sample can be simultaneously tested. A commercial PCR assay, Cepheid's GeneXpert system (Sunnyvale, CA), can test for a variety of targets in less than an hour, including sample preparation and thermocycling, but a different sample cartridge must be used for each target. Our device can test for the presence of up to seven targets simultaneously. Since many respiratory infections present with similar symptoms, testing for multiple organisms will save time.

For the development of the device, real-time data was collected, but it may not be needed for all applications. In the developmental stages, collection of real-time data helps pinpoint experimental obstacles such as air bubbles or fluid evaporation. Monitoring the C_t values and the shape of the amplification curves also makes it easier to determine if experimental changes are inhibiting PCR.[41] For a simple diagnostic device, end-point detection by measuring only the initial and final fluorescence of the reactions would be satisfactory for determining a positive or negative response. This would simplify the data processing requirements of a reader device designed to operate the chip. For other applications, like the detection of oral microbes used as biomarkers for diseases such as pancreatic cancer, the concentration of the organism is important rather than just its presence.[42] For those applications, quantitative real-time data would need to be collected.

The pre-spotting of primers used for primer delivery with the 3-well chip in Chapter 3 was tested with this chip, but was not successful. Those experiments and an alternative strategy to deliver different primer sets to each well prior to DNA extraction are discussed in Chapter 5. The design of additional primer and probe sets would also be useful for this device. Because primers sets are not multiplexed in the wells, new primer and probe sets only need to be specific to the targeted organism and compatible with the thermocycling temperatures. This also means that the primer and probe sets on a chip can be combined in any fashion and chips can be tailored to specific diseases or groups of symptoms.

4.5 Tables and Figures

Table 4.1. Primer and probe sequences for the target organisms and genes. The probes are double-quenched and have a 6-FAM attached to the 5′ end, an Iowa Black Dark Quencher FQ attached to the 3′ end, and an internal ZEN quencher.

Organism/gene	Sequence
S. mutans/16S rRNA	
forward	5′-TCTTGATTGGACAGGTCAAGGAAA-3′
reverse	5′-ACGGCCATTTGGTACATCAACCT-3′
probe	5′-/6-FAM/AACCCGGTG/ZEN/CCAATGATGTTTGGGTT-/IaBkQ/-3′
S. aureus/nuc	
forward	5′-GGTGTAGAGAAATATGGYCCTGAAGC-3′
reverse	5′-AGCCAAGCCTTGACGAACTAAAGC-3′
probe	5′-/6-FAM/TGGACGTGG/ZEN/CTTAGCGTATATTTATGCT-GA/IaBkQ/-3′
MRSA*/mecA*	
forward	5′-CTGGAACTTGTTGAGCAGAGGTTCT-3′
reverse	5′-ACTGCTATCCACCCTCAAACAGGT-3′
probe	5′-/6-FAM/GACGTCATA/ZEN/TGAAGGTGTGCTTACAAGTG-C/IaBkQ/-3′

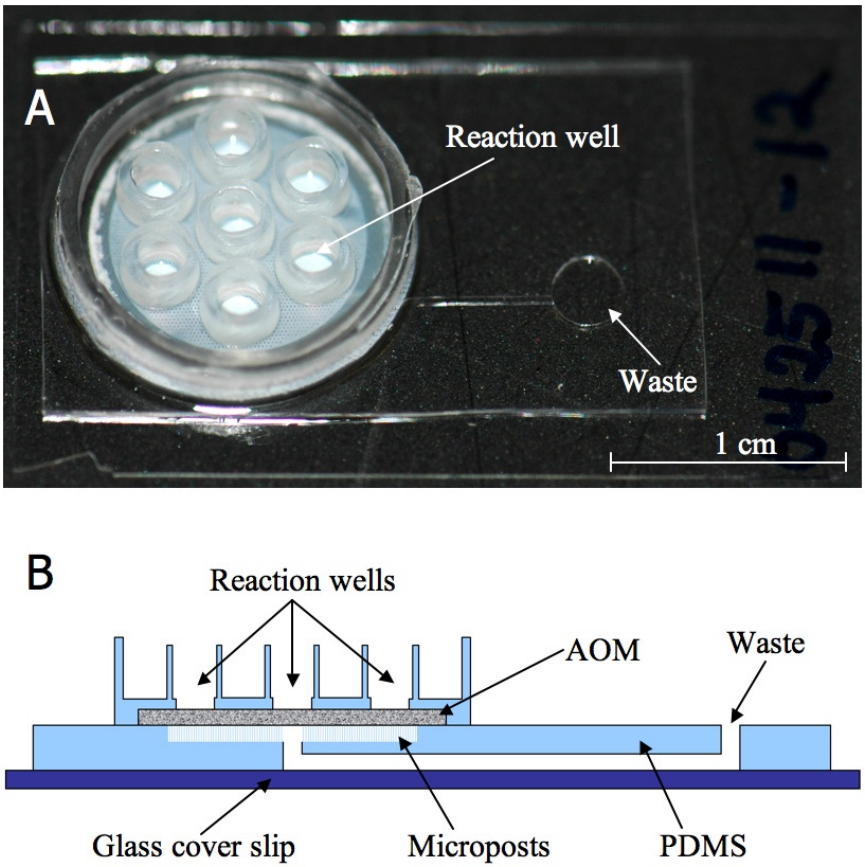

Figure 4.1. An image of the 7-well rt-PCR chip (A) and a schematic of its cross-section (B). The schematic is not to scale.

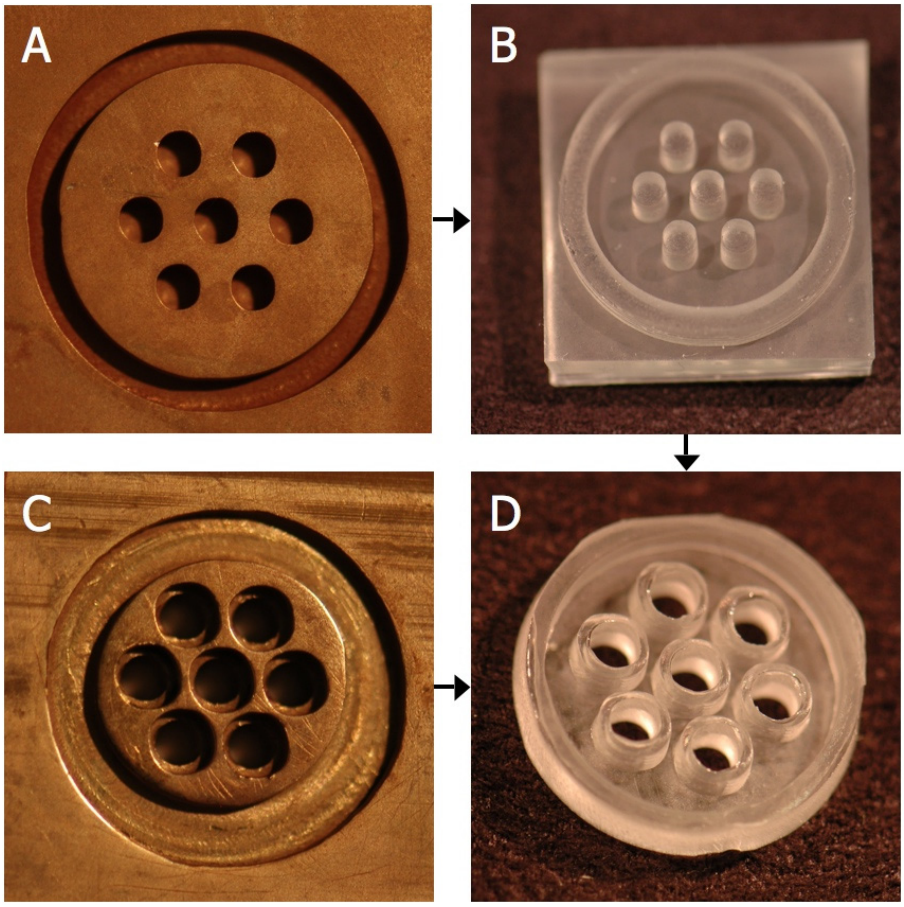

Figure 4.2. Images of the molds used to make the 7-well PDMS reservoirs. A brass master (A) is used to cast the PDMS half of the reservoir mold (B) which is mated to a second brass master (C) to form a double-sided mold used to cast the 7-well PDMS reservoirs (D). The entire piece in B is 2.54 cm square.

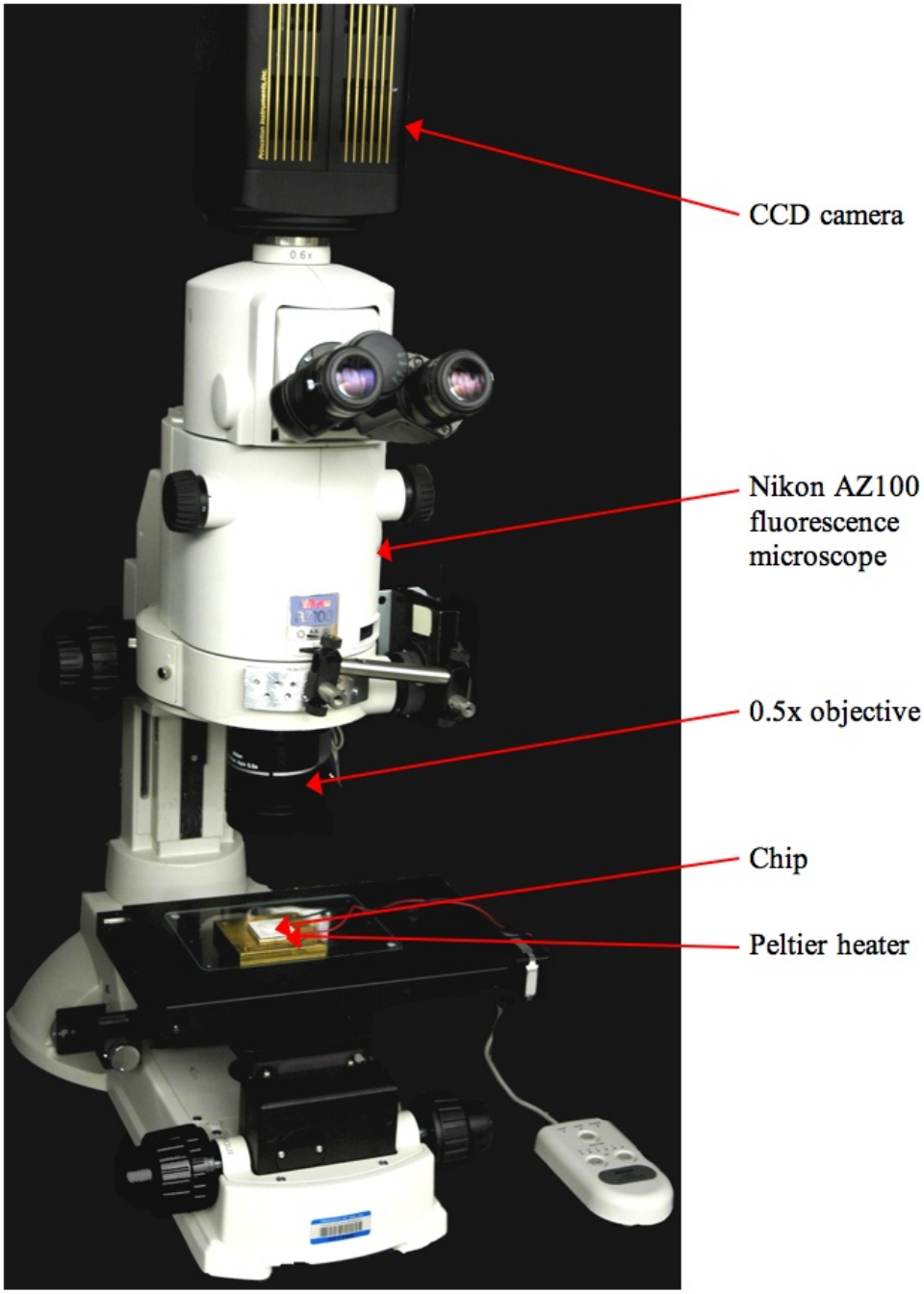

Figure 4.3. Image of the rt-PCR instrument set-up including the microscope, camera, and Peltier heater used for thermocycling the chip. The custom heat sink built in-house is not shown.

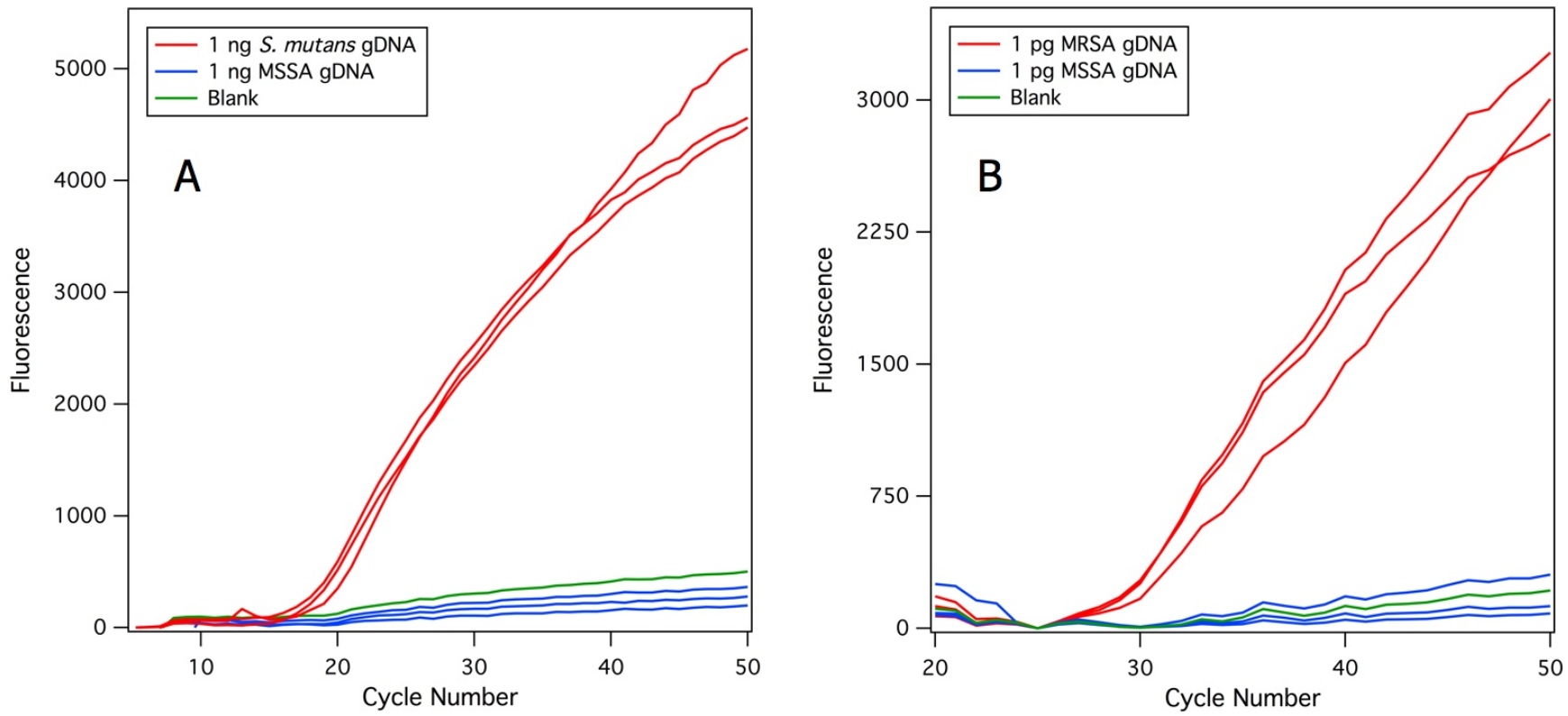

Figure 4.4. Real-time amplification plots for *S. mutans 16S rRNA* primers with *S. mutans* and MSSA gDNA (A) and for *S. aureus mecA* primers with MRSA and MSSA gDNA (B). In (A), 1 ng of gDNA was used for the sample, while in (B), 1 pg of gDNA was used. Both primer sets were found to be specific for their intended targets.

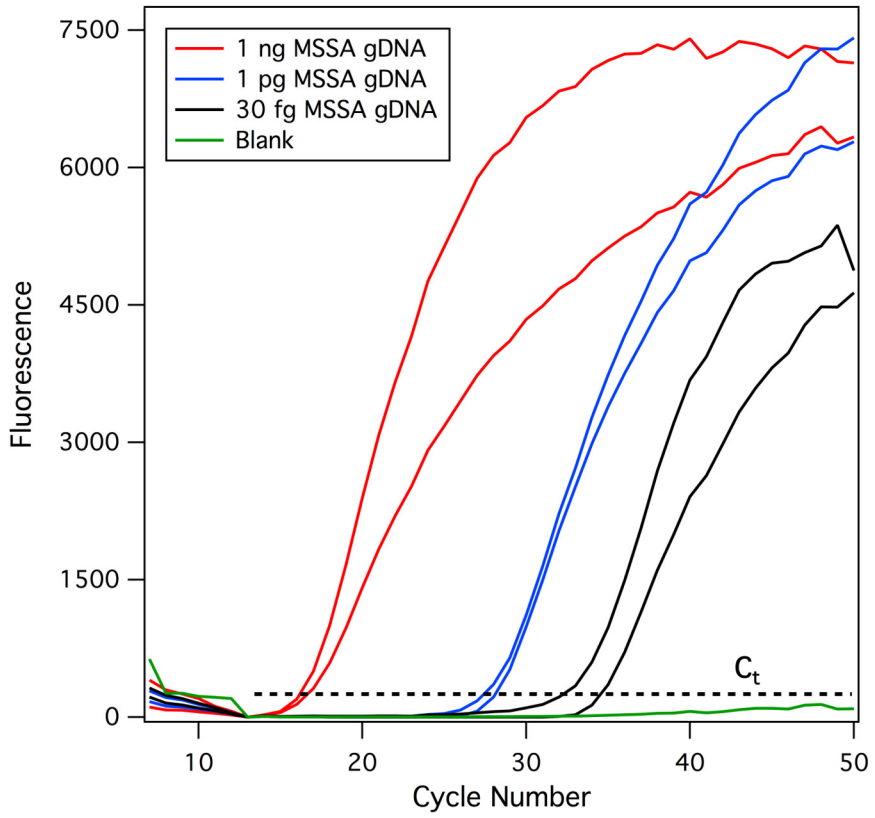

Figure 4.5. Real-time amplification plot for varying amounts of MSSA gDNA testing the limit of detection of the *S. aureus nuc* primer set. 1 ng of MSSA gDNA corresponds to 3×10^5-4×10^5 copies, 1 pg of MSSA gDNA corresponds to 300-400 copies, and 30 fg of MSSA gDNA corresponds to 8-12 copies. A dashed C_t line is shown on the plot. C_t value is a good indicator of starting concentration of template and duplicate reactions shown on this plot have nearly the same values. Amplification is first detected at a later cycle for wells containing a smaller amount of template DNA.

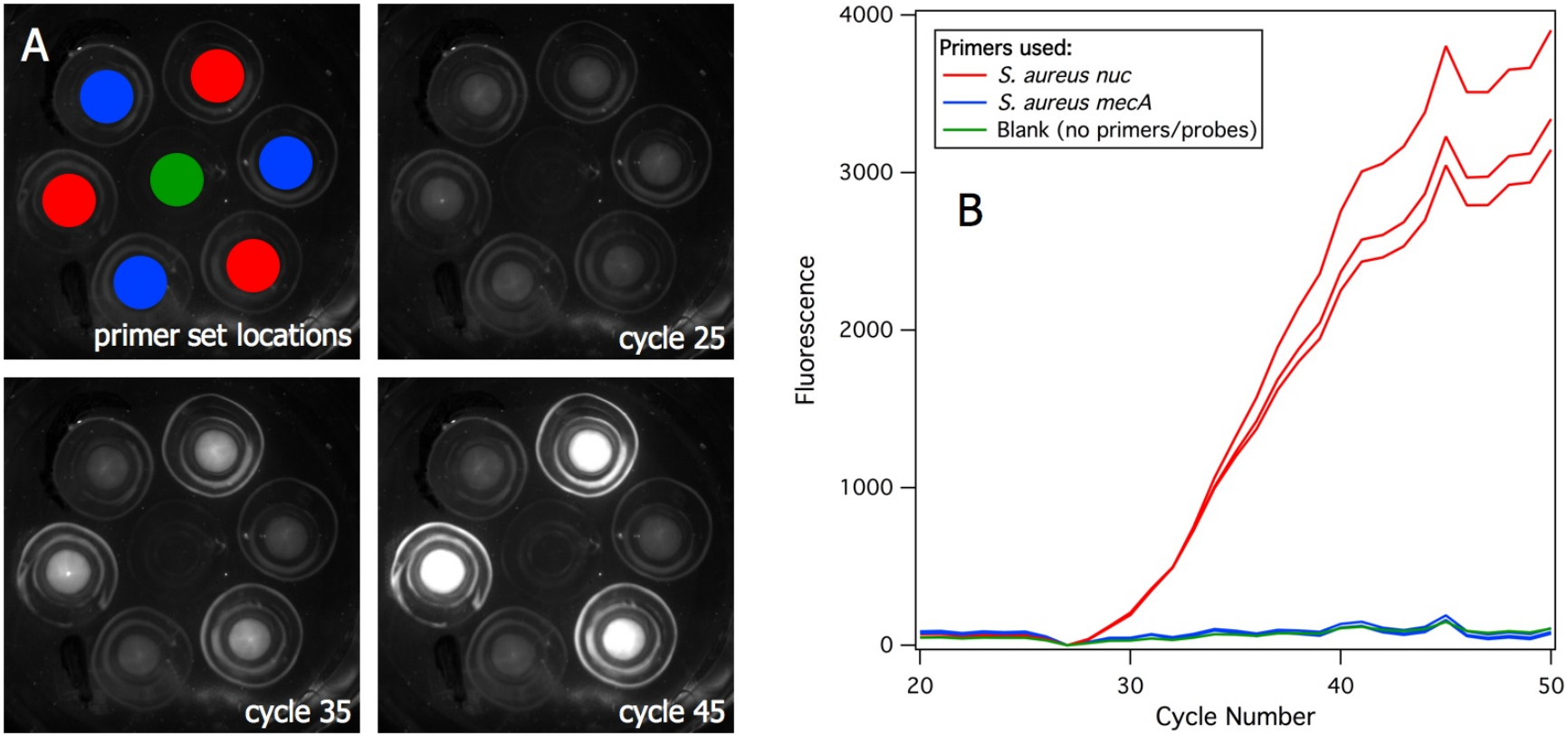

Figure 4.6. Fluorescence Images (A) and amplification plot (B) from testing for cross-contamination. The upper left image in A shows the primer set added to each well (colors correspond to the legend in B) and the other images were taken following cycles 25, 35, and 45. The real-time amplification plot for *S. aureus nuc* and *mecA* genes (B) demonstrates that there is no cross-contamination between wells. Each well contained 1 pg of MSSA gDNA as the sample. There are three wells for each primer set and one blank well without primers or probes.

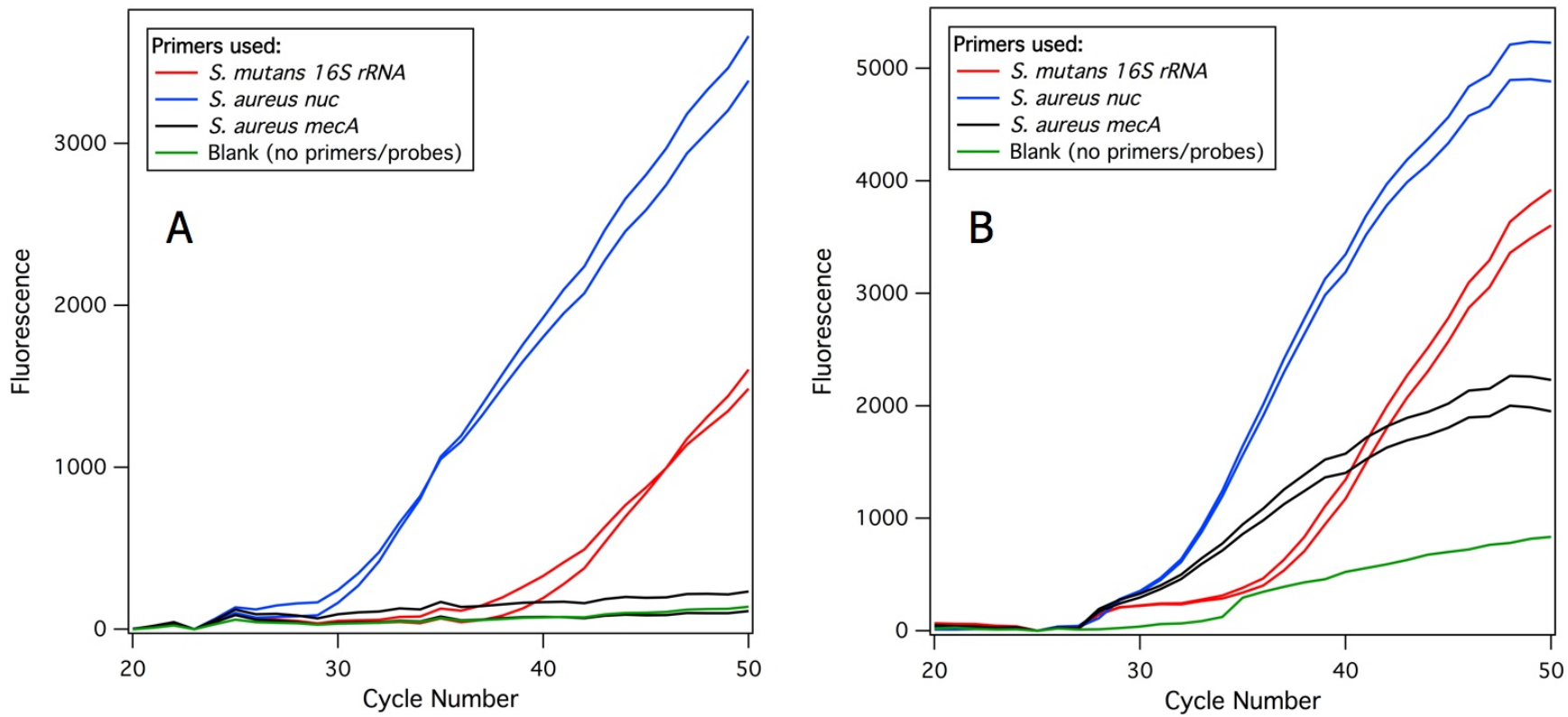

Figure 4.7. Real-time amplification plots showing simultaneous detection of multiple genes. In each plot there are two wells corresponding to each of the three primer sets and one blank well without primers or probes. In (A), the sample was 1 pg of gDNA from both *S. mutans* and MSSA. Positive results are seen for both the *S. mutans 16S rRNA* and *S. aureus nuc* primer sets. In (B), the sample was 1 pg of gDNA from both *S. mutans* and MRSA. Positive results are seen for all three primer sets.

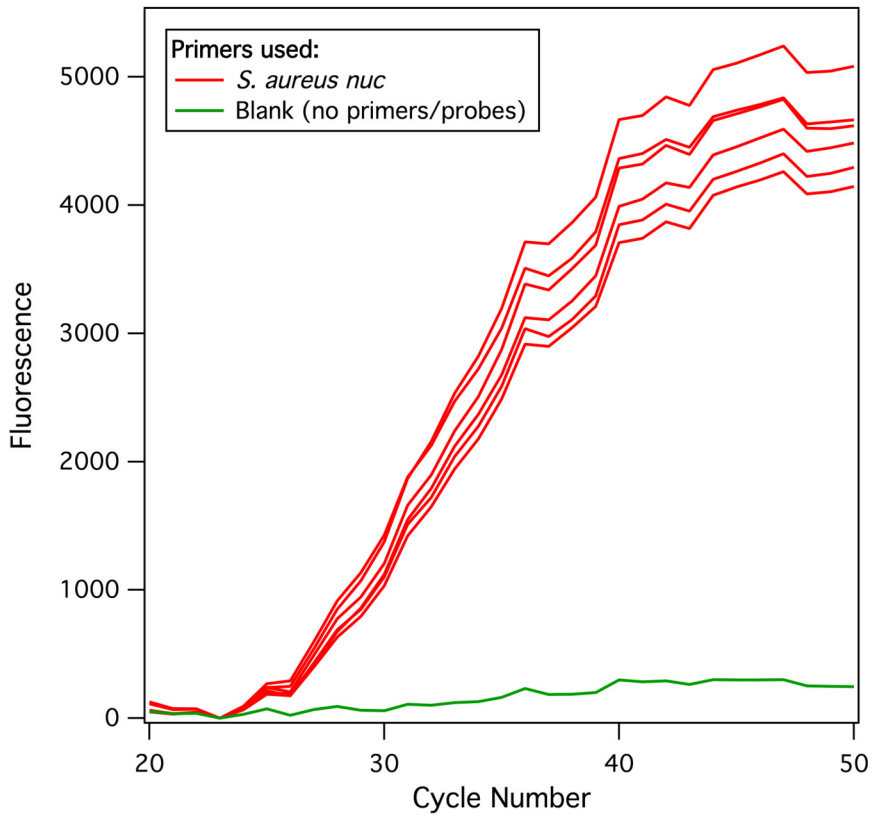

Figure 4.8. Real-time amplification plot for DNA extracted from MSSA cell lysate. Each well used 10 μL of MSSA cell lysate as the sample with six wells containing *S. aureus nuc* primers and probes and one blank well with no primers or probes. Positive results are seen for all six *S. aureus nuc* wells, but not for the blank well.

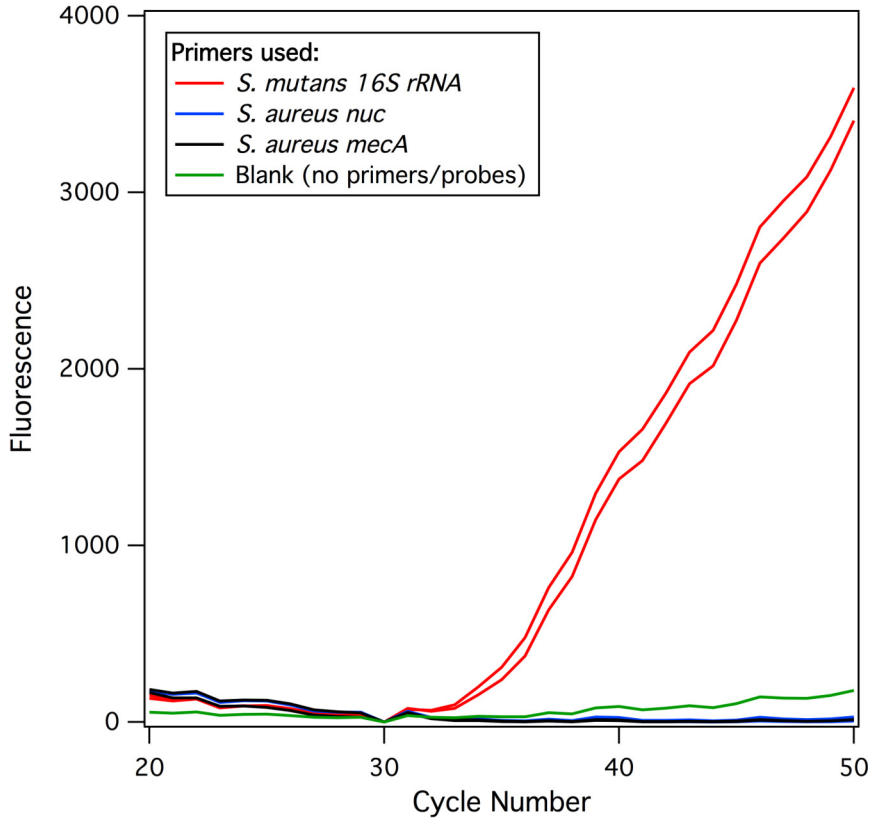

Figure 4.9. Real-time amplification plot for DNA extracted from whole saliva. Each well used 10 μL of thermally lysed whole saliva as the sample while the primers were varied between the wells. There are two wells corresponding to each of the three primer sets and one blank well without any primers or probes. Positive results are seen only for *S. mutans*, the control organism.

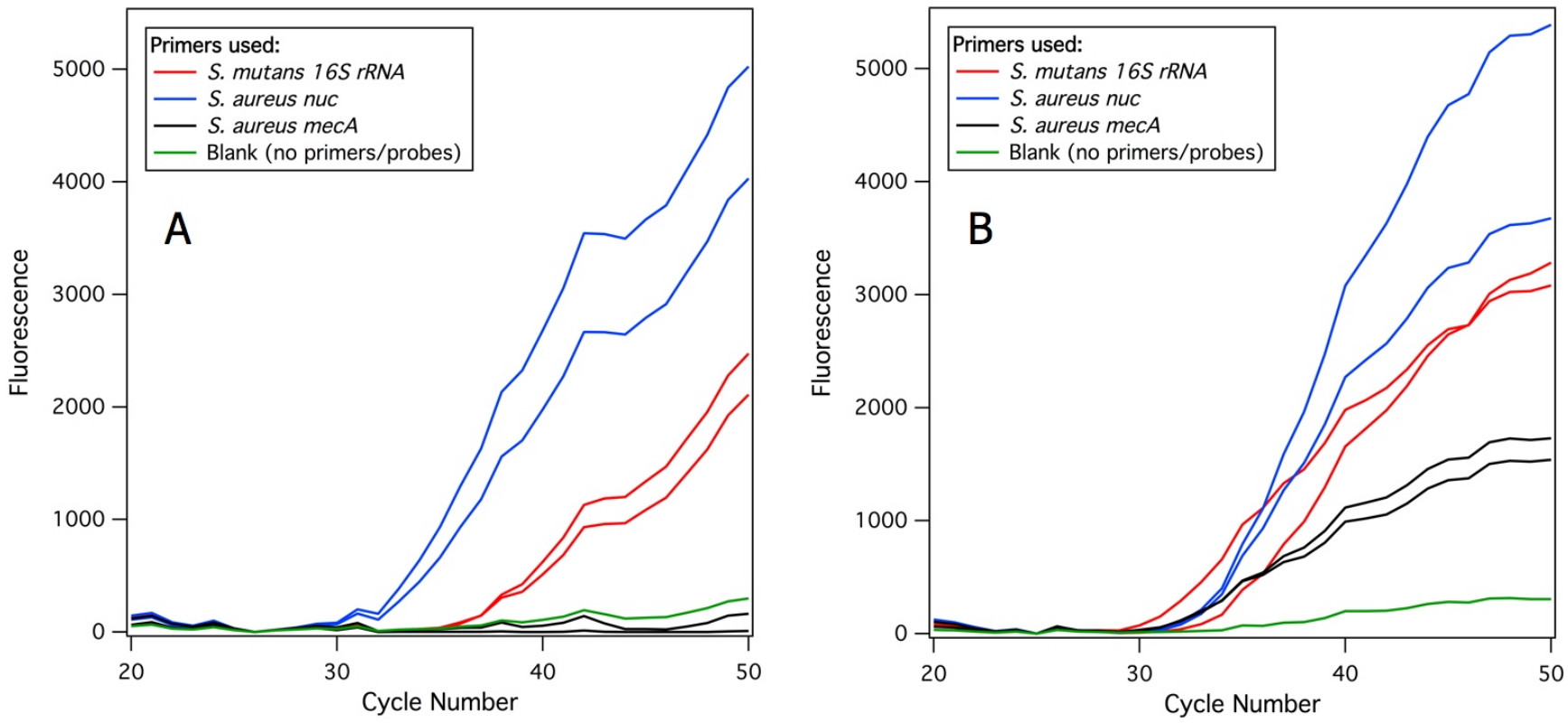

Figure 4.10. Real-time amplification plots for DNA extracted from whole saliva spiked with 0.33 pg (100-125 copies) of (A) MSSA or (B) MRSA gDNA. Each well used 10 μL of spiked whole saliva as the sample while the primers were varied between wells. In each plot there are two wells corresponding to each of the three primer sets and one blank well without primers or probes. (A) Positive results are seen for *S. mutans 16S rRNA* and *S. aureus nuc*, but not for *S. aureus mecA*. (B) Positive results are seen for all three primer sets.

4.6 References

1. Chen, L.; Manz, A.; Day, P. J. R., Total nucleic acid analysis integrated on microfluidic devices. *Lab on a Chip* 2007, *7*, (11), 1413-1423.

2. Kim, J.; Johnson, M.; Hill, P.; Gale, B. K., Microfluidic sample preparation: cell lysis and nucleic acid purification. *Integrative Biology* 2009, *1*, (10), 574-586.

3. Liu, P.; Mathies, R. A., Integrated microfluidic systems for high-performance genetic analysis. *Trends in Biotechnology* 2009, *27*, (10), 572-581.

4. Mariella, R., Sample preparation: the weak link in microfluidics-based biodetection. *Biomedical Microdevices* 2008, *10*, (6), 777-784.

5. Schulze, H.; Giraud, G.; Crain, J.; Bachmann, T. T., Multiplexed optical pathogen detection with lab-on-a-chip devices. *Journal of Biophotonics* 2009, *2*, (4), 199-211.

6. Chen, D.; Mauk, M.; Qiu, X.; Liu, C.; Kim, J.; Ramprasad, S.; Ongagna, S.; Abrams, W.; Malamud, D.; Corstjens, P.; Bau, H., An integrated, self-contained microfluidic cassette for isolation, amplification, and detection of nucleic acids. *Biomedical Microdevices* 2010, *12*, (4), 705-719.

7. Easley, C. J.; Karlinsey, J. M.; Bienvenue, J. M.; Legendre, L. A.; Roper, M. G.; Feldman, S. H.; Hughes, M. A.; Hewlett, E. L.; Merkel, T. J.; Ferrance, J. P.; Landers, J. P., A fully integrated microfluidic genetic analysis system with sample-in-answer-out capability. *Proceedings of the National Academy of Sciences of the United States of America* 2006, *103*, (51), 19272-19277.

8. Liu, R. H.; Yang, J.; Lenigk, R.; Bonanno, J.; Grodzinski, P., Self-Contained, Fully Integrated Biochip for Sample Preparation, Polymerase Chain Reaction Amplification, and DNA Microarray Detection. *Analytical Chemistry* 2004, *76*, (7), 1824-1831.

9. Prakash, A. R.; De La Rosa, C.; Fox, J. D.; Kaler, K. V. I. S., Identification of respiratory pathogen *Bordetella pertussis* using integrated microfluidic chip technology. *Microfluidics and Nanofluidics* 2008, *4*, (5), 451-456.

10. Sauer-Budge, A. F.; Mirer, P.; Chatterjee, A.; Klapperich, C. M.; Chargin, D.; Sharon, A., Low cost and manufacturable complete microTAS for detecting bacteria. *Lab on a Chip* 2009, *9*, (19), 2803-2810.

11. Thaitrong, N.; Toriello, N. M.; Del Bueno, N.; Mathies, R. A., Polymerase Chain Reaction-Capillary Electrophoresis Genetic Analysis Microdevice with In-Line Affinity Capture Sample Injection. *Analytical Chemistry* 2009, *81*, (4), 1371-1377.

12. Waters, L. C.; Jacobson, S. C.; Kroutchinina, N.; Khandurina, J.; Foote, R. S.; Ramsey, J. M., Microchip device for cell lysis, multiplex PCR amplification, and electrophoretic sizing. *Analytical Chemistry* 1998, *70*, (1), 158-162.

13. Yeung, S.-W.; Lee, T. M.-H.; Cai, H.; Hsing, I.-M., A DNA biochip for on-the-spot multiplexed pathogen identification. *Nucleic Acids Research* 2006, *34*, (18), e118.

14. Keer, J. T., Quantitative Real-time PCR Analysis. In *Essentials of Nucleic Acid Analysis: A Robust Approach*, Keer, J. T.; Birch, L., Eds. Royal Society of Chemistry: Cambridge, UK, 2008; pp 132-166.

15. Mackay, I. M., Real-time PCR in the microbiology laboratory. *Clincal Microbiology and Infection* 2004, *10*, (3), 190-212.

16. Park, S.; Zhang, Y.; Lin, S.; Wang, T.-H.; Yang, S., Advances in microfluidic PCR for point-of-care infectious disease diagnostics. *Biotechnology Advances* 2011, *29*, (6), 830-839.

17. Saunders, N. A., An Introduction to Real-Time PCR. In *Real-Time PCR: An Essential Guide*, Edwards, K.; Logan, J.; Saunders, N., Eds. Horizon Bioscience: Norfolk, UK, 2004; pp 1-11.

18. Higuchi, R.; Dollinger, G.; Walsh, P. S.; Griffith, R., Simultaneous Amplification and Detection of Specific DNA Sequences. *Bio/Technology* 1992, *10*, (4), 413-417.

19. Espy, M. J.; Uhl, J. R.; Sloan, L. M.; Buckwalter, S. P.; Jones, M. F.; Vetter, E. A.; Yao, J. D. C.; Wengenack, N. L.; Rosenblatt, J. E.; Cockerill, F. R.; Smith, T. F., Real-TIme PCR in Clinical Microbiology: Applications for Routine Laboratory Testing. *Clinical Microbiology Reviews* 2006, *19*, (1), 165-256.

20. Zhang, C. S.; Xing, D., Miniaturized PCR chips for nucleic acid amplification and analysis: latest advances and future trends. *Nucleic Acids Research* 2007, *35*, (13), 4223-4237.

21. Zhang, C. S.; Xu, J. L.; Ma, W. L.; Zheng, W. L., PCR microfluidic devices for DNA amplification. *Biotechnology Advances* 2006, *24*, (3), 243-284.

22. Mothershed, E. A.; Whitney, A. M., Nucleic acid-based methods for the detection of bacterial pathogens: Present and future considerations for the clinical laboratory. *Clinica Chimica Acta* 2006, *363*, (1-2), 206-220.

23. Holland, P. M.; Abramson, R. D.; Watson, R.; Gelfand, D. H., Detection of specific polymerase chain reaction product by ulitizing the 5′ → 3′ exonuclease activity of *Thermus aquaticus* DNA polymerase. *Proceedings of the National Academy of Sciences of the United States of America* 1991, *88*, (16), 7276-7280.

24. Lee, M. A.; Squirrell, D. J.; Leslie, D. L.; Brown, T., Homogeneous Fluorescent Chemistries for Real-Time PCR. In *Real-Time PCR: An Essential Guide*, Edwards, K.; Logan, J.; Saunders, N., Eds. Horizon Bioscience: Norfolk, UK, 2004; pp 31-70.

25. Lie, Y. S.; Petropoulos, C. J., Advances in quantitative PCR technology: 5′ nuclease assays. *Current Opinion in Biotechnology* 1998, *9*, (1), 43-48.

26. Edwards, K., Performing Real-Time PCR. In *Real-Time PCR: An Essential Guide*, Edwards, K.; Logan, J.; Saunders, N., Eds. Horizon Bioscience: Norfolk, UK, 2004; pp 71-83.

27. Huang, Q. Y.; Zheng, L. L.; Zhu, Y. M.; Zhang, J. F.; Wen, H. X.; Huang, J. W.; Niu, J. J.; Zhao, X. L.; Li, Q. G., Multicolor Combinatorial Probe Coding for Real-Time PCR. *Plos One* 2011, *6*, (1), e16033.

28. Birch, L.; Bailey, C. L.; Anderson, M. T., Multiplex PCR and Whole Genome Amplification. In *Essentials of Nucleic Acid Analysis: A Robust Approach*, Keer, J. T.; Birch, L., Eds. Royal Society of Chemistry: Cambridge, UK, 2008; pp 167-188.

29. SantaLucia, J., Jr., Physical Principles and Visual-OMP Software for Optimal PCR Design. In *PCR Primer Design*, Yuryev, A., Ed. Humana Press: Totowa, NJ, 2007; pp 3-33.

30. Liu, H.-B.; Ramalingam, N.; Jiang, Y.; Dai, C.-C.; Hui, K. M.; Gong, H.-Q., Rapid distribution of a liquid column into a matrix of nanoliter wells for parallel real-time quantitative PCR. *Sensors and Actuators B-Chemical* 2009, *135*, (2), 671-677.

31. Liu, J.; Hansen, C.; Quake, S. R., Solving the "World-to-Chip" Interface Problem with a Microfluidic Matrix. *Analytical Chemistry* 2003, *75*, (18), 4718-4723.

32. Matsubara, Y.; Kerman, K.; Kobayashi, M.; Yamamura, S.; Morita, Y.; Tamiya, E., Microchamber array based DNA quantification and specific sequence detection from a single copy via PCR in nanoliter volumes. *Biosensors & Bioelectronics* 2005, *20*, (8), 1482-1490.

33. Ramalingam, N.; Liu, H.-B.; Dai, C.-C.; Jiang, Y.; Wang, H.; Wang, Q.; Hui, K. M.; Gong, H.-Q., Real-time PCR array chip with capillary-driven sample loading and reactor sealing for point-of-care applications. *Biomedical Microdevices* 2009, *11*, (5), 1007-1020.

34. Ashcroft, B. A.; Oosterkamp, T., AutoMicromanager: A microscopy scripting toolkit for LABVIEW and other programming environments. *Review of Scientific Instruments* 2010, *81*, (11), 4.

35. Edelstein, A.; Amodaj, N.; Hoover, K.; Vale, R.; Stuurman, N., Computer Control of Microscopes Using µManager. In *Current Protocols in Molecular Biology*, John Wiley & Sons, Inc.: 2001.

36. Al-Talib, H.; Yean, C. Y.; Al-Khateeb, A.; Hassan, H.; Singh, K.-K. B.; Al-Jashamy, K.; Ravichandran, M., A pentaplex PCR assay for the rapid detection of methicillin-resistant *Staphylococcus aureus* and Panton-Valentine Leucocidin. *Bmc Microbiology* 2009, *9*, 113.

37. Hu, D.-L.; Omoe, K.; Inoue, F.; Kasai, T.; Yasujima, M.; Shinagawa, K.; Nakane, A., Comparative prevalence of superantigenic toxin genes in meticillin-resistant and meticillin-susceptible *Staphylococcus aureus* isolates. *Journal of Medical Microbiology* 2008, *57*, (9), 1106-1112.

38. Kilic, A.; Muldrew, K. L.; Tang, Y.-W.; Basustaoglu, A. C., Triplex real-time polymerase chain reaction assay for simultaneous detection of *Staphylococcus aureus* and coagulase-negative staphylococci and determination of methicillin resistance directly from positive blood culture bottles. *Diagnostic Microbiology and Infectious Disease* 2010, *66*, (4), 349-355.

39. Rasband, W. S. ImageJ, U.S. National Institutes of Health, Bethesda, MD, USA. http://imagej.nih.gov/ij/, 1997-2011

40. Petti, S.; Pezzi, R.; Cattaruzza, M. S.; Osborn, J. F.; Darca, A. S., Restoration related salivary Streptococcus mutans level: A dental caries risk factor? *Journal of Dentistry* 1997, *25*, (3-4), 257-262.

41. Kolari, K.; Satokari, R.; Kataja, K.; Stenman, J.; Hokkanen, A., Real-time analysis of PCR inhibition on microfluidic materials. *Sensors and Actuators B-Chemical* 2008, *128*, (2), 442-449.

42. Farrell, J. J.; Zhang, L.; Zhou, H.; Chia, D.; Elashoff, D.; Akin, D.; Paster, B. J.; Joshipura, K.; Wong, D. T. W., Variations of oral microbiota are associated with pancreatic diseases including pancreatic cancer. *Gut* 2012, *61*, (4), 582-588.

CHAPTER 5

PRIMER DELIVERY, RESTRICTION ENZYMES, AND FUTURE DIRECTIONS FOR THE PCR CHIP

5.1 Introduction

The PCR chip described in Chapter 4 integrates DNA extraction, amplification, and amplicon detection, and is easy to use, but the different primer and probe sets must still be pipetted into the individual wells following DNA extraction. This step increases the potential for user error and the storage and dispensing of multiple solutions makes automation more complex. Except for the specific primers and probes, all reagents are the same in each well; therefore, having preloaded primers and probes would simplify chip operation. Primer delivery strategies to eliminate this extra pipetting step are described in this chapter. The use of an intercalating dye (SYBR Green I) for amplicon detection instead of TaqMan probes and the resulting problems with non-specific amplification are also described. The use of restriction enzymes to digest the gDNA before amplification to improve reproducibility and signal is also explored.

Many strategies for PCR primer and reagent delivery have been described in the literature. The simplest method is to dry the primers onto the surface of the reaction vessel. Many microfluidic chips using dried primers have been described,[1-4] and this strategy was used for primer delivery with the 3-well chip described in Chapter 3. Another approach is to cover or encapsulate the primers and other reagents in paraffin wax.[5-7] The wax melts during the initial denaturing step of PCR, releasing reagents into

the solution. An added benefit of using wax is that after the initial melting, it can form a layer on top of the reaction mixture to help prevent evaporation. Primers have also been covalently coupled to microspheres, with PCR occurring at the surface of the bead.[8, 9] The Walt group has performed rolling-circle amplification, an isothermal technique, using oligonucleotides attached to microspheres through a biotin-streptavidin linkage that remains intact.[10] We have also taken advantage of biotin-streptavidin binding to couple primers to microspheres and deliver them to the PCR reaction.[11] For our microspheres, the streptavidin-biotin linkage remains intact during DNA extraction steps at room temperature but is broken during the initial heating steps of PCR, releasing the primers and probes into solution.[12] These primer beads can be loaded into the wells of a PCR chip before DNA extraction and the primers will be released as amplification begins.

Another possible improvement to the PCR assay is to incorporate restriction enzyme digestion prior to PCR. PCR efficiency is usually better for smaller sized templates,[13] and one way to reduce the size of template DNA in a controlled, reproducible manner is to use restriction enzymes. These endonucleases recognize specific DNA sequences and then cleave both strands of double-stranded DNA into fragments. Class I enzymes cleave the DNA at random sites unrelated to the recognition sequence.[14, 15] Class II enzymes are much more useful since they cleave the DNA close to or within the recognition site, usually 4-8 bp long, and they are the most commonly utilized.[14, 15] Class III enzymes also cleave the DNA at a specific site, but it is usually 20-30 bp away from the recognition sequence.[14] Two different enzymes may often recognize the same sequence (isoschizomers) but can sometimes cleave the DNA at different positions (neoschizomers).[14] Class II enzymes are particularly useful for

applications like DNA mapping, to find the position of functional sites, and DNA fingerprinting, to identify species, strains, or even individuals from their gDNA.[14, 15] Less commonly, restriction enzymes are used to digest gDNA samples before PCR to improve amplicon yields and reduce non-specific amplification.[13, 16, 17] Enzymes are chosen that will not cleave within the targeted sequence but will cleave peripheral regions that may non-specifically bind primers.[16, 17] Pre-PCR digestion also makes circular bacterial gDNA linear, which can make the template DNA more available to the primers.[17]

5.2 Materials and Methods

Materials and Reagents

Biotinylated forward and reverse primers for *S. mutans 16S rRNA*, *S. aureus nuc*, and *S. aureus mecA* with the sequences listed in table 4.1 were purchased from Integrated DNA Technologies (Coralville, IA). ProMag 3 series streptavidin coated magnetic microspheres with a mean diameter of 3.28 μm were purchased from Bangs Laboratories, Inc. (Fishers, IN). Tween 20 was purchased from Bio-Rad (Hercules, CA). PCR tubes (200 μL) were obtained from Eppendorf (Hauppauge, NY). Class II restriction enzymes MwoI, Bpu10I, and EcoRV-HF, and 10x NEBuffer 3 were purchased from New England BioLabs (Ipswich, MA). Parafilm M was obtained from Bemis Company, Inc. (Neenah, WI). Petri dishes, 10 mm x 15 mm, were obtained from BD Falcon (Franklin Lakes, NJ). Purified gDNA from *S. mutans* (ATCC 25175), MSSA (ATCC 25923), and MRSA (ATCC 700699) was purchased from ATCC (Manassas, VA). Forward and reverse *S. mutans 16S rRNA* primers with AT-rich flaps, 10x PCR buffer, and 10,000x SYBR Green I nucleic acid gel stain were purchased from Invitrogen (Carlsbad, CA). Primers

and purified gDNA were resuspended following the instructions provided by their respective manufacturers. DNase, RNase, and protease free water water, DNase/RNase free polyurethane amplification tape (PCR tape), lithium chloride (LiCl), and Trizma base were purchased from Sigma-Aldrich (St. Louis, MO). Tris Hydrochloride (Tris-HCl) buffer, sodium chloride (NaCl), potassium chloride (KCl), and magnesium chloride ($MgCl_2$) were purchased from Thermo Fisher Scientific (Waltham, MA). TTL buffer was prepared with 100 mM Tris-HCl, 0.1% Tween 20, 1 M LiCl, and a pH of 8.0. TT buffer was prepared with 250 mM Tris-HCl, 0.1% Tween 20, and a pH of 8.0. Mock PCR buffer was prepared with 20 mM Trizma, 50 mM KCl, 2.5 mM $MgCl_2$, and a pH of 8.5. Unless otherwise noted, all dilutions were made with DNase, RNase, and protease free water.

Primer Beads

Primer beads were made by coupling biotinylated primers to streptavidin coated magnetic microspheres. The primer sequences are the same as the forward and reverse primer sequences listed in table 4.1, with the addition of a biotin attached to the 5′ ends with a C6 spacer arm. One set of beads was made for each primer set, with a 1:1 mixture of both forward and reverse primers coupled to the beads unless otherwise noted. To couple primers to the beads, the beads were first washed and resuspended in TTL buffer. Biotinylated primers were diluted in TTL buffer and combined to make the oligonucleotide mixture with a concentration of 0.4 mM total primers, 0.2 mM each of the forward and reverse primers. The oligonucleotide mixture was added to the beads in TTL buffer to make a solution with 2 nmol primers/mg beads and incubated for at least 15 min at room temperature while shaking with a vortex mixer (Fisher Scientific,

Waltham, MA). The beads were then washed twice with TT buffer and resuspended in mock PCR buffer for storage.

Primer Delivery

Primer delivery experiments were carried out using the 7-well rt-PCR chips described in Chapter 4. DNA extraction and PCR were performed as described in section 4.2 with the same thermocycling program, instrument set-up, and data analysis. For experiments using spotted primers or primer beads, the primers and probes were omitted from the PCR master mix. For primer spotting, the same primers and probes used in Chapter 4 were spotted into the wells prior to DNA extraction. Tube-mounted AOMs were the same as those described in Chapter 3, and experiments with them were carried out as previously described. For primer bead experiments, the TaqMan probes were not used. Instead, 1x SYBR Green was added to the master mix for detection. A 0.5 μL volume of primer beads, corresponding to approximately 500 nM delivered primers, was used in each reaction well instead of the primers and probes usually added with the master mix.

Restriction Enzyme Digestions

Restriction enzymes that cut close to the target region for each primer set but do not cut within any of the target regions were chosen using NEBcutter v2.0 on the New England BioLabs website.[18] The restriction enzyme digestions were performed in PCR tubes and incubated using an Eppendorf Mastercycler personal (Eppendorf). The digestions were performed in 10 or 20 μL volumes containing 1x NEBuffer 3, 0.2 units/μL EcoRV-HF enzyme, 0.2 units/μL Bpu10I enzyme, and 1 pg/μL gDNA from each of type of gDNA in the sample. The digestions were incubated at 37 °C for 30 min,

then MwoI enzyme was added to a concentration of 0.2 units/μL and the digestion was incubated at 60 °C for another 30 min. One μL volumes of the digestion reactions were then used as samples for PCR. PCR in tubes was performed with primer beads and the same PCR master mix used for on-chip PCR but with a 10 μL volume and without SYBR Green. PCR products from PCR performed in tubes were analyzed with the Agilent 2100 Bioanalyzer (Agilent, Santa Clara, CA). On-chip PCR with digested template was performed with primer beads, SYBR Green, and the same PCR master mix as usual.

5.3 Results and Discussion

Primer Spotting and On-Chip PCR

After using the 7-well PCR chips to perform rt-PCR of gDNA captured on-chip with an AOM, the primer spotting technique described in Chapter 3 was tested with the real-time primer and probe sets. Each well of a 7-well PCR chip was spotted with 2.5 pmol of each primer and 1.25 pmol of probe from the *S. aureus nuc* primer and probe set and dried at room temperature. PCR master mix and gDNA were then added to the wells, with 1 pg MSSA gDNA added to three wells, 1 pg MRSA gDNA added to three wells, and one well left as a blank, with water used in place of the gDNA solution. DNA capture was not performed in this experiment. The chip was thermocycled and the amplification plot is shown in figure 5.1. Amplification was seen in all six positive wells, although it was detected later for one of the wells containing MSSA gDNA. Amplification is also detected in the blank well, possibly due to a small amount of template migrating into the blank well below the membrane. While experiments in Chapter 4 demonstrated no detectable cross-contamination of primers and probes between wells, even a very small amount of template cross-contamination is much easier

to detect. The chip was designed to use the same template in all wells, so a small amount of template cross contamination is not a concern with regard to future experiments.

With this initial success, combining primer spotting and DNA capture with the real-time primers and probes was tested. Each well of a chip was spotted with 2.5 pmol of each primer and 1.25 pmol of probe from the *S. mutans 16S rRNA* primer and probe set, and dried at room temperature. Ten μL of solution containing 1 pg of *S. mutans* gDNA was filtered through six wells, and water was used in the seventh well (the blank). PCR master mix was then added to all wells and the chip was thermocycled. No amplification was detected. Since previous experiments described in Chapter 3 combining pre-spotted primers with DNA extraction were successful, these results were surprising. From this experiment, it was unclear whether the DNA capture step eluted the pre-spotted primers and probes or if the pre-spotted primers interfered with DNA capture.

To determine the cause of PCR failure for pre-spotted primers combined with DNA extraction, primer spotting was tested using a 200 mM NaCl solution in place of the DNA solution. Template DNA was added to the wells with the master mix. *S. aureus nuc* primers and probes were spotted and dried into each well and 10 μL of the NaCl solution was filtered through the AOM in three wells to simulate the DNA capture step. The NaCl solution was used in place of water because the addition of NaCl was previously found to increase DNA capture and might increase primer retention if the primers were indeed being eluted. The remaining four wells were used as positive controls, with pre-spotted primers but no NaCl wash or DNA capture step. Master mix and 1 pg of MSSA gDNA was then added to all seven wells and the chip was thermocycled. The amplification plot is shown in figure 5.2A. While the positive

controls show amplification as expected, the wells incorporating a wash step do not. This indicates that the primers and probes are eluted during DNA capture steps with this chip design. Since primer spotting combined with DNA capture was previously successful with the 3-well chip, it is possible that the primers also remained on the AOM for this chip but that the probes did not. To determine if successful amplification did occur, the PCR products from the experiment were analyzed with the Bioanalyzer. The gel representation of the results is shown in figure 5.2B. The expected product (180 bp) is seen for the four positive controls that did not incorporate a wash step, while a weak product band is seen for just one of the three wells that did use a wash step. Though amplification occurred in that well, no product was seen from the other two wells, indicating that with these primer sets and chip design both primers and probes are eluted during DNA capture.

To further investigate solutions for integrating primer preloading onto the 7-well chips, the previous experiment was repeated with tube-mounted AOMs. The goal was to repeat the previous PCR failure and then use the tube-mounted AOMs to test out potential solutions. After primer spotting and washing, the AOMs were punched out into clean PCR tubes, PCR reagents and gDNA were added, and PCR was performed on the bench top thermocycler with a 10 μL reaction volume rather than the 5 μL volume used on-chip. Nine tube-mounted AOMs were spotted with primers and probes, and dried as before. The amount of primers and probes spotted onto the AOMs was doubled since the reaction volume was doubled. Three tube-mounted AOMs were positive controls that did not use a wash step. Another three were washed with 10 μL of DNase/RNase free water, and the final three were washed with 10 μL of 200 mM NaCl. For each set of three tube-

mounted AOMs, two reactions were carried out with 1 pg MSSA gDNA and one was left as a blank. The Bioanalyzer results are shown in figure 5.3. The expected product band is seen for all tubes that contained gDNA, and no difference between those that incorporated a wash step and the positive controls was observed. This experiment indicated that the tube-mounted AOMs did not correlate well to the chip and should not be used to explore ways to make primer spotting work on-chip.

One possible reason for PCR failure in previous on-chip experiments was that the amount of primers, enough for a 1x primer and probe concentration in the final reaction volume, was too small. Increased amounts of primers were spotted into the wells, from 3x to 10x. The experiment was performed with *S. aureus nuc* primers and probes, and with 1 pg MSSA gDNA used in all wells except the blank. Two wells and the blank used 3x primers and probes, another two wells used 4x primers and probes, and the final two wells used 10x primers and probes. All wells were washed with 10 μL of DNase/RNase free water after the primers and probes were dried in the wells. No amplification was seen for any amount of primers and probes. Although it is not yet know why preloading of the primer sets worked for the 3-well chips with *gyrB* primers and the tube-mounted AOMs but doesn't work for the 7-well chips and rt-PCR primer sets, it may be due to an increased surface area of AOM exposed in the 3-well chips and tube-mounted AOMs. With a larger surface area, the AOMs will have more sites for capturing oligonucleotides as well as gDNA. It is also likely that longer template DNA is more strongly captured than short oligonucleotides, and the primers are eluted by the template during the DNA capture step. With even 10x pre-spotted primers resulting in failed PCR, other primer delivery strategies were explored.

Primer Beads and On-Chip PCR

Primer beads, with oligonucleotides attached through a biotin-streptavidin linkage, are a different way to deliver the primers to each well before DNA extraction. The primers' attachment to the microspheres prevents their removal, unlike pre-spotting directly onto the AOM. The initial sets of beads were functionalized with either a forward or reverse primer. Another set of beads was functionalized with an equal mixture of forward and reverse primers. The first on-chip experiment with the primer beads was to determine if the primers would remain on the beads during DNA extraction. A mixture of primer beads with only the forward and reverse *S. aureus nuc* primers was added to three wells, primer beads with both *S. aureus nuc* primers were added to another three wells, and the final well was left as a blank with no primers. Then 10 μL of 100 pg/mL MSSA gDNA was filtered through each well, master mix containing SYBR Green was added and overlaid with mineral oil, and the chip was thermocycled. The amplification plot is shown in figure 5.4. Amplification was seen from all wells except the blank, showing that the primer beads retain the primers during DNA extraction and release them during the initial heating steps. The primer concentration was sufficient for PCR and no inhibition due to the presence of the microspheres was observed. Since beads with both primers worked just as well as a mixture of forward primer and reverse primer bead sets and required only one pipetting step to load onto the chip instead of two, beads with both primers were used for all future experiments.

Storage of Primer Beads On-chip

With successful primer delivery and PCR amplification using the primer beads demonstrated, the potential on-chip storage of the beads was explored. For two chips, *S.*

aureus nuc primer beads were loaded into five of the seven wells. One well was left empty to be used as a blank and another was left empty to use as a positive control with fresh primer beads loaded on the day of the experiment. After primer bead loading, the reservoirs of the chips were covered with PCR tape, the chips were placed into Petri dishes sealed shut with Parafilm. One chip was stored at 4 °C while the other chip was stored at room temperature.

The chip stored at 4 °C was tested 39 days later. Fresh primer beads, from a different batch than the beads stored on the chip, were loaded into the positive control well. DNA extraction was performed with 1 pg of MSSA gDNA filtered through each well. The chip was thermocycled, and the amplification plot is shown in figure 5.5. All wells showed successful amplification although amplification is detected later for the fresh primer beads compared to those stored on-chip. This could be due to some batch-to-batch variation in the primer beads, or some unexpected inhibition of the PCR in the positive control well. It was unknown whether the streptavidin-biotin linkage attaching the primers to the microspheres would remain intact for more than a month in solution, much less dried in the wells of a chip. This experiment shows that the streptavidin-biotin linkage does remain intact during storage, retaining the primers on the beads, and preventing them from being eluted during DNA extraction.

The chip stored at room temperature was tested 62 days after loading the primers. The same procedure used for the chip stored at 4 °C was used for this chip. Primer beads from a different batch than the beads stored on-chip were again used for the positive control well. The amplification plot is shown in figure 5.6. The plot shows even better results for this chip than for the chip stored at 4 °C, which was unexpected since the

primer beads in solution are stored at 4°C. The start of detectable amplification is closely grouped for the wells with stored beads, and only slightly later for the positive control with fresh beads. This shows that the streptavidin-biotin linkage attaching the primers to the beads can remain intact for more than 2 months at room temperature without adversely affecting DNA extraction or PCR. This is useful for a POC device, since the various sets of primer beads can be loaded into wells at the time of manufacture and the loaded chips can be stored by clinicians at room temperature until needed.

Primer Dimers

One potential problem with the primer beads is that they do not include a probe for product detection. Instead, SYBR Green I intercalating dye is added into the master mix. Unlike the TaqMan probes, intercalating dyes like SYBR Green are not specific to a particular sequence, detecting any double stranded DNA including non-specific amplification such as primer dimers. Primer dimers are formed when the 3′ ends of two primers anneal to each other with subsequent amplification by the polymerase.[19, 20] The primer dimers not only compete with the intended target for PCR reagents, potentially inhibiting PCR, but also will be detected by intercalating dyes.[20, 21] The presence of primer dimers is easily determined with gel electrophoresis. Primer dimers will show up as a band approximately double the size of the primers.

To determine whether primer dimers were forming during on-chip PCR with primer beads, a simple PCR chip, with a 7-well reservoir and AOM affixed directly onto a glass cover slip with PDMS, was loaded with *S. aureus nuc* primer beads in all wells. Master mix was then added to all wells, and 1 pg of MSSA gDNA was added to four of the wells while the remaining three were left as blanks. The chip was thermocycled, and

the PCR products were collected off-chip and analyzed with the Bioanalyzer. The amplification plot and Bioanalyzer results are shown in figure 5.7. In the plot, all wells show amplification, including the blanks. The false positives are explained by the Bioanalyzer results, which show primer dimer formation in nearly all of the wells. Even in lanes 3 and 4, which correspond to the traces showing the earliest detectable amplification, there are very weak primer dimer bands. One of the other wells with template DNA shows bands for both products and primer dimers (lane 1), while the final MSSA gDNA well shows only primer dimers and no product (lane 6). Primer dimer bands are also seen for all of the blank wells. As the amplification plot demonstrates, with these experimental parameters it is impossible to tell desired amplification from undesired, non-specific amplification without further analysis. This could lead to false positives for a POC device relying on rt-PCR detection with SYBR Green.

The products from the on-chip storage of primer beads could not be analyzed with the Bioanalyzer, so there is no way to know whether the amplification detected was of the target DNA or of the primers. However, whether the products were from the target or from primer dimers, the amplification results do indicate that the primers are retained on-chip through storage and subsequent DNA extraction.

Following the detection of primer dimers from PCR with primer beads, a variety of strategies were tested to reduce or eliminate their formation. The first attempt was to add primer flaps to the PCR primers. Primer flaps were described by Afonina et al. and are AT-rich 12-bp regions (AATAAATCATAA) added to the 5′ end of both the forward and reverse primers.[22] They were found to increase signal intensity during PCR for reactions with probes or SYBR Green, and in some cases, improve PCR performance and

C_t values. These flaps were added to the *S. mutans 16S rRNA* primers and tested with a simple chip and the same experimental conditions used for the previous experiment but with *S. mutans* gDNA instead of MSSA gDNA. Since this was an initial test and biotinylated primers are significantly more expensive, these primers were not coupled to beads but instead were added to the master mix for a final concentration of 500 nM of each primer. The amplification plot and Bioanalyzer results are shown in figure 5.8. No primer dimers were seen in three of the wells with gDNA, although the fourth well with gDNA (lane 6) showed no product band and only a very weak primer dimer band. The primer dimer bands were also very weak for the blanks, but were easily detectable with the SYBR Green in the amplification plot. One blank was also a false positive, with a product band but no primer dimer band (lane 5). The source of contamination for that well is unknown, but it was not a problem in future experiments. While the primer flaps did reduce primer dimer formation, they did not eliminate it sufficiently enough to reliably distinguish positive and negative results for unknown samples.

The next avenue explored for primer dimer elimination was to increase the annealing temperature. Increased annealing temperatures lead to decreased PCR efficiency but increased specificity.[23] Annealing temperature optimization for the primer sets was first performed in PCR tubes with an Applied Biosystems Veriti 96 Well Thermal Cycler (Applied Biosystems, Foster City, CA). The reactions were performed with the same 5 μL volume and reagent concentrations used on-chip. Four sets of reactions were carried out: *S. aureus nuc* primer beads with MSSA gDNA, *S. aureus mecA* beads with MRSA gDNA, *S. mutans 16S rRNA* beads with *S. mutans* gDNA, and *S. mutans 16S rRNA* primers with flaps with *S. mutans* gDNA. For each primer/template

combination, the annealing temperature was varied from 64 °C to 74 °C in increments of 2 °C. At each annealing temperature there was one blank reaction and one positive control containing 1 pg template DNA. The PCR products were analyzed on the Bioanalyzer following thermocycling. The Bioanalyzer results for *S. aureus nuc*/MSSA and *S. mutans 16S rRNA* with flaps/*S. mutans* are shown in figure 5.9. For *S. aureus nuc* primer beads (figure 5.9A), primer dimers form with a 64 °C annealing temperature, but not at higher annealing temperatures. At 72 °C and above, amplification of the target fails. For this primer set an annealing temperature of 66-70 °C is optimal to reduce primer dimer formation. For *S. aureus mecA* beads, primer dimers are only seen at 64 °C while amplification of the target fails at 70 °C and above, giving an annealing temperature range of 66-68 °C. For *S. mutans 16S rRNA* beads, amplification fails at 66 °C, but primer dimers still form at both 64 and 66 °C. No useful annealing temperature range was found for the *S. mutans 16S rRNA* beads. The results were more unusual for the *S. mutans 16s rRNA* primers with flaps (figure 5.9B). Amplification fails at 70 °C and above, but primer dimers formed at every annealing temperature tested. This suggests that the primer flaps are unsuited for the *S. mutans 16S rRNA* primer sequences. The addition of the primer flaps may result in the 3′ end of one of the primers forming a complex more stable than usual primer dimers, or impurities remaining from the synthesis of a longer oligonucleotide facilitated the formation of primer dimers.

The annealing temperature optimization experiments indicated that for *S. aureus nuc* and *mecA* primer beads, increasing the annealing temperature to at least 66 °C should eliminate primer dimers. Since the current annealing temperature used on-chip is 66 °C, there may be a difference between the solution temperature and Peltier stage temperature.

A 68 °C annealing temperature was tested with the *S. aureus nuc* primer beads, MSSA gDNA, and a simple chip. Three wells contained 1 pg MSSA gDNA as the sample, three wells were blanks without template DNA but still contained primer beads, and the final well was a blank without template or primers. After thermocycling, the PCR products were analyzed for primer dimers with the Bioanalyzer. The amplification plot and Bioanalyzer results are shown in figure 5.10. The amplification plot shows what appears to be amplification in the blank wells containing primer beads, especially compared to the blank well without primers. Unfortunately, noise was a problem for this experiment, which was later found to be due to fluctuations in the intensity of the Nikon Intensilight (Nikon Instruments Inc., Melville, NY) used with the microscope. The Bioanalyzer results confirm the conclusions drawn from the amplification plot, with primer dimers in most of the blank wells and two of the wells with template DNA, including one positive control well with failed amplification of the target sequence (lane 5). Since *S. aureus nuc* was the primer set most tolerant of higher annealing temperatures, these results indicate that raising the annealing temperature may not eliminate primer dimers on-chip. The annealing temperature cannot be raised further without making both of the other primer sets incompatible with the thermocycling program and preventing them from being used on the same chip as the *S. aureus nuc* primers.

Another strategy to reduce primer dimer formation is to reduce the concentration of primers in solution. This was tested with the *S. aureus nuc* primer beads, MSSA gDNA, and a simple chip. Four wells contained 1 pg MSSA gDNA as the sample and three wells were blanks without template. All wells contained half the amount of primer beads used in previous experiments. No amplification was detected from any of the

wells. While this strategy eliminated primer dimer formation, it also eliminated product formation. An alternative strategy to either reduce primer dimers or change how the products are detected will need to found for the primer beads to eliminate the potential for false positives with a chip used in a clinical setting.

Template Digestion with Restriction Enzymes

Performing a restriction enzyme digestion of the template DNA before PCR can improve PCR efficiency. Three enzymes that will cut the template DNA within a few base pairs of the target sequences were tested for compatibility with PCR by performing amplification of digested template in a tube-based reaction. Separate digestions of template gDNA for each of the three targets were performed with a 1 pg/μL concentration of gDNA. One μL of digested DNA was then used as template for PCR in tubes. For each target there were four blanks (two without template and two without primers), four positive controls with undigested template, and four reactions with digested template. The MSSA gDNA was paired with *S. aureus nuc* primer beads, the MRSA gDNA was paired with *S. aureus mecA* beads, and the *S. mutans* gDNA was paired with *S. mutans 16S rRNA* beads. An annealing temperature of 68 °C was used to prevent primer dimer formation. The concentration of PCR products from each reaction was determined with the Bioanalyzer. The average product concentration for each template/primer set pair with undigested and digested template is listed in table 5.1. When the standard deviations are taken into consideration, there is no significant difference between the results for undigested and digested template for MSSA and MRSA. For *S. mutans*, no amplification was detected for the undigested template. This was likely due to the higher annealing temperature. That product was detected for

digested *S. mutans* template indicates that enzyme digestion does not inhibit PCR and may improve annealing.

PCR with digested template was then tested on-chip with MRSA gDNA, *S. aureus mecA* primer beads, and a simple chip. The digestion was performed off-chip as previously described. Three reaction wells contained digested template gDNA, three wells contained undigested template gDNA (positive controls), and the final well was a blank containing primers but no template. The usual annealing temperature of 66 °C was used. The amplification plot and Bioanalyzer results are shown in figure 5.11. Bubbles were a problem for one of the wells with digested template and that trace has been removed from the amplification plot, but the Bioanalyzer results for that well are shown. Amplification was successful for all wells with digested or undigested DNA. The Bioanalyzer results confirm amplification of the target region, although the product bands are weaker for two of the wells with digested DNA and one of the positive controls. For this experiment, the concentration of products measured by the Bioanalyzer may be lower than the concentration that was present on-chip. The amount of solution collected from each well was small, and there was more gelation from BSA than had been seen in previous experiments. Those factors made it difficult to prevent mineral oil from making up part of the 1 μL samples used with the Bioanalyzer. The Bioanalyzer results also show that primer dimers were not a problem for most wells, including the blank, in this experiment, although that may be due to experimental variation or underestimation of product concentrations rather than the enzyme digestion. These results do show that restriction digestion of the template DNA does not inhibit PCR, although the improvement in the results was modest with this chip design.

5.4 Conclusions and Future Directions

We have developed a primer delivery method for the microfluidic rt-PCR device that is compatible with DNA extraction with AOMs. Primers spotted directly onto the AOM, as in Chapter 3, were washed off during the DNA extraction step. Instead, biotinylated primers were coupled to streptavidin-coated microspheres that were added into the reaction wells. The beads are too large to travel through the pores of the AOM, and the streptavidin-biotin linkage firmly anchors the primers during DNA extraction. The initial heating steps of PCR break the streptavidin-biotin linkage, releasing the primers. The primer beads were successfully used to perform on-chip PCR with DNA extraction. Further experiments found they could be stored on-chip for at least 39 days at 4 °C or 62 days at room temperature and still be used for PCR.

Only primers were coupled to the microspheres, so SYBR Green was used for product detection instead of the fluorescently labeled probes used in Chapter 4. One disadvantage of SYBR Green is that it does not detect specific sequences, so it will detect unintended amplification products such as primer dimers. Bioanalyzer analysis of products from PCR with primer beads found that primer dimers were a recurring problem with these experimental conditions. The addition of AT-rich primer flaps to the *S. mutans 16S rRNA* primers was tested to eliminate primer dimers, but was ultimately unsuccessful. The annealing temperature was also optimized for each primer set. Higher annealing temperatures appeared to be beneficial for the *S. aureus nuc* and *mecA* primer sets in tubes, but were unsuccessful on-chip. Reducing the concentration of primers in the reaction was tested, but was also unsuccessful on-chip under the current experimental parameters.

Primer dimers can cause false positives when used with non-specific intercalating dyes, so a means to eliminate them or a more specific detection strategy must be found. One possibility is to couple the probes to the beads along with the primers. Although biotinylated dual-quenched probes have not been previously described and the probes already have a fluorescent dye on one end and a quencher on the other, it may still be possible to biotinylate them either internally or as a second modification to one end. SYBR Green was used for detection at first rather than adding an untested probe modification as an additional unknown variable into the experiments. Another possibility is to continue using SYBR Green for detection, but perform a melting curve analysis after the completion of PCR. In a melting curve analysis, the temperature of the solution is gradually increased from 50 °C to 95 °C. As the double stranded DNA denatures, the fluorescence signal from SYBR Green decreases greatly. A plot of the derivative of the fluorescence with respect to temperature (*dF/dT*) vs. temperature will show peaks at the melting temperatures for any DNA present.[24] Primer dimers have a lower melting temperature than longer PCR products, so the presence of primer dimers or specific amplification can be determined. Melting curve analysis was attempted using our set-up, but the noise from the Intensilight was too great to determine a sharp melting temperature. New light sources are currently being investigated, so this may be a possibility in the future. Current work in the Ramsey group suggests that reducing the reaction volume may also reduce primer dimer formation as the total number of molecules is reduced (results not published). Work to design and fabricate chips with much smaller reaction volumes is ongoing.

We have also found three restriction enzymes that are compatible with the target sequences for which our primers were designed. The digested gDNA could be successfully amplified both in tubes and on-chip without PCR inhibition. For *S. mutans* gDNA in tubes, the digested template was amplified even when the annealing temperature was too high for the undigested template. A further use for the digested DNA could be to use the primer beads for specific DNA extraction from samples, eliminating the need for DNA extraction with the AOM and providing a means of selective sample concentration. Since the enzymes were selected to cut near one end of the target sequence, the digested DNA may be able to hybridize to the primers on the beads. A mixture of beads for a pool of targets could be incubated with digested template DNA and then the beads with hybridized template could be loaded into individual reaction wells with a greatly decreased reaction volume. A general master mix could then be added, and thermocycling could begin. The beads would need to be encoded in some way, similar to the antibody-functionalized microspheres from Chapter 2, so that the results from each bead could be attributed to the appropriate target. If the reaction wells are small enough for reactions with single primer beads, an array large enough for digital PCR may be possible, and the amount of template might be quantified directly, without using C_t values and a calibration curve.[2, 25, 26]

Another potential improvement would be to include a reference dye for normalization of the fluorescent signal. This could simplify data analysis and eliminate the need to subtract an image from a few cycles before amplification to account for well-to-well variations in the baseline fluorescent signal. Developing a reader instrument for the chip, particularly one that includes automated reagent loading, would make it more

user friendly. If the chip requires the user to pipette reagents into each well, even if the same volume of the same solution is used for all wells, there is greater potential for user error. Automation of all chip operation after saliva sample introduction would be ideal. Finally, primer sets for additional organisms with annealing temperatures compatible with the three sets currently in use, and potentially with the three restriction enzymes, would expand the usefulness of the device. Multiple, non-biotinylated primer sets for *H. influenzae*, *S. pneumoniae*, and *S. salivarius* were designed, but they either had problems with primer dimer formation or annealing temperatures disparate from those used for the *S. aureus* and *S. mutans* primer sets. If an alternative approach is found with reduced primer dimer formation (such as using lower reaction volumes), some of those primer sets could be retested.

5.5 Tables and Figures

Table 5.1. Average concentration of products from PCR with undigested and digested template for three template and primer set combinations. No products were detected from PCR with undigested *S. mutans* gDNA.

Template/primer set	Concentration of PCR products (ng/μL)	
	Undigested template	**Digested template**
MSSA/*S. aureus nuc*	4.11 ± 0.32	3.52 ± 0.42
MRSA/*S. aureus mecA*	2.07 ± 0.32	1.81 ± 0.08
S. mutans/*S. mutans 16S rRNA*	-	0.36 ± 0.14

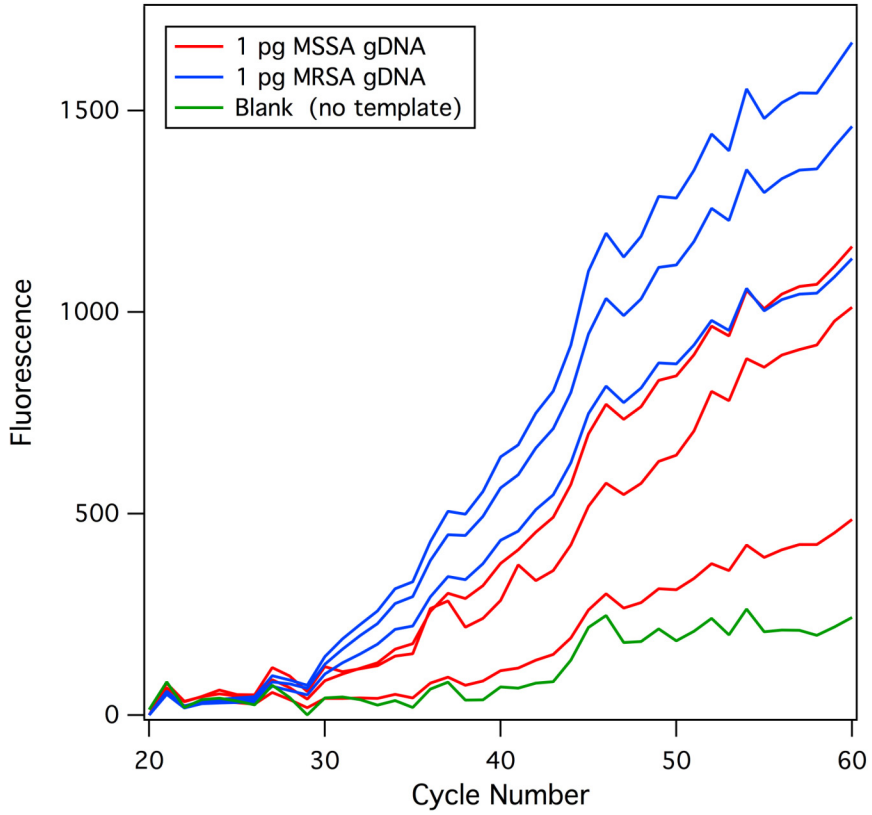

Figure 5.1. Real-time amplification plot for MSSA and MRSA gDNA with *S. aureus nuc* primers and probes pre-spotted into the wells. DNA extraction with the AOM was not performed. Positive results are seen for all wells containing template DNA. Possible amplification in the blank well indicates that it may have become contaminated with a small amount of template.

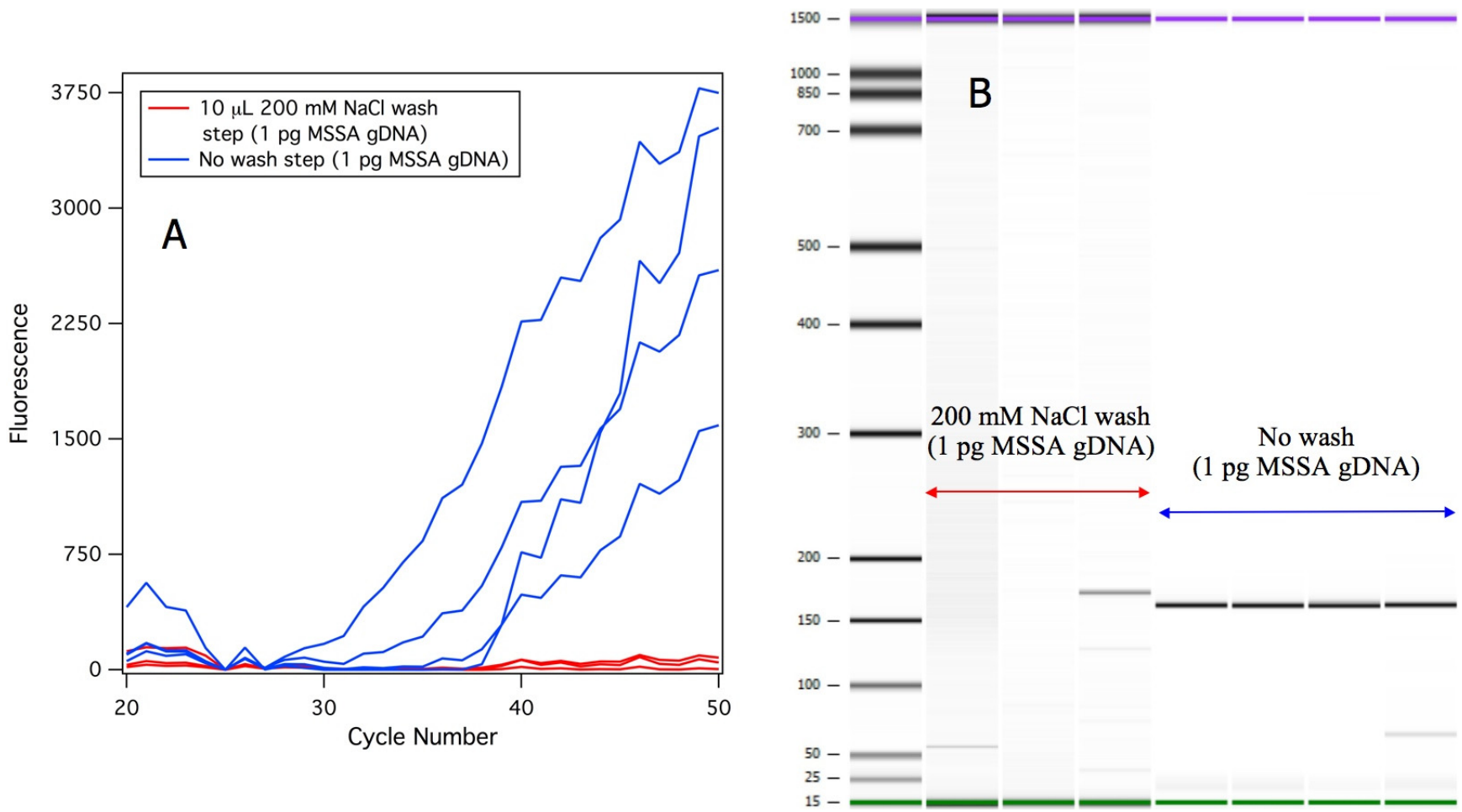

Figure 5.2. Real-time amplification plot (A) and Bioanalyzer results (B) for MSSA gDNA with and without a wash step after pre-spotting *S. aureus nuc* primers and probes. The wash step with 200 mM NaCl simulated DNA extraction. The wells with a wash step did not show detectable amplification in the plot and showed little or no product (180 bp) in the Bioanalyzer results. Amplification was successful for wells without a wash step, indicating that the primers and probes are washed away during DNA extraction.

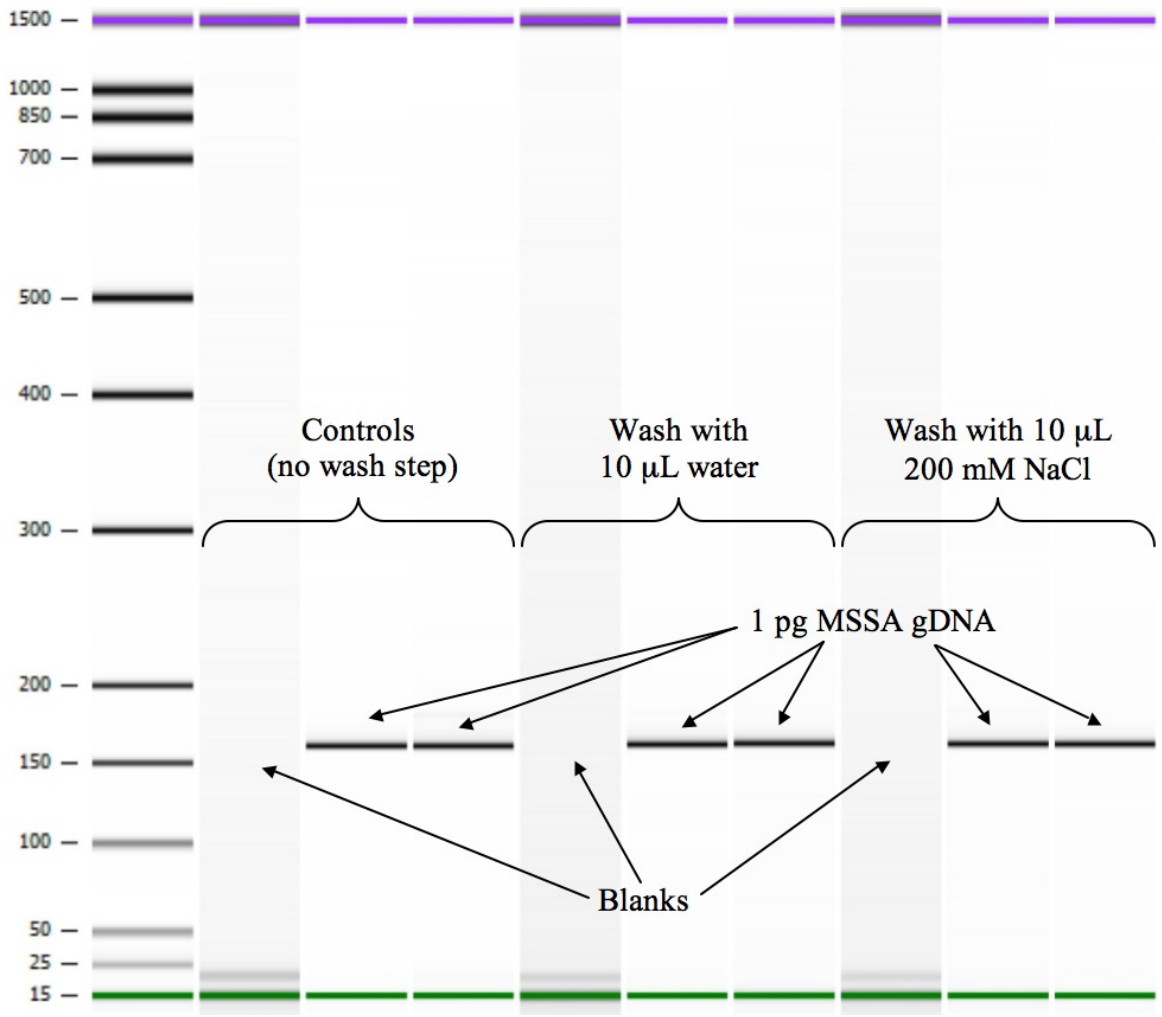

Figure 5.3. Results of PCR of MSSA gDNA with *S. aureus nuc* primers pre-spotted onto tube-mounted AOMs. Primers and probes were spotted onto all of the tube-mounted AOMs. The first set of three were used as positive controls without a wash step, the second set of three were washed with DNase/RNase free water, and the third set were washed with 200 mM NaCl. Amplification was seen from all reactions containing gDNA, whether or not a wash step was performed.

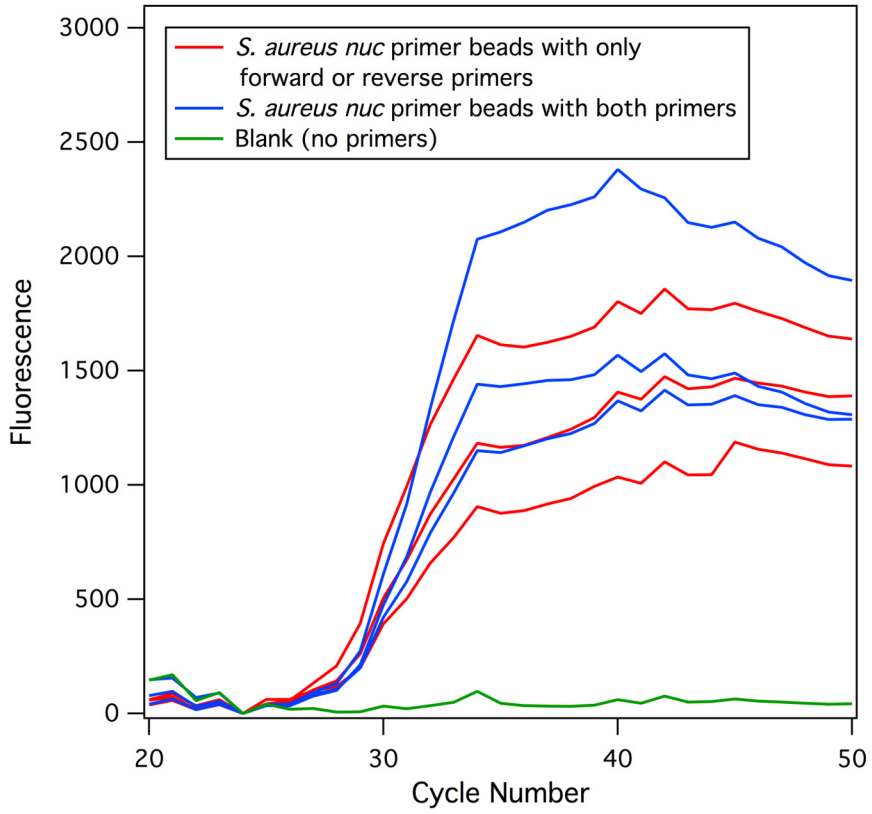

Figure 5.4. Real-time amplification plot of the *S. aureus nuc* gene using primer beads. A mixture of primer beads for the forward and reverse primers were added to three wells, primer beads with both primers were added to another three wells, and the final well was a blank with no primer beads. Each well contained 1 pg MSSA gDNA as the sample. Template DNA was extracted onto the AOM after adding the primer beads into the wells. Amplification is seen from all wells with primers, demonstrating that the primers are retained on the beads through the DNA extraction step.

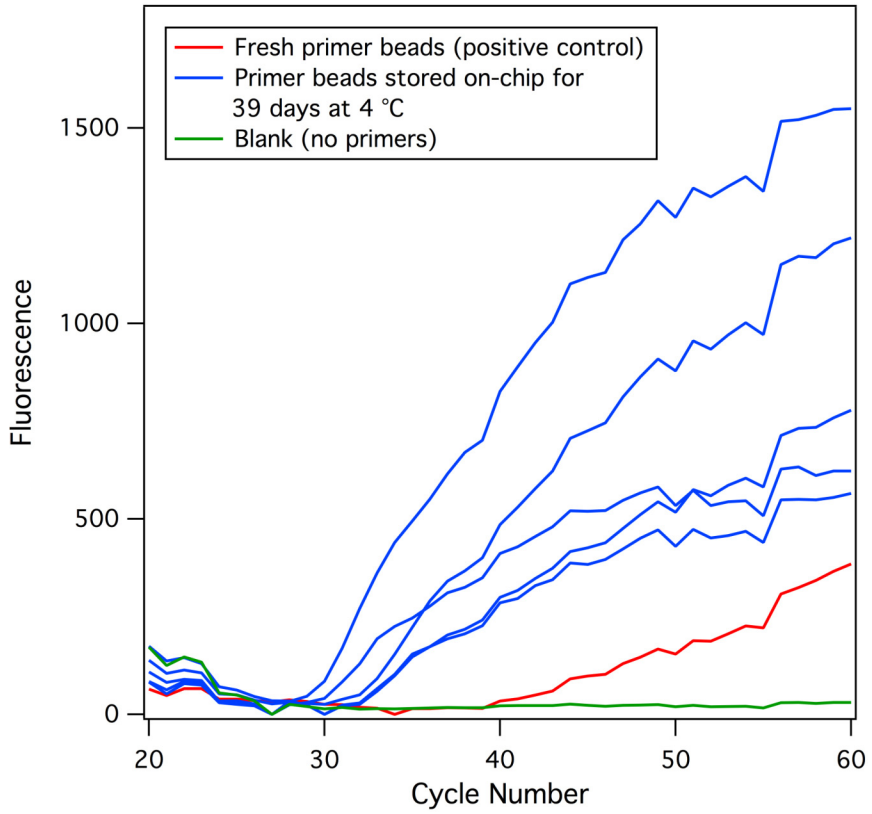

Figure 5.5. Real-time amplification plot with *S. aureus nuc* primer beads stored on-chip for 39 days at 4 °C. Primer beads were loaded into five wells of a chip before storing it for 39 days. On the day PCR was performed, fresh primer beads, from a new batch, were added to a sixth well. The final well was left as a blank. Each well contained 1 pg MSSA gDNA, extracted onto the AOM, as the sample. Amplification was seen from all wells containing primers, so the primer beads can be stored on-chip for at least 39 days at 4 °C and still be used for PCR.

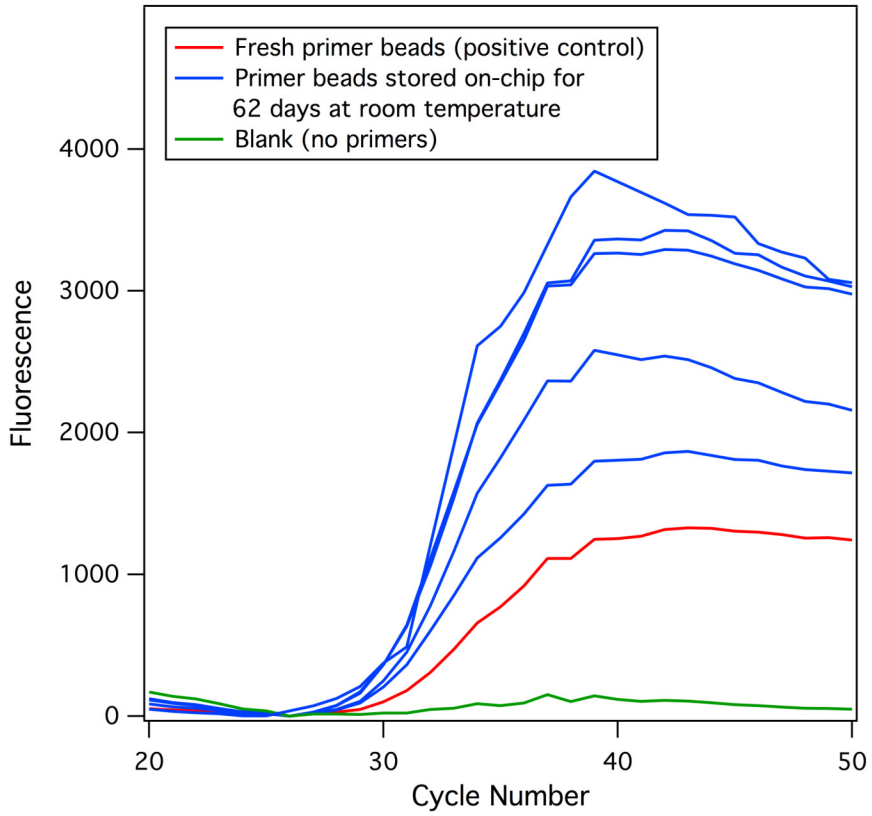

Figure 5.6. Real-time amplification plot with *S. aureus nuc* primer beads stored on-chip for 62 days at room temperature. Primer beads were loaded into five wells of a chip before storing it for 62 days. On the day PCR was performed, fresh primer beads, from a new batch, were added to a sixth well. The final well was left as a blank. Each well contained 1 pg MSSA gDNA, extracted onto the AOM, as the sample. Amplification was seen from all wells containing primers, indicating that the primer beads can be stored on-chip for at least 62 days at room temperature and still be used for PCR.

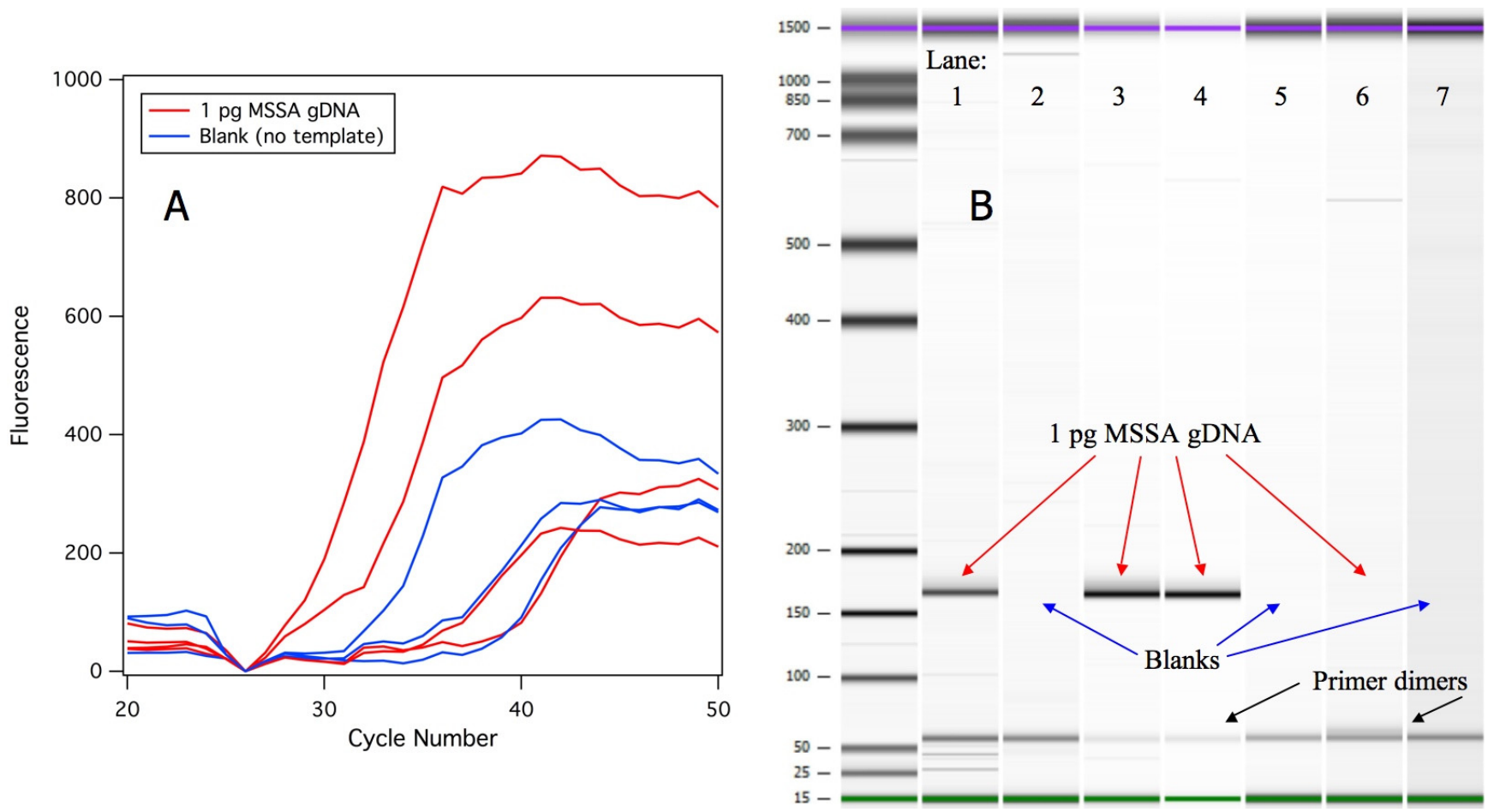

Figure 5.7. Real-time amplification plot (A) and Bioanalyzer results (B) from PCR with *S. aureus nuc* beads showing primer dimers. Four wells of a chip contained 1 pg MSSA gDNA, while three wells were blanks with no template DNA. Primer beads were added to all wells. Amplification was detected from all wells, including the blanks. The Bioanalyzer results show that the amplification from the blank wells (lanes 2, 5, and 7) and some of the wells containing gDNA (lanes 1 and 6) was due to primer dimers.

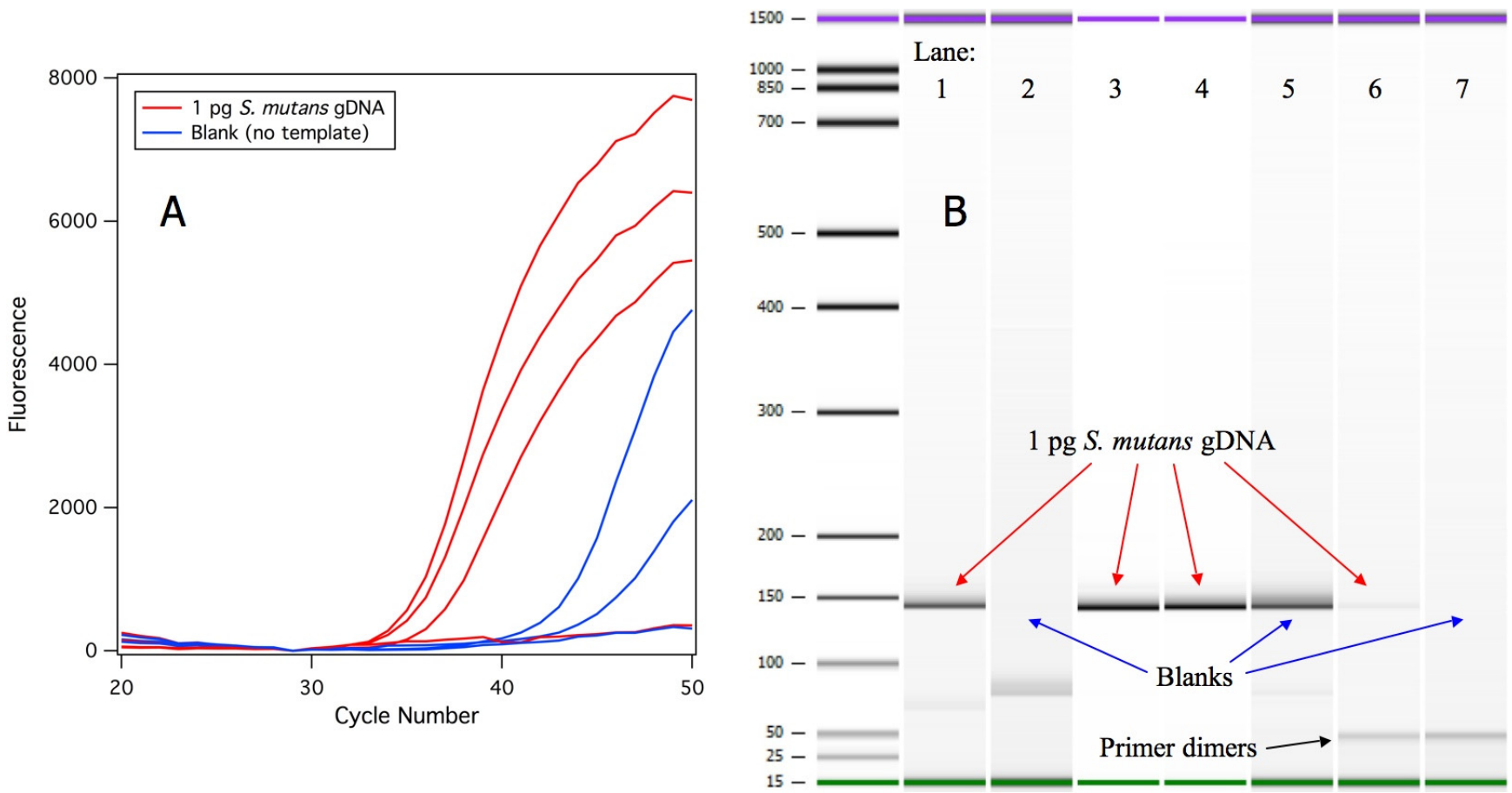

Figure 5.8. Real-time amplification plot (A) and Bioanalyzer results (B) from PCR with *S. mutans 16S rRNA* primers with flaps. Four wells of a chip contained 1 pg *S. mutans* gDNA, while three wells were blanks with no template DNA. Primers were added to all wells. Amplification was detected from three wells containing DNA and two blank wells, and one well containing DNA was a false negative. The Bioanalyzer results show primer dimers for several of the wells and product for one of the blank wells (lane 5), due to unknown contamination with template DNA.

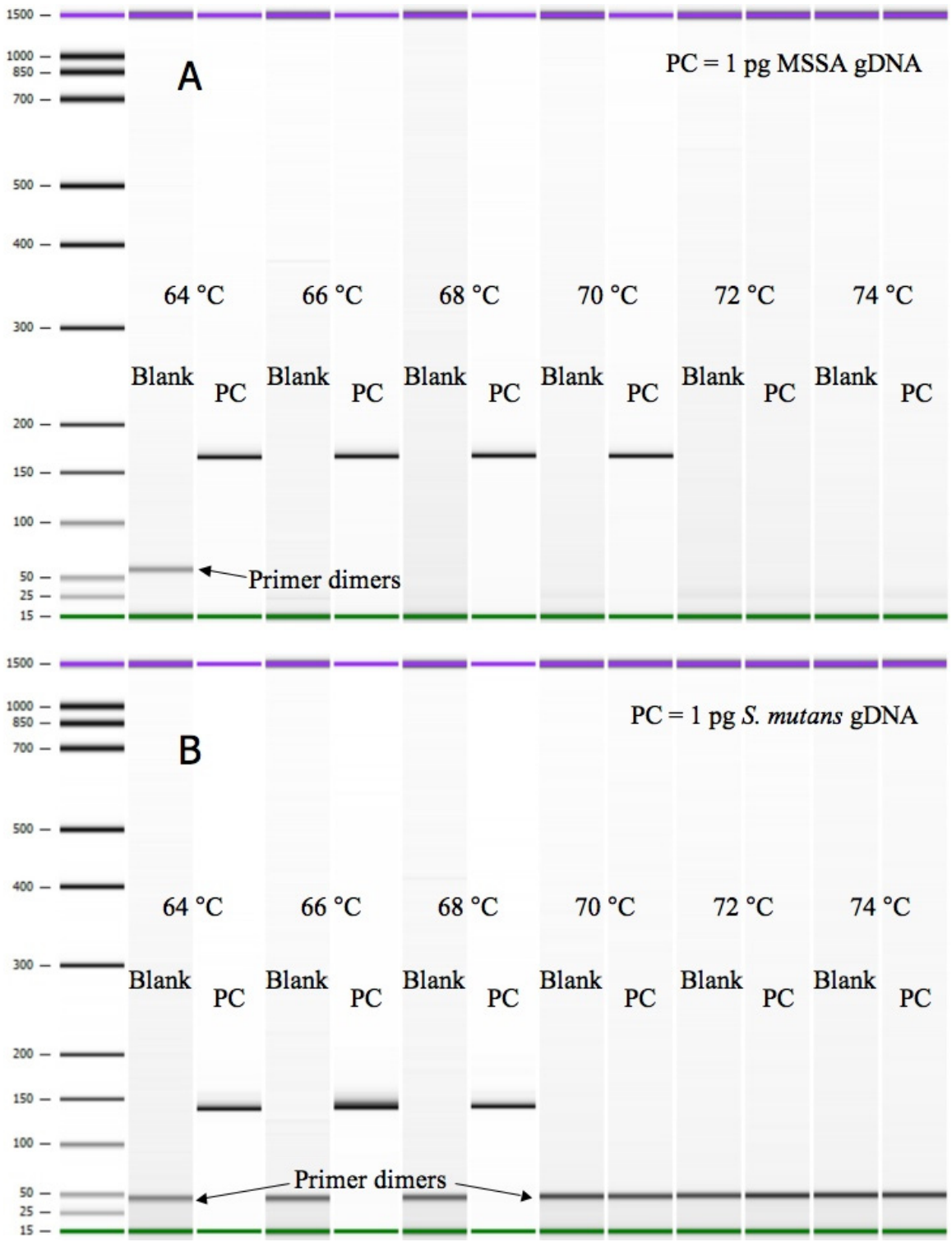

Figure 5.9. Results of annealing temperature optimization for *S. aureus nuc* primer beads (A) and *S. mutans 16S rRNA* primers with flaps (B). The annealing temperature was varied from 64-74 °C with a blank and positive control (PC) with 1 pg of MSSA (A) or *S. mutans* (B) gDNA at each temperature. Primer dimers form at every temperature for *S. mutans* primers with flaps, but 66-70 °C eliminated them for the *nuc* primer beads.

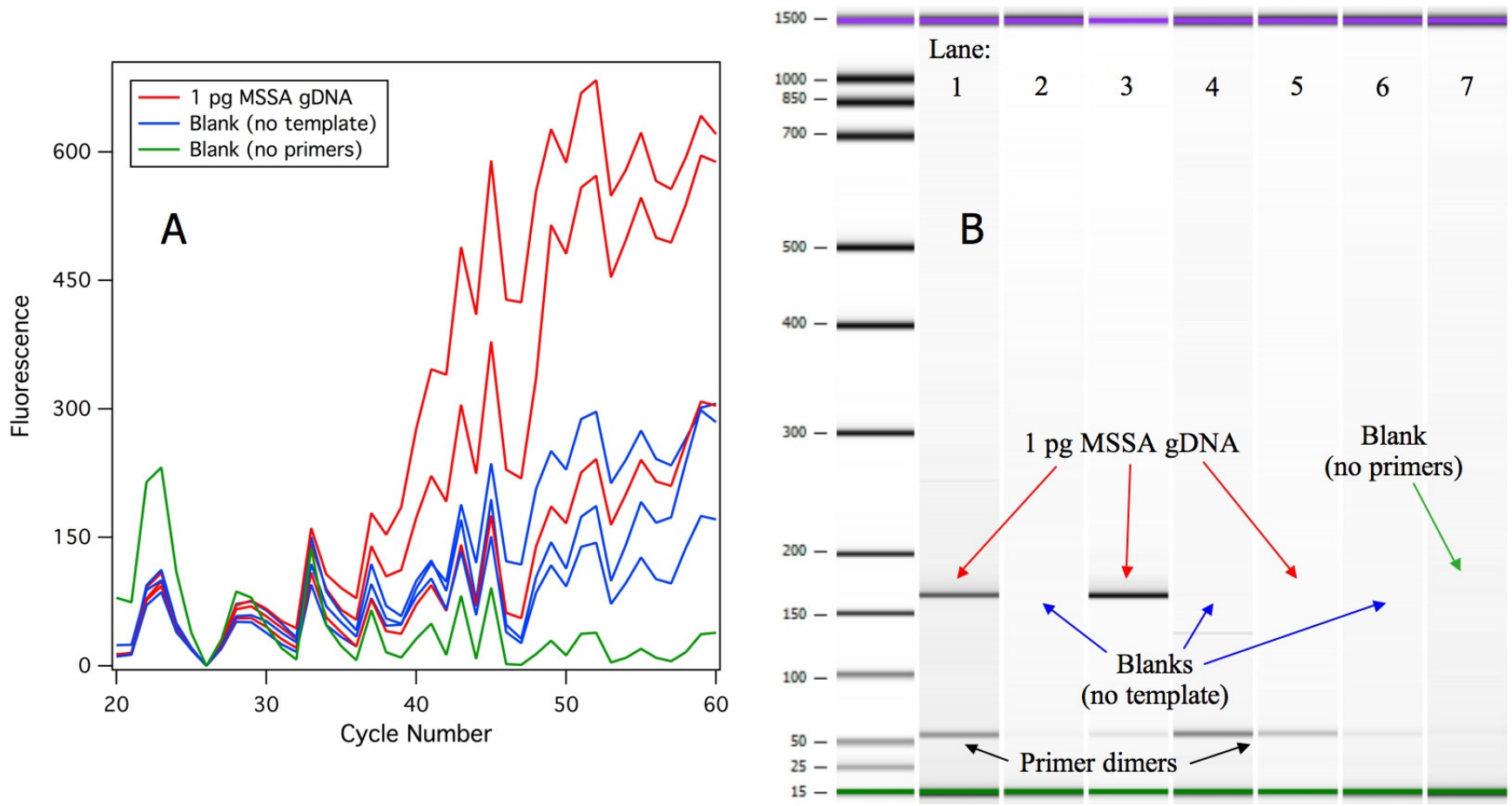

Figure 5.10. Real-time amplification plot (A) and Bioanalyzer results (B) from on-chip PCR with *S. aureus nuc* primer beads and an annealing temperature of 68 °C. Three wells contained 1 pg MSSA gDNA, three wells were blanks without template DNA, and the final well was a blank without primers. All wells but the final blank contained *S. aureus nuc* primer beads. Amplification was seen for all wells containing primers, and the Bioanalyzer shows primer dimers forming in many of the wells. Amplification failed in one well containing template DNA. The noise in the amplification plot was caused by fluctuations in the intensity of the light source.

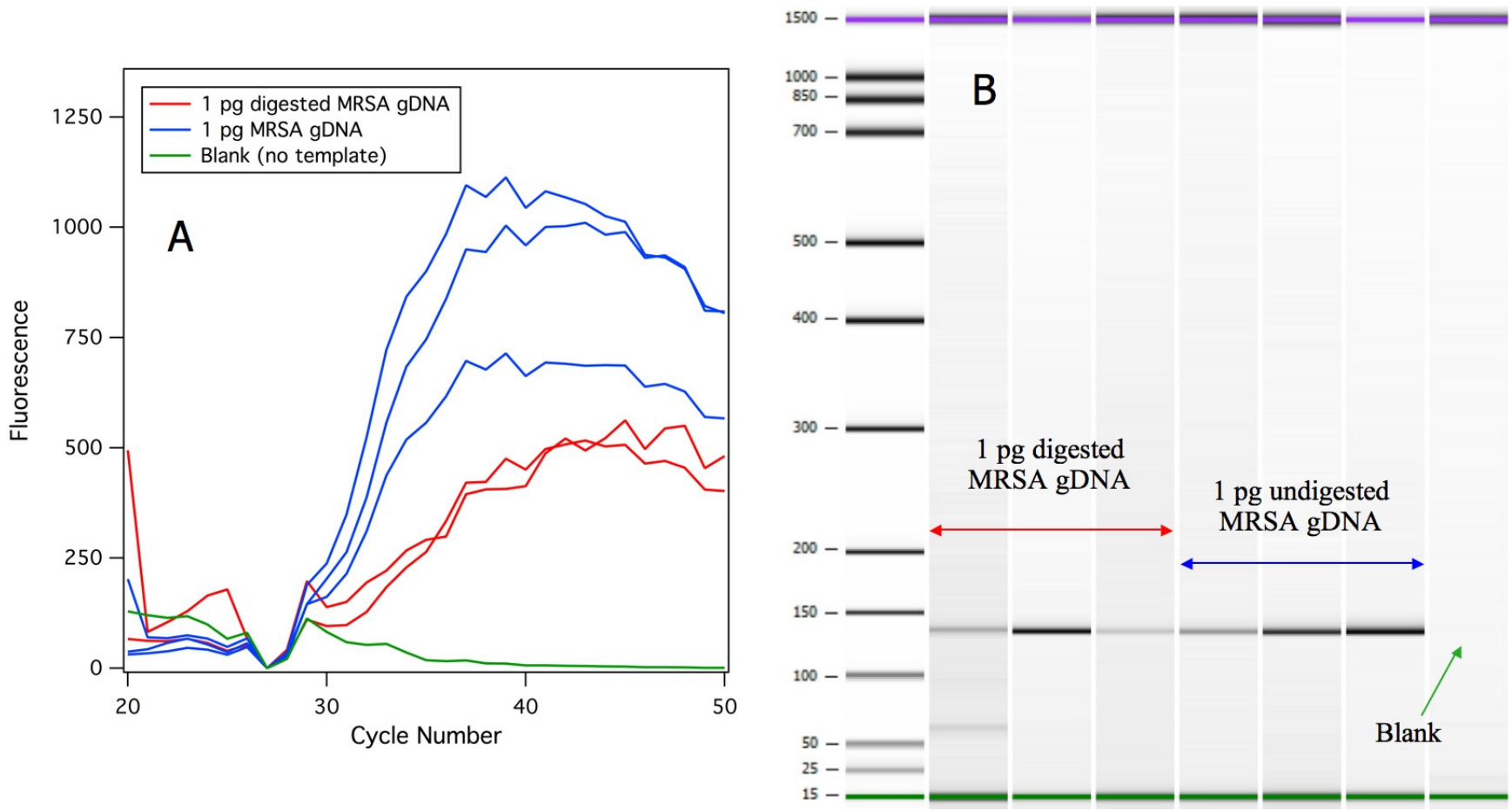

Figure 5.11. Real-time amplification plot (A) and Bioanalyzer results (B) for on-chip PCR of digested MRSA gDNA. Three of the wells contained 1 pg digested MRSA gDNA, three wells contained 1 pg undigested MRSA gDNA, and the final well was a blank. All wells contained *S. aureus mecA* primer beads. The plot shows amplification for all wells containing template DNA, and the Bioanalyzer results confirm that the amplification is of the target gene, not just from primer dimers.

5.6 References

1. Liu, H.-B.; Ramalingam, N.; Jiang, Y.; Dai, C.-C.; Hui, K. M.; Gong, H.-Q., Rapid distribution of a liquid column into a matrix of nanoliter wells for parallel real-time quantitative PCR. *Sensors and Actuators B-Chemical* 2009, *135*, (2), 671-677.

2. Matsubara, Y.; Kerman, K.; Kobayashi, M.; Yamamura, S.; Morita, Y.; Takamura, Y.; Tamiya, E., On-Chip Nanoliter-Volume Multiplex TaqMan Polymerase Chain Reaction from A Single Copy Based on Counting Fluorescence Released Microchambers. *Analytical Chemistry* 2004, *76*, (21), 6434-6439.

3. Ramalingam, N.; Liu, H.-B.; Dai, C.-C.; Jiang, Y.; Wang, H.; Wang, Q.; Hui, K. M.; Gong, H.-Q., Real-time PCR array chip with capillary-driven sample loading and reactor sealing for point-of-care applications. *Biomedical Microdevices* 2009, *11*, (5), 1007-1020.

4. Ramalingam, N.; Rui, Z.; Liu, H.-B.; Dai, C.-C.; Kaushik, R.; Ratnaharika, B.; Gong, H.-Q., Real-time PCR-based microfluidic array chip for simultaneous detection of multiple waterborne pathogens. *Sensors and Actuators B: Chemical* 2010, *145*, (1), 543-552.

5. Chen, D.; Mauk, M.; Qiu, X.; Liu, C.; Kim, J.; Ramprasad, S.; Ongagna, S.; Abrams, W.; Malamud, D.; Corstjens, P.; Bau, H., An integrated, self-contained microfluidic cassette for isolation, amplification, and detection of nucleic acids. *Biomedical Microdevices* 2010, *12*, (4), 705-719.

6. Kim, J.; Byun, D.; Mauk, M. G.; Bau, H. H., A disposable, self-contained PCR chip. *Lab on a Chip* 2009, *9*, (4), 606-612.

7. Qiu, X. B.; Mauk, M. G.; Chen, D. F.; Liu, C. C.; Bau, H. H., A large volume, portable, real-time PCR reactor. *Lab on a Chip* 2010, *10*, (22), 3170-3177.

8. Kumaresan, P.; Yang, C. J.; Cronier, S. A.; Blazej, R. G.; Mathies, R. A., High-Throughput Single Copy DNA Amplification and Cell Analysis in Engineered Nanoliter Droplets. *Analytical Chemistry* 2008, *80*, (10), 3522-3529.

9. Liu, P.; Mathies, R. A., Integrated microfluidic systems for high-performance genetic analysis. *Trends in Biotechnology* 2009, *27*, (10), 572-581.

10. Konry, T.; Hayman, R. B.; Walt, D. R., Microsphere-Based Rolling Circle Amplification Microarray for the Detection of DNA and Proteins in a Single Assay. *Analytical Chemistry* 2009, *81*, (14), 5777-5782.

11. Ramsey, J. M.; Henley, W. H.; Oblath, E. A. Microfluidic Devices, Solid Supports for Reagents, and Related Methods. *US Patent Application 61/651,648* filed May 2012.

12. Holmberg, A.; Blomstergren, A.; Nord, O.; Lukacs, M.; Lundeberg, J.; Uhlén, M., The biotin-streptavidin interaction can be reversibly broken using water at elevated temperatures. *Electrophoresis* 2005, *26*, (3), 501-510.

13. Cha, R. S.; Thilly, W. G., Specificity, Efficiency, and Fidelity of PCR. *PCR Methods and Applications* 1993, *3*, (3), S18-S29.

14. Pingoud, A.; Alves, J.; Geiger, R., Restriction Enzymes. In *Enzymes of Molecular Biology*, Burrell, M. M., Ed. Humana Press: Totowa, NJ, 1993; pp 107-200.

15. Roberts, R. J., Restriction Endonucleases. *CRC Critical Reviews in Biochemistry* 1976, *4*, (2), 123-1664.

16. Her, C.; Weinshilboum, R. M., Endonuclease-Mediated Long PCR and Its Application to Restriction Mapping. *Current Issues in Molecular Biology* 1999, *1*, (2), 77-88.

17. Sharma, J. K.; Gopalkrishna, V.; Das, B. C., A simple method for elimination of unspecific amplifications in polymerase chain reaction. *Nucleic Acids Research* 1992, *20*, (22), 6117-6118.

18. Vincze, T.; Posfai, J.; Roberts, R. J., NEBcutter: a program to cleave DNA with restriction enzymes. *Nucleic Acids Research* 2003, *31*, (13), 3688-3691.

19. Das, S.; Mohapatra, S. C.; Hsu, J. T., Studies on primer-dimer formation in polymerase chain reaction (PCR). *Biotechnology Techniques* 1999, *13*, (10), 643-646.

20. Rychlik, W., Selection of Primers for Polymerase Chain Reaction. *Molecular Biotechnology* 1995, *3*, (2), 129-134.

21. Brownie, J.; Shawcross, S.; Theaker, J.; Whitcombe, D.; Ferrie, R.; Newton, C.; Little, S., The elimination of primer-dimer accumulation in PCR. *Nucleic Acids Research* 1997, *25*, (16), 3235-3241.

22. Afonina, I.; Ankoudinova, I.; Mills, A.; Lokhov, S.; Huynh, P.; Mahoney, W., Primers with 5' flaps improve real-time PCR. *BioTechniques* 2007, *43*, (6), 770-774.

23. Bailey, C. L.; Birch, L.; McDowell, D. G., PCR: Factors Affecting Reliability and Validity. In *Essentials of Nucleic Acid Analysis: A Robust Approach*, Keer, J. T.; Birch, L., Eds. Royal Society of Chemistry: Cambridge, UK, 2008; pp 101-131.

24. Keer, J. T., Quantitative Real-time PCR Analysis. In *Essentials of Nucleic Acid Analysis: A Robust Approach*, Keer, J. T.; Birch, L., Eds. Royal Society of Chemistry: Cambridge, UK, 2008; pp 132-166.

25. Park, S.; Zhang, Y.; Lin, S.; Wang, T.-H.; Yang, S., Advances in microfluidic PCR for point-of-care infectious disease diagnostics. *Biotechnology Advances* 2011, *29*, (6), 830-839.

26. Zhang, C. S.; Xing, D., Miniaturized PCR chips for nucleic acid amplification and analysis: latest advances and future trends. *Nucleic Acids Research* 2007, *35*, (13), 4223-4237.